

Teilchenphysik Seminar

# Silicon Photomultipliers

Principle, Performance and Some Applications

Christian Joram  
CERN / PH Department



## The “classical” application domains of photodetectors in particle physics

- ❑ **Calorimetry**
  - Readout of organic and inorganic scintillators, lead glass, scint. or quartz fibres → Blue/VIS, usually 10s – 10000s of photons
  
- ❑ **Particle Identification**
  - Detection of Cherenkov light → UV/blue → single photons
  - Time Of Flight → Usually readout of organic scintillators (not competitive at high momenta)
  - Transition radiation (X-rays, not covered in this talk)
  
- ❑ **Tracking**
  - Readout of scintillating fibres, blue-green, few photons

- ❖ 158,000 photodetectors in the LHC experiments
- ❖ 4,45 M readout channels
- ❖ 35.4 m<sup>2</sup> photosensitive area

## ... and beyond particle physics

- ❑ **Medical imaging**
  - Nuclear Medicine: PET & SPECT ( $\gamma$ -camera) → Readout of inorganic scintillators
  
- ❑ **Analytical, industrial, ...**

C.J., Photodetection in the LHC experiments, NIM A 695 (2012) 13-22

- A novel type of photodetector has emerged over the last ~15 years (too late for LHC!)
- by now reached a reasonable level of maturity
  - a number of attractive features, but also some serious limitations.
  - It has many names like Silicon PM (SiPM), Geiger APD (G-APD), Metal Resistive layer Semiconductor (MRS-APD), Multi Photon Pixel Counter (MPPC), SiPM, SPM,...
- SiPM is by now the most used name (I don't like it).

## Outline

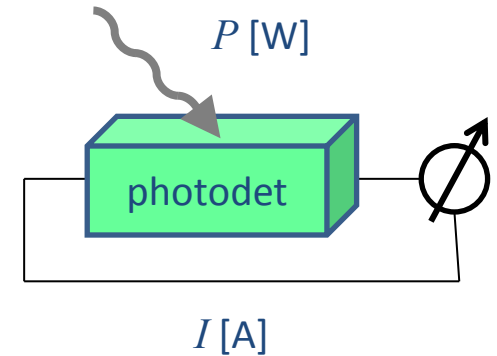
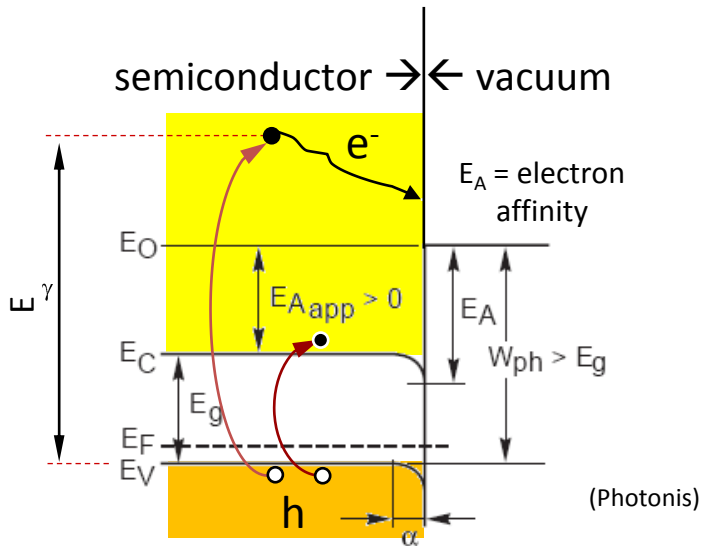
- Requirements on photodetectors
- Principle of operation of the Silicon Photomultiplier
- AX-PET – Demonstration of an axial PET scanner
- The Digital SiPM
- Extension of AX-PET by TOF
- SiPM R&D for a SciFi tracker for LHCb and Calorimetry for ILC

## "Typical" requirements on a photodetector

- High sensitivity  $S \stackrel{Q}{=} \frac{I[A]}{P[W, \lambda]}$  or  $QE \stackrel{Q}{=} \frac{N_{pe}}{N_\gamma}$   $S[mA/W] \approx \frac{QE[\%] \cdot \lambda[nm] \cdot e}{hc} = \frac{QE[\%] \cdot \lambda[nm]}{124}$
- What really counts: Photon detection Efficiency  $PDE = QE \cdot \epsilon_{coll} \cdot \epsilon_{aval} \cdot \epsilon_{fill} \cdot \epsilon \dots$
- High gain  $M = \frac{N_e}{N_{pe}}$   $M > 10^5 \rightarrow$  we have a chance to see single photons
- Small signal fluctuations, low Excess Noise Factor F  $ENF = \frac{\sigma_{out}^2}{\sigma_{in}^2}$   $ENF = 1 + \frac{\sigma_M^2}{M^2}$   
 ENF impacts energy resolution  $\frac{\sigma_E}{E} = \sqrt{\frac{ENF}{N_{pe}}}$  general definition (M = 1) (M ≠ 1)
- Low dark noise / current
- Fast timing properties (rise time, fall time, dead time)
- Large dynamic range with good linearity
- For certain applications: Radiation hardness, magnetic field compatibility, compactness, cost

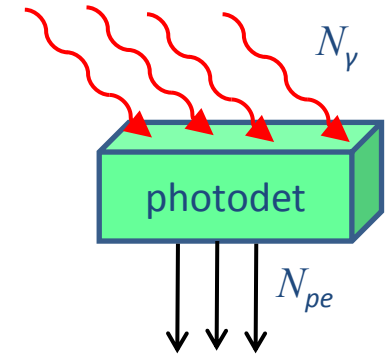
# Basics of photodetection

Many photosensitive materials are semiconductors, but photoeffect can also be observed from gases and liquids.



Internal photoeffect

External photoeffect



Internal photoeffect:  $E_\gamma > E_g$

External photoeffect:  $E_\gamma > E_g + E_A$

## Photodetectors

### Gas

External photoeffect

TMAE  
TEA +  
Csl

MWPC  
GEM  
...

### "Vacuum"

External photoeffect

Avalanche gain  
Process

Dynodes → PMT

Continuous dynode  
→ Channeltron, MCP

Multi-Anode devices

Other gain process  
= Hybrid tubes

Silicon  
anode

HPD  
HAPD  
(G-APD-HPD)

Lumines-  
cent anodes

SMART/Quasar  
X-HPD

### Solid state

Internal photoeffect

PIN-diode

APD

SiPM

Digital SiPM

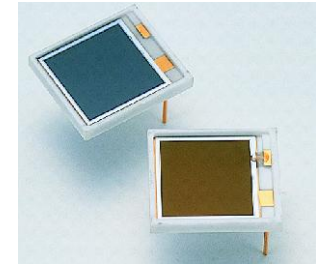
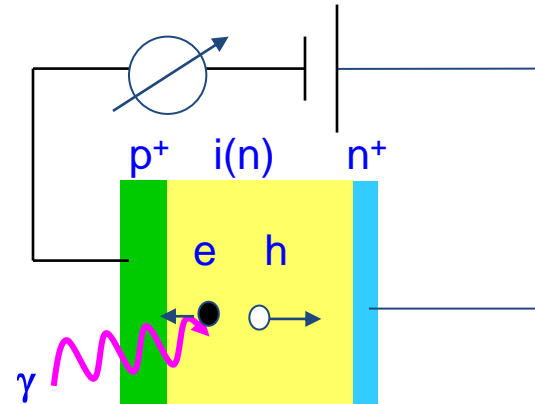
CMOS imager

CCD

Doesn't exist as 'real' device  
Proposed by G. Barbarino et al., NIM A 594 (2008) 326-331  
Proof of principle by CJ et al., NIM A 621 (2010) 171-176

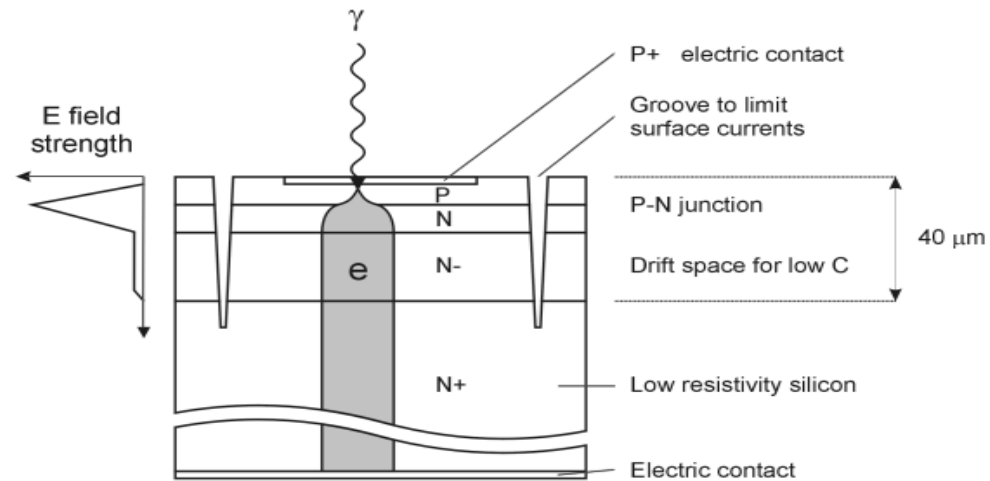
## (Si) – Photodiodes (PIN diode)

- P(I)N type
- p layer very thin ( $<1 \mu\text{m}$ ), as visible light is rapidly absorbed by silicon
- High QE (80% @  $\lambda \approx 700\text{nm}$ )
- Gain = 1

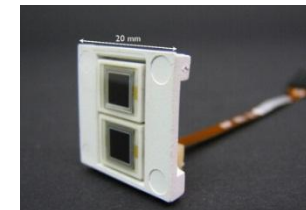


## Avalanche photodiode (APD)

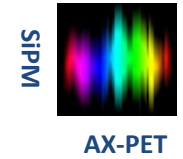
- High reverse bias voltage: typ. few 100 V
- Special doping profile  $\rightarrow$  high internal field ( $>10^5 \text{ V/cm}$ )  $\rightarrow$  avalanche multiplication
- Avalanche stops due to statistical fluctuations.
- Gain: typ.  $O(100)$
- Rel. high gain fluctuations (excess noise from the avalanche). CMS ECAL APD:  $\text{ENF} = 2 @ G=50$ .
- Very high sensitivity on temp. and bias voltage  $\Delta G = 3.1\%/V$  and  $-2.4 \%/K$



Hamamatsu S8148.  
(140.000 pieces used in CMS barrel ECAL).



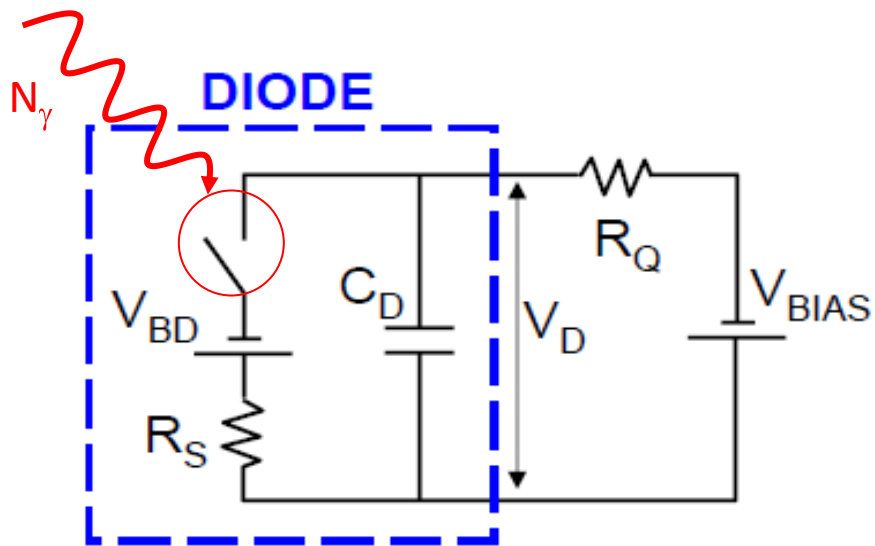
# PIN → APD → Geiger mode Avalanche Photodiode (GM-APD)



How to obtain higher gain (= single photon detection) without suffering from excessive noise ?

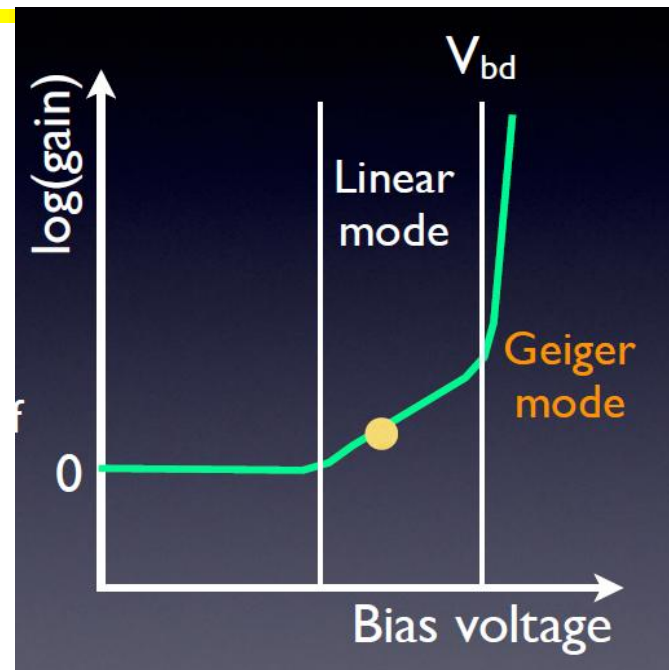
Operate APD cell in Geiger mode (= full discharge), however with (passive/active) **quenching**.

Photon conversion + avalanche short circuit the diode. A single photon (or anything else) is sufficient!

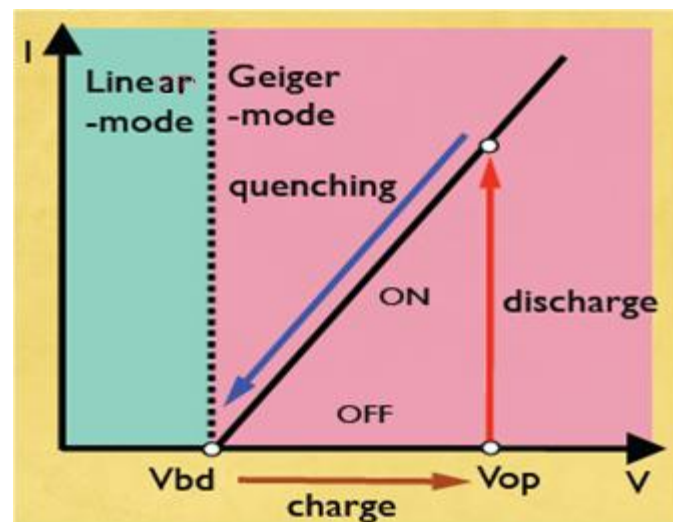


J. Haba, RICH2007

A single-cell GM-APD is just a **binary** device (=switch). Info on  $N_\gamma$  is lost by the Geiger avalanche. It will become more interesting when we combine many cells in one device ...



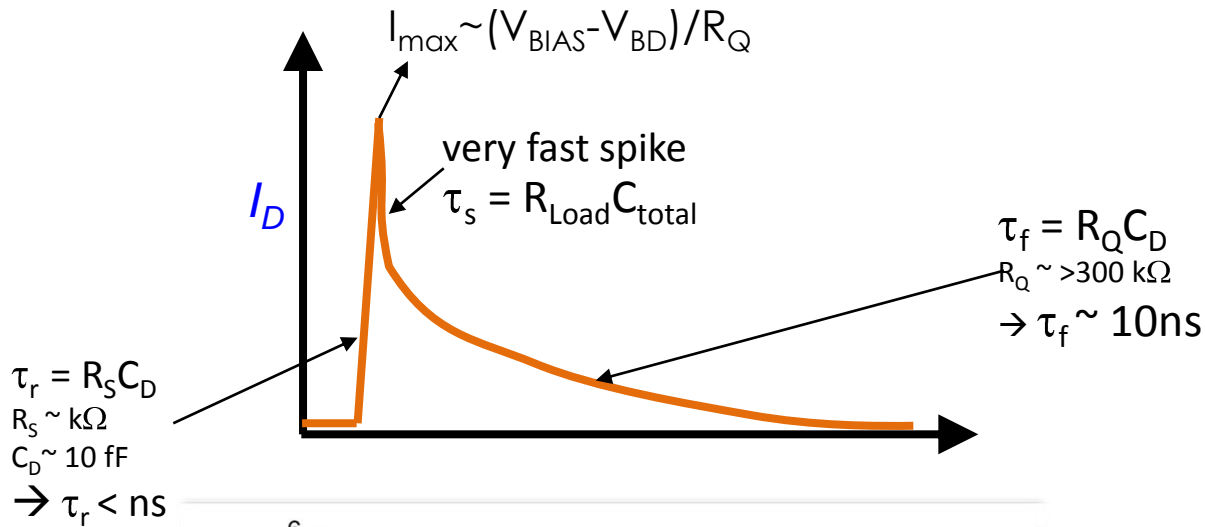
J. Haba, RICH2007



J. Haba, RICH2007

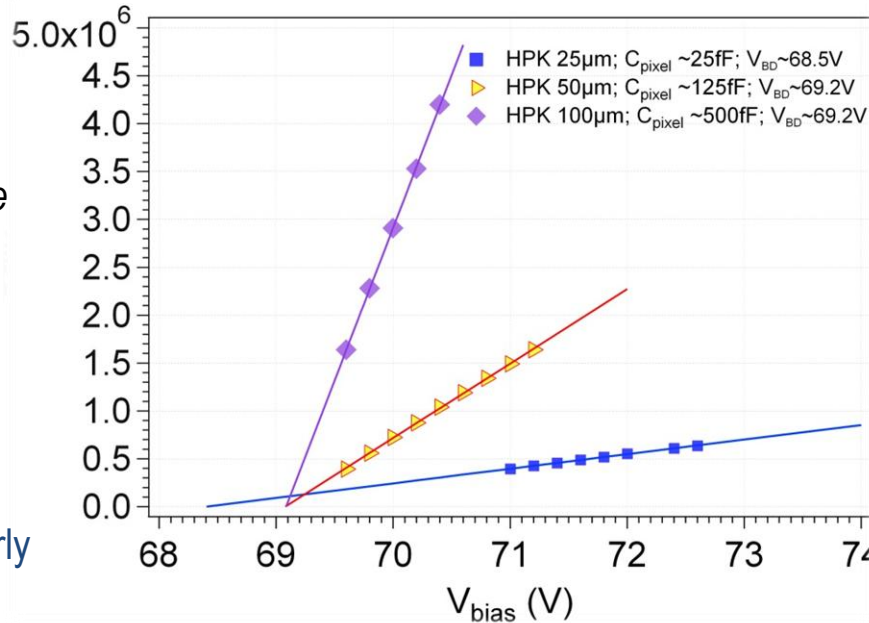


The avalanche formation is **intrinsically very fast**, because **confined to a small space**.



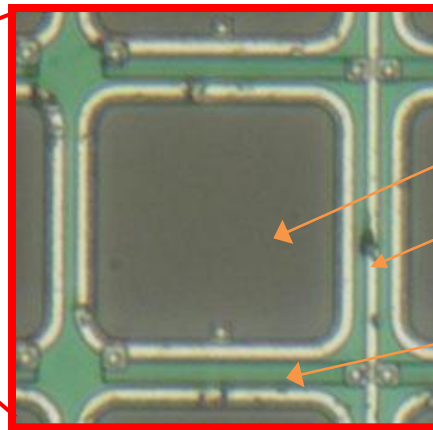
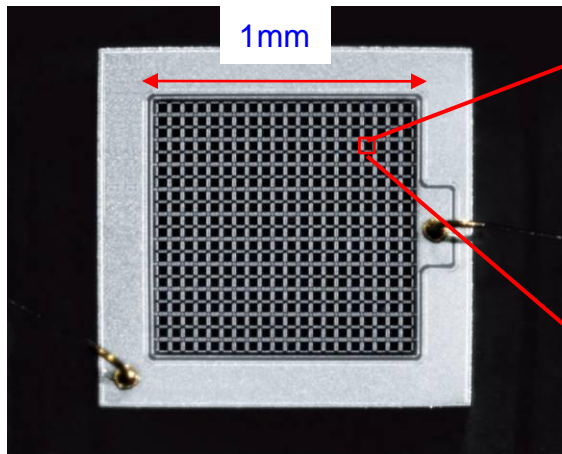
$$\begin{aligned}
 \text{Gain} &= Q / e \\
 &= I_{max} \cdot \tau / e \\
 &= \underbrace{(V_{BIAS} - V_{BD})}_{\Delta V \text{ (overvoltage)}} C_D / e
 \end{aligned}$$

- $G \sim 10^5 - 10^6$  at rel. low bias voltage ( $< 100$  V)
- $dG/dT$  and  $dG/dV$  similarly critical as for APD.



- The slope of the linear fit of  $G(V_{bias})$  is the pixel capacitance
- $C_{pixel}$  and hence  $G$  increase with the pixel geometrical dimensions and the depletion depth.
- $C_{pixel} \sim \epsilon_0 \epsilon_r S / d$
- $C_{pixel} = O(10-100 \text{ fF})$

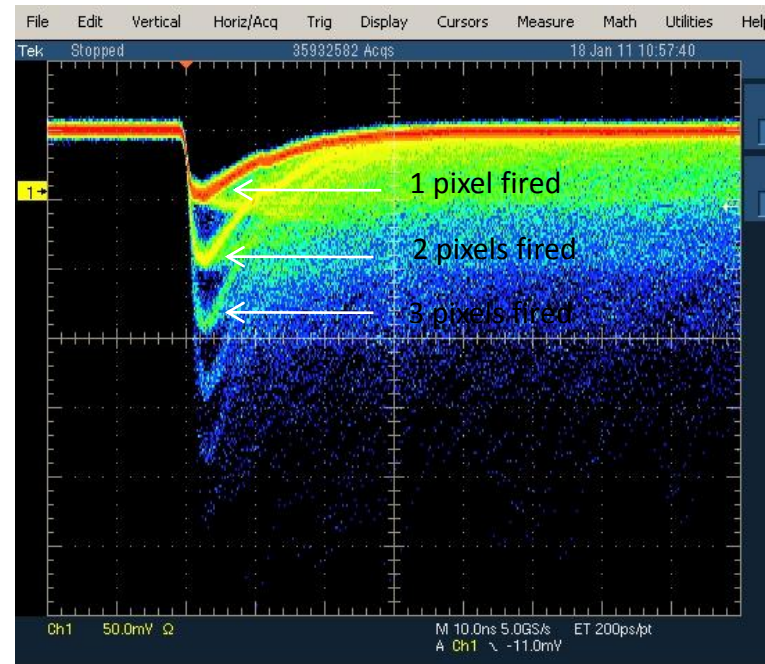
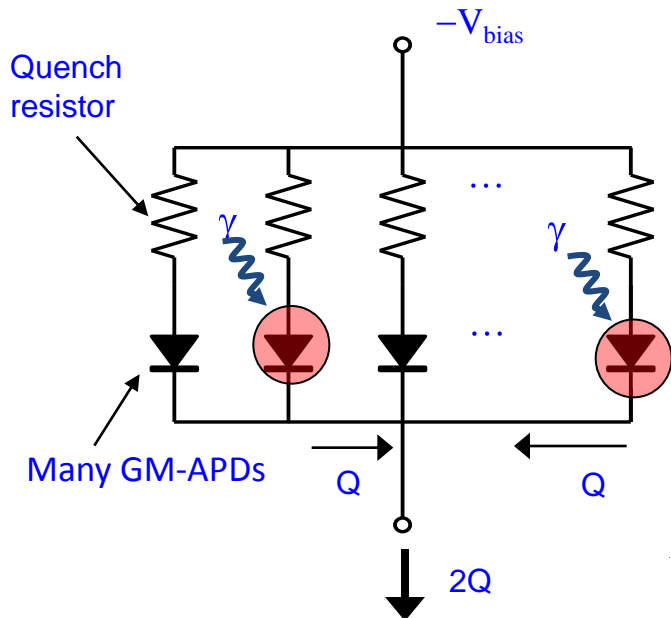
# Multi pixel GM-APD, called SiPM, G-APD, MPPC, ...



100 – several 1000 pix / mm<sup>2</sup>  
 GM-APD  
 Bias bus  
 Quench resistor

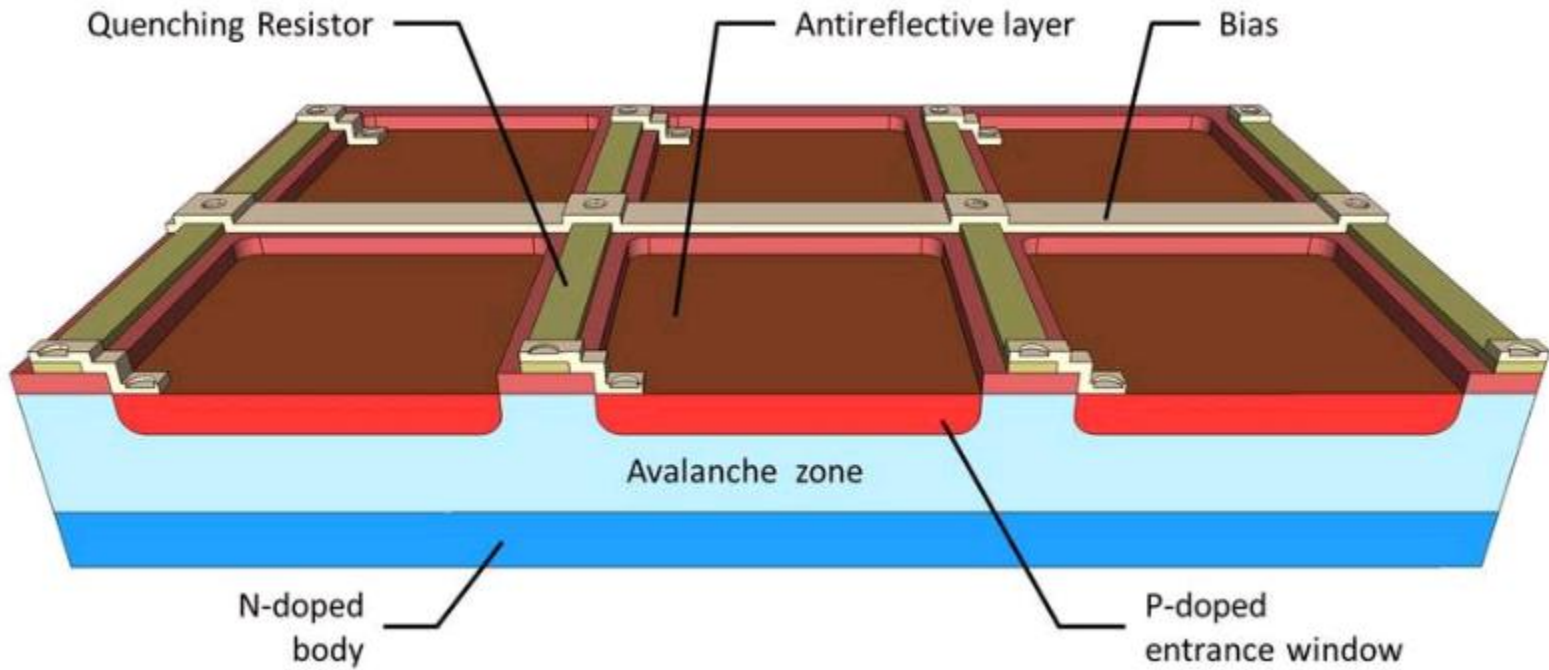
*Only part of surface is photosensitive!*

Sizes up to 6x6 mm<sup>2</sup> now standard.



The operation of many binary devices in parallel leads to a quasi-analog detector with very nice properties (photon counting).

Schematic representation of a blue sensitive pn structure

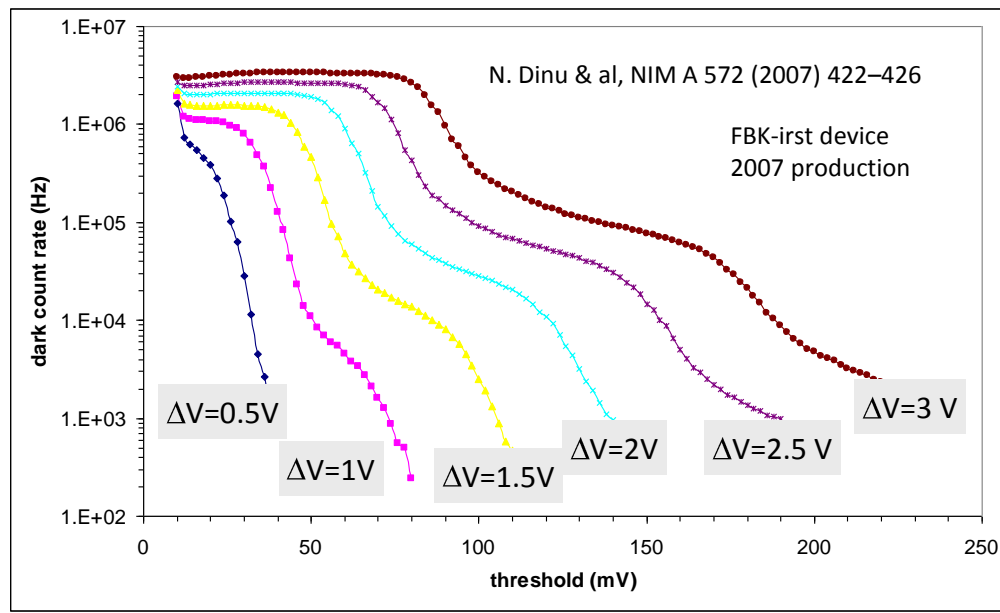
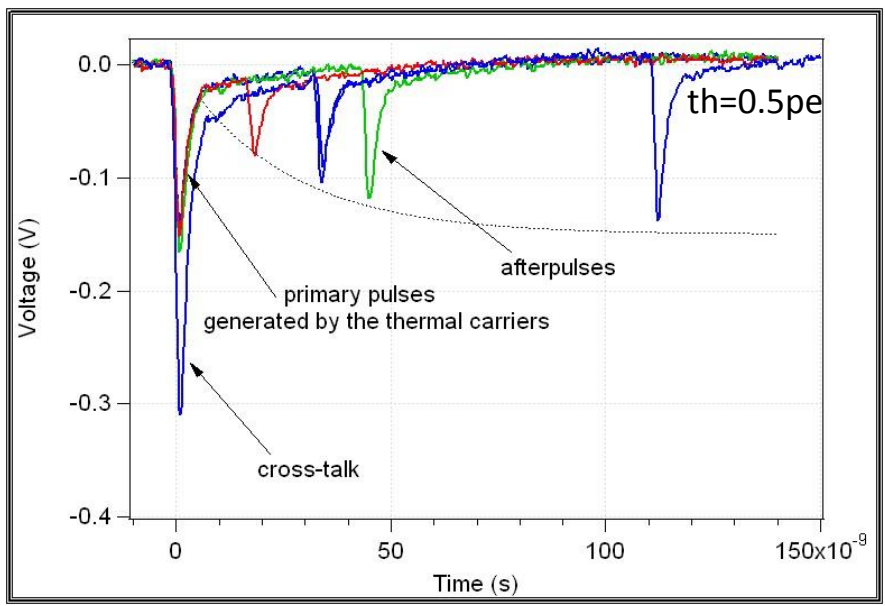
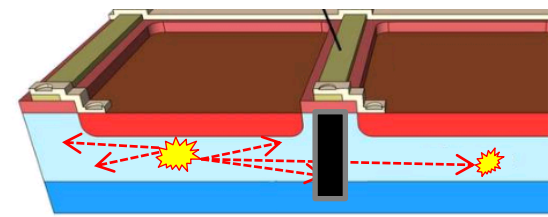


Source: <http://www.ketek.net/products/sipm-technology/microcell-construction/>

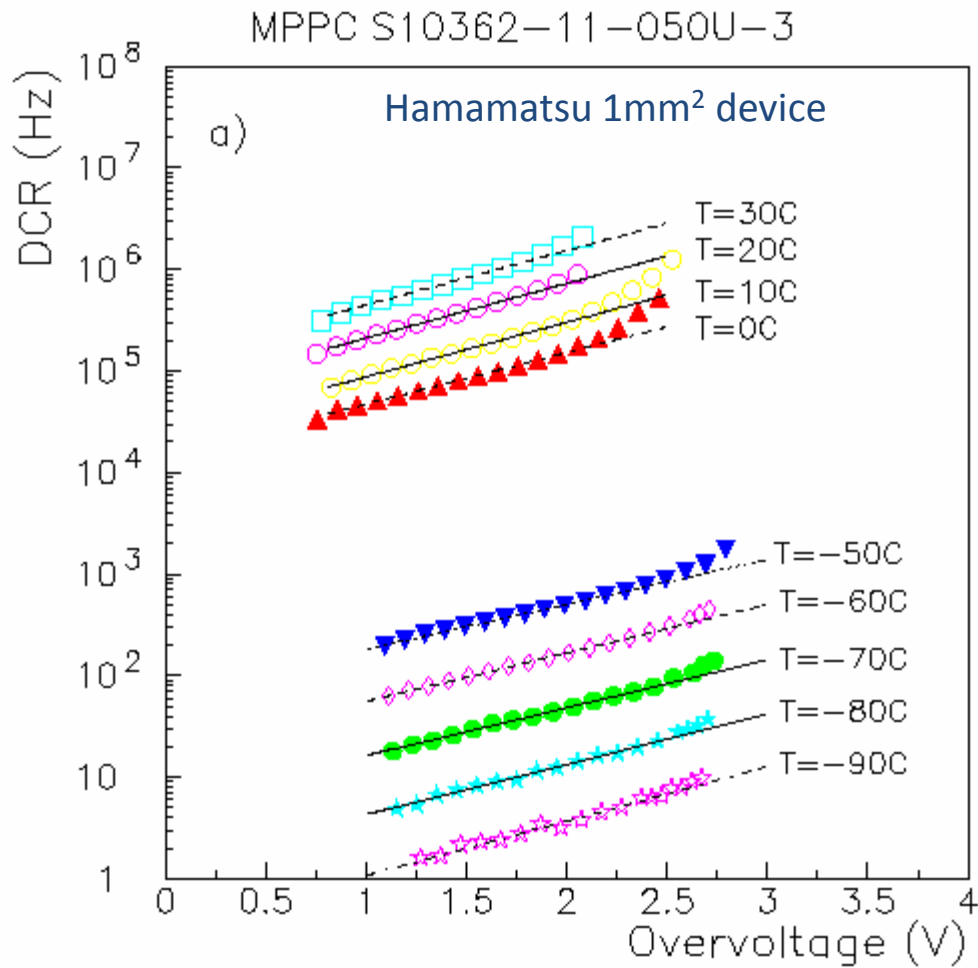
# Dark counts due to ...

- **Thermal/tunneling** : thermal/ tunneling carrier generation in the bulk or in the surface depleted region around the junction
- **After-pulses** : carriers trapped during the avalanche discharging and then released triggering a new avalanche during a period of several 100 ns after the breakdown
- **Optical cross-talk**:  $10^5$  carriers in an avalanche plasma emit on average 3 photons with an energy higher than 1.14 eV (A. Lacaita et al. IEEE TED 1993). These photons can trigger an avalanche in an adjacent  $\mu$ cell.

- Limit gain, increase threshold
- add trenches btw  $\mu$ cells



... and/or cool



Reduce noise by a factor  $\sim 2$  every 8 K

Overvoltage must take into account the T-dependence of  $V_{BD}$

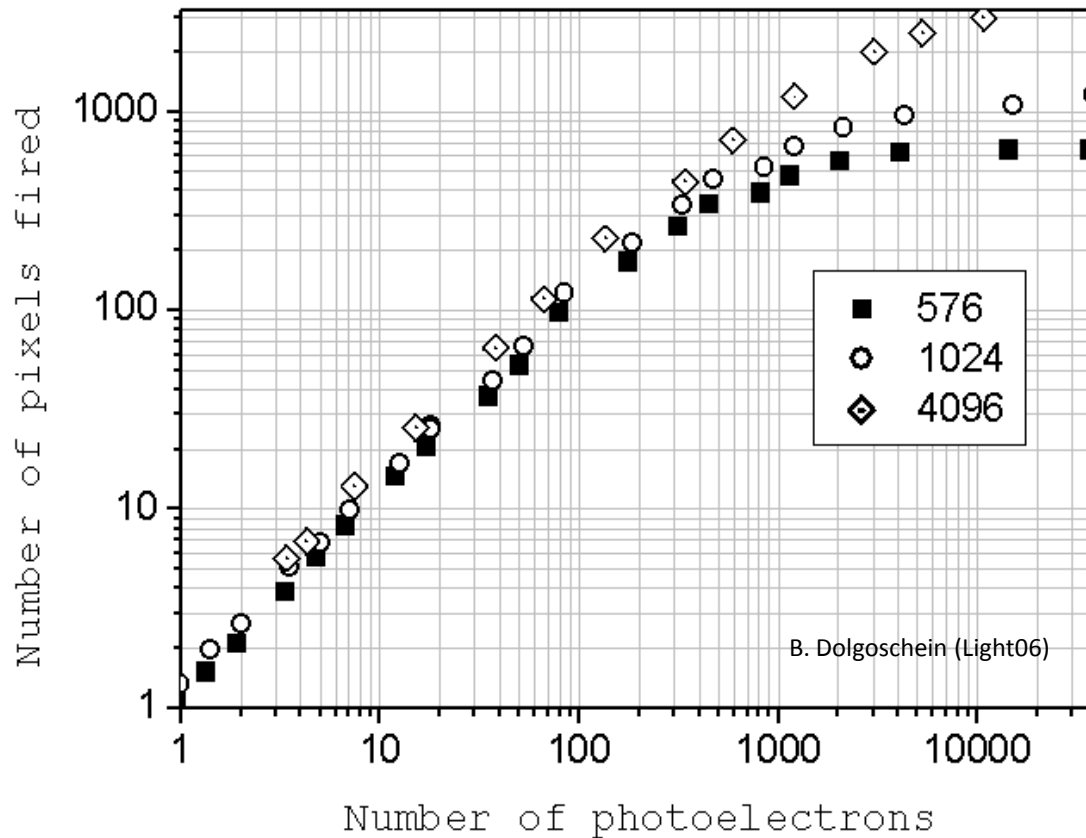
N. Dinu et al., *NSS Conf Record (NSS/MIC), 2010 IEEE*, vol., no., pp.215-219,

## Limited linearity

is simply a consequence of the limited of available pixels. Some pixels get  $\geq 2$  hits.

$$N_{fired} = N_{available} \left( 1 - \exp\left(-\frac{N_{\gamma, true}}{N_{available}}\right) \right)$$

$$\begin{aligned} N_{true}/N_{available} &\sim 0.5 \\ \rightarrow N_{fired}/N_{true} &\sim 0.8 \end{aligned}$$





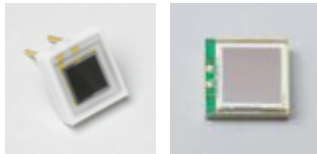
# SiPM designs (just examples)

**Hamamatsu HPK** (<http://jp.hamamatsu.com/>)  
 25x25 $\mu\text{m}^2$ , 50x50 $\mu\text{m}^2$ , 100x100 $\mu\text{m}^2$  pixel size

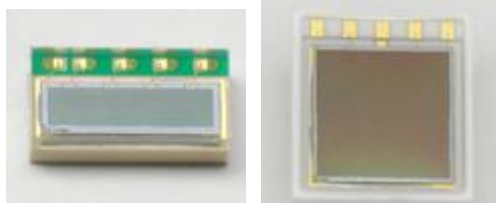
1x1mm<sup>2</sup>



3x3mm<sup>2</sup>



Arrays



1x4mm<sup>2</sup>  
1x4 channels

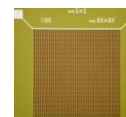
6x6 mm<sup>2</sup>  
2x2 channels

**FBK-IRST**  
 50x50 $\mu\text{m}^2$  pixel size

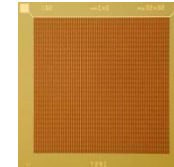
1x1mm<sup>2</sup>



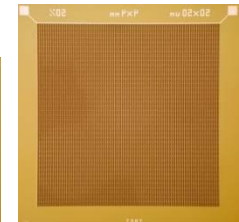
2x2mm<sup>2</sup>



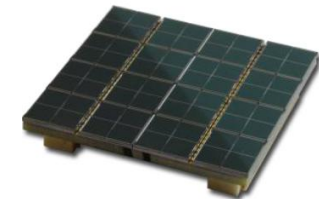
3x3mm<sup>2</sup>



4x4mm<sup>2</sup>



4x4mm<sup>2</sup>  
2x2 channels

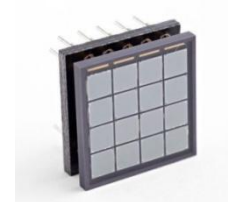


3x3 cm<sup>2</sup>  
8x8 channels

**SensL** (<http://sensl.com/>)  
 20x20 $\mu\text{m}^2$ , 35x35 $\mu\text{m}^2$ , 50x50 $\mu\text{m}^2$ , 100x100 $\mu\text{m}^2$  pixel size



3.16x3.16mm<sup>2</sup>  
4x4 channels



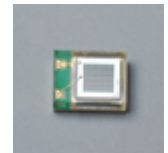
3.16x3.16mm<sup>2</sup>  
4x4 channels



6 x 6 cm<sup>2</sup>  
16x16 channels



	PMT	SiPM
QE (VIS)	0.2-0.4	0.2-0.7
Gain	$10^6$ @ O(kV)	$10^6$ @ O(50V)
Timing	$T_r \sim O(1\text{ns})$ $TTS \sim O(100\text{ ps})$	$T_r \sim O(1\text{ns})$ $TTS O(100\text{ ps})$
Dynamic range	$O(10^6)$	$O(10^3)$
ENF	1.1-1.5	$\sim 1$
Dark noise rate	$O(\text{kHz}/\text{cm}^2)$	$O(\text{MHz}/\text{mm}^2)$
Single photon sensitivity/ counting	☹/☹	☺/☺
Magnetic field immunity	☹	☺
Robustness & compactness	☹☹	☺☺







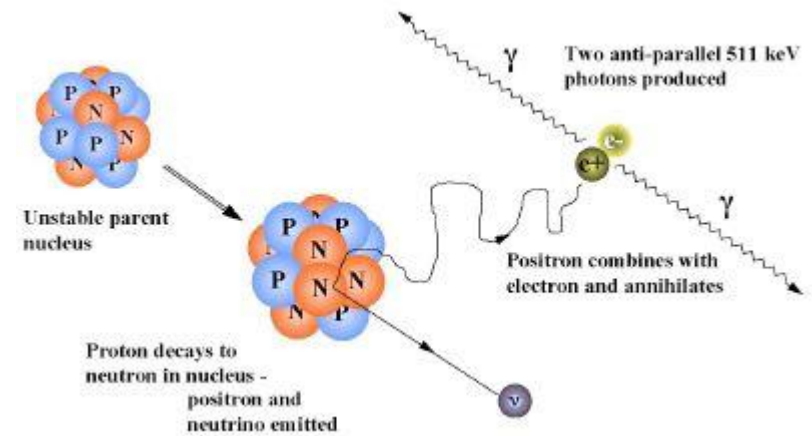
# A new geometrical concept for a PET scanner with SiPM readout.

P. Beltrame et al., The AX-PET demonstrator—Design, construction and characterization, NIM A 654 (2011) 546-559  
P. Beltrame et al., The AX-PET Concept: New Developments And Tomographic Imaging, 2011 IEEE NSS Conf. Rec. MIC22-5

- **Positron Emission** :  $p \rightarrow n + e^+ \nu_e$

$\beta^+$  decay of various radionuclides

Radionuclide	Half life	$E_{\max} e^+$ (MeV)
$^{11}\text{C}$	20.4 min	0,96
$^{15}\text{O}$	122 sec	1,73
$^{18}\text{F}$	109,8 min	0,63
$^{22}\text{Na}$	2.6 years	0,55



- **Positron Annihilation** :  $e^+e^- \rightarrow \gamma\gamma$  ( $E_\gamma = 511 \text{ keV}$ ). 2 photons emitted almost “back-to-back”

The above two processes define the **fundamental limits** to the spatial resolution of PET

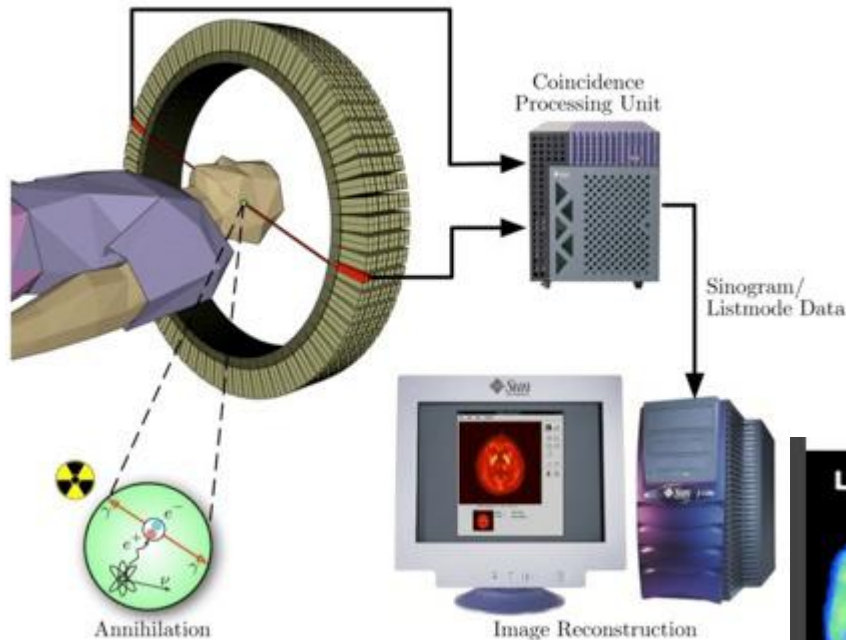
- ▶ **Finite positron range ( $\rho$ )**: annihilation position  $\neq$  emission point,  $\rho$  depends on the energy of the positron (i.e. on the radioisotope).  $\rho \sim \text{mm}$
- ▶ **Non-collinearity of the 2 photons**: residual momentum of the  $e^+e^-$  at the annihilation  $\Rightarrow$  the 2 photons are emitted with a small deviation from  $180^\circ$  ( $\Delta\theta \sim 0.5^\circ$ )  $\Rightarrow$  blurring of the spatial resolution  $R_{\text{FWHM}} \sim 0.0022 \times D$  [mm]

### PET detector principle :

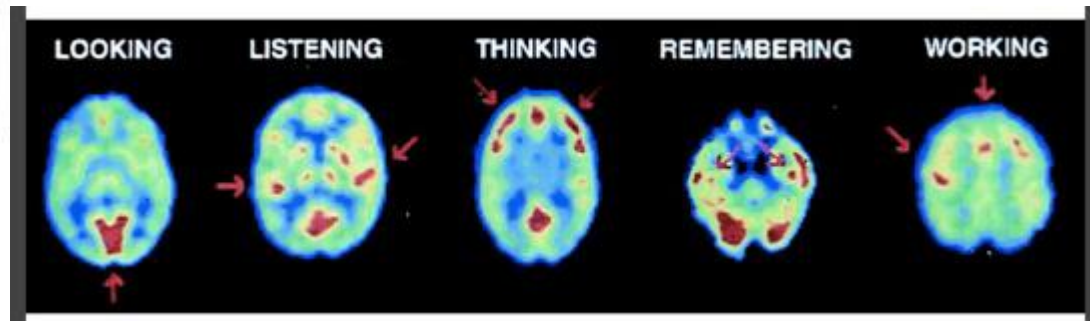
- coincidence of two 511 keV photons define a line of record.
- Take projections under all angle
- (2/3D) Tomographic reconstruct of data

### In practice...

1. Inject the radiotracer into the body (0.1-0.2 mCi per kg body weight)
2. Wait for up-taking period (~h)
3. Acquire data (~0.5 h for full body)
4. Feed the data into the reconstruction algorithms
5. (2/3D) image of the activity concentration



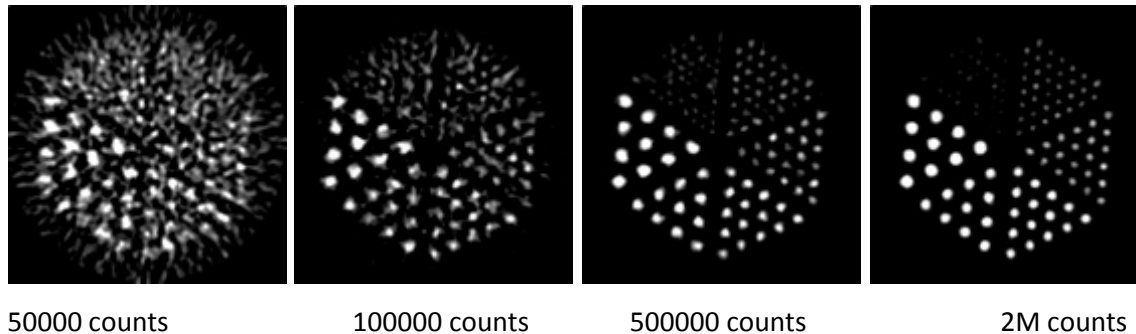
PET is an **“in-vivo” functional imaging** technique  
**It produces** a (quantitative) image of the radio-tracer concentration  
 Use of F-18 labeled glucose → image of the bodies metabolism



## Quality of a PET image depends on

- Detector resolution → crystal size and readout type)
- Counting statistics → efficiency, detector thickness, scintillator material
- Scatter fraction (Compton scattering in body and detector) → energy resolution
- Accidental coincidences and pile-up → coincidence window
- ...

Statistics matters ...



A. Del Guerra, CERN  
Academic Training 2009

## The challenges in PET are today (and since a long time)

- Improve resolution (approach physical limits)
- Improve efficiency
- Reduce background
- Combine it with other imaging modalities, in particular MRI

The Axial PET concept was conceived to simultaneously optimize resolution and efficiency.

- Crystals need to have a minimum thickness  $L$

Efficiency for pair detection  $\epsilon_2 = \left(1 - e^{-L/\lambda_a}\right)^2$

$\lambda_a$  = photon attenuation length of crystal

$L = \lambda_a \rightarrow \epsilon_2 \sim 40\%$ ,  $L = 2 \lambda_a \rightarrow \epsilon_2 \sim 75\%$ , ...

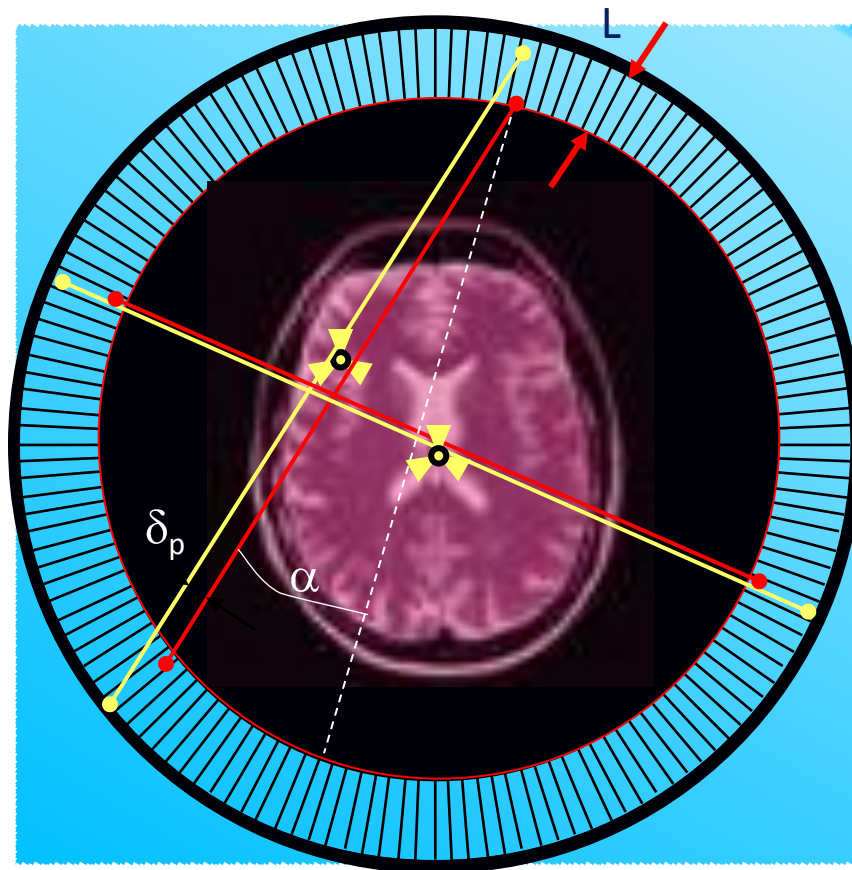
$\lambda_a = 1-2$  cm (depending on material, see below)

- A standard PET does not measure the depth of interaction (DOI) in the crystal.

This introduces a parallax error  $\delta_p = L \cdot \sin \alpha$

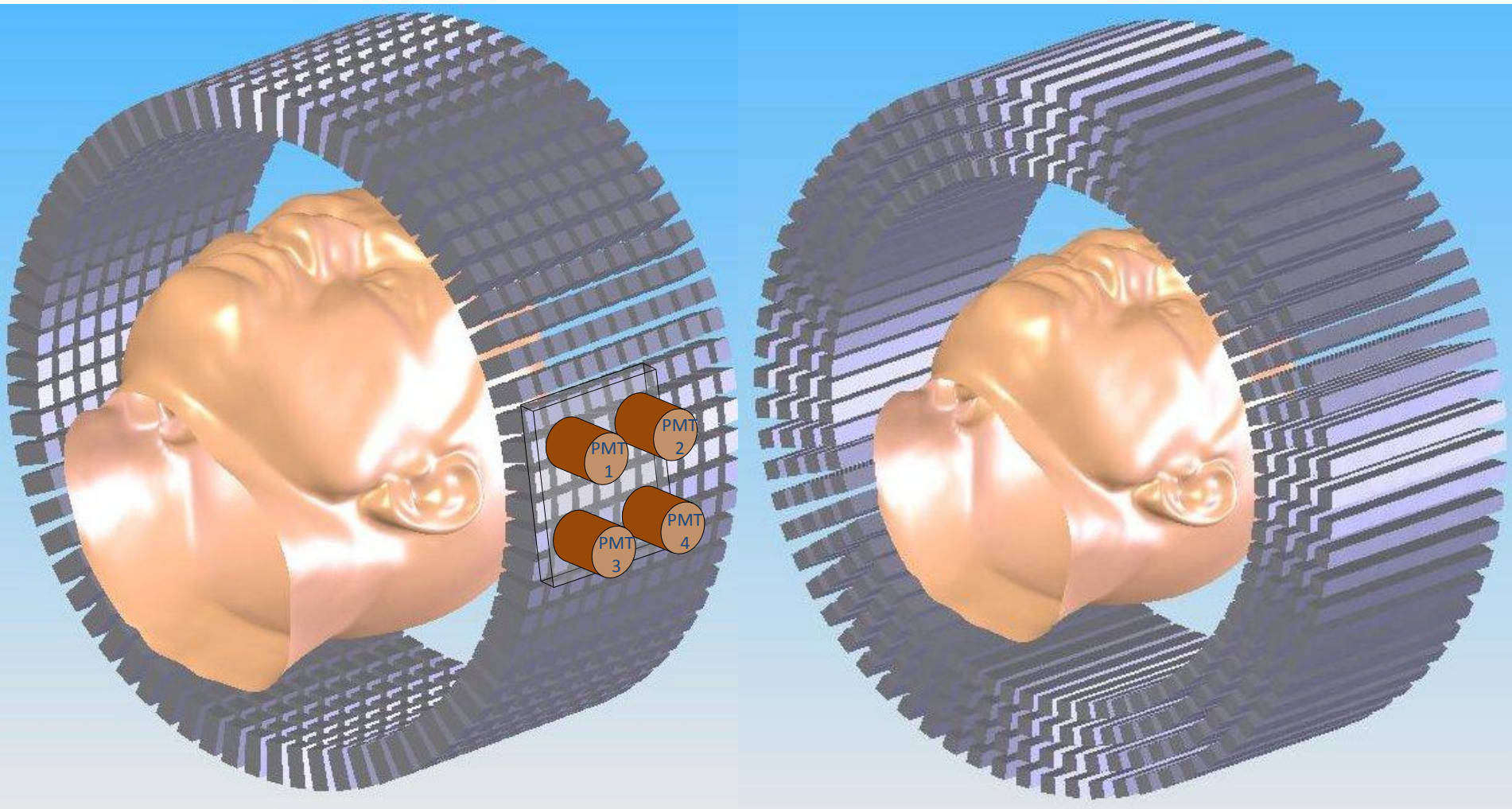
- The resolution in the off-center region degrades significantly

- Solution: reduce  $L$  ( $\rightarrow$  bad  $\epsilon_2$ ) OR measure DOI OR invent a different geometry



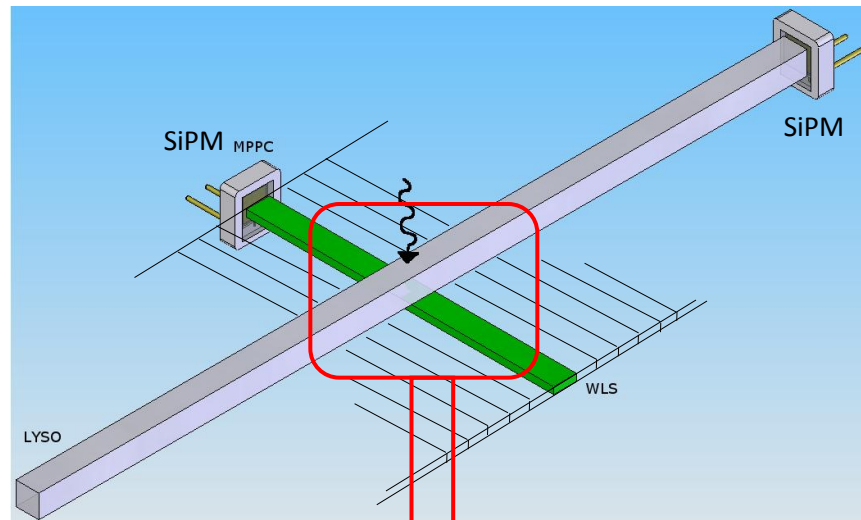
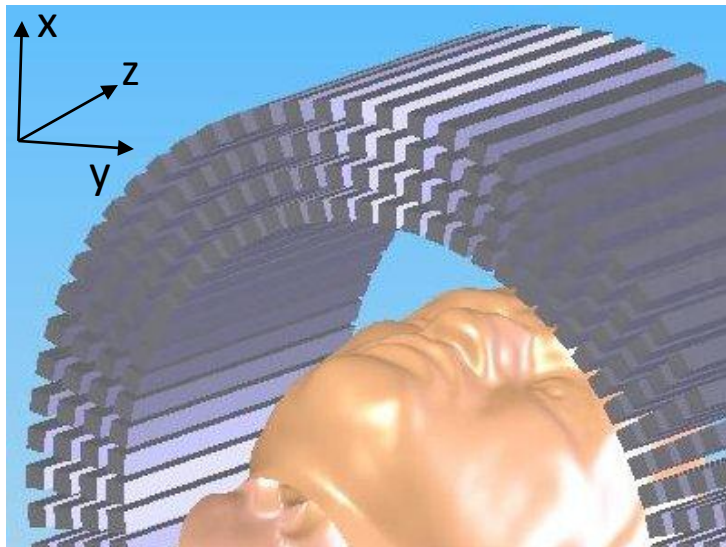
“Standard” radial PET geometry





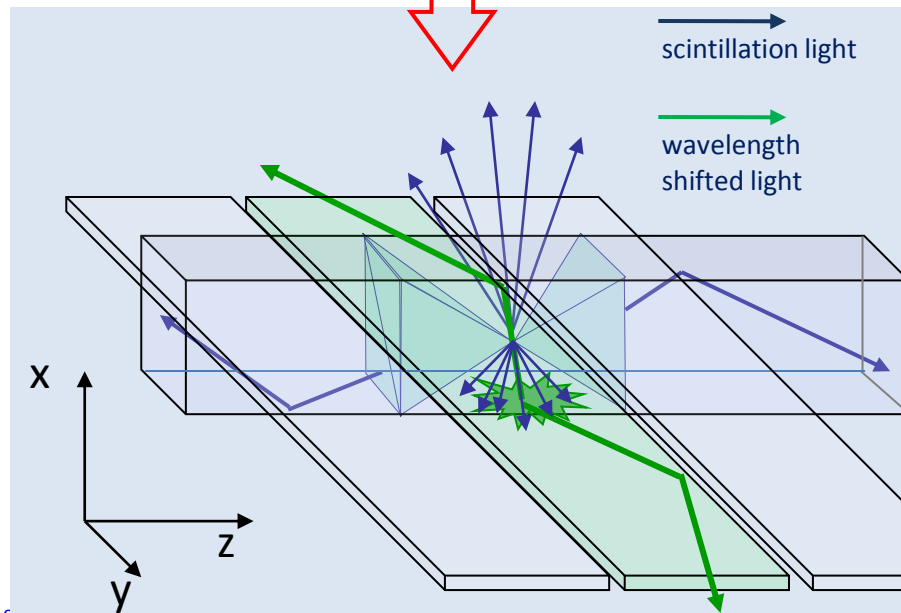
From short radially oriented,  
block readout crystals ...

... to long, axially oriented, individually  
readout crystals



- Individual readout of crystals. Crystal address gives transverse coordinates (x,y)
- Small crystal cross section → **parallax error practically negligible !**
- Additional layers allow to increase sensitivity
- → **Spatial resolution and sensitivity are decoupled and can be optimized independently**

- ❖ **How to read crystals ?**
- ❖ **How to measure axial coordinate ?**

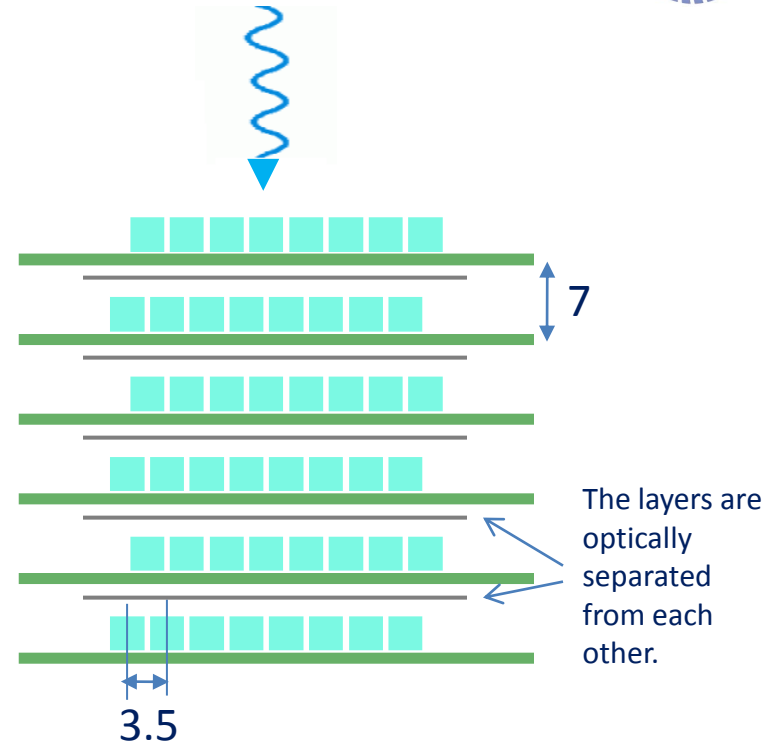
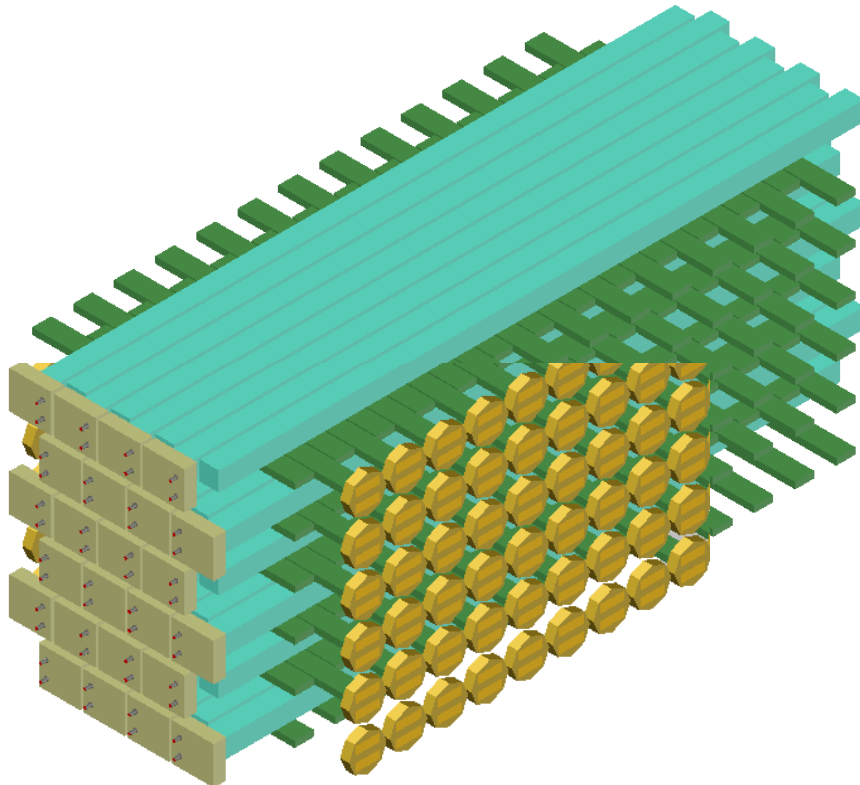


Since 2008, the **AX-PET collaboration** (Bari, Cagliari, CERN, Michigan, Ohio, Oslo, Tampere, Valencia, Zurich, < 10 FTE ) has built and tested a fully operational **PET demonstrator scanner**.



It consists only of **two camera modules** à

- 48 crystals (6 layers x 8 crystals)
- 156 WLS strips (6 layers x 26 strips)



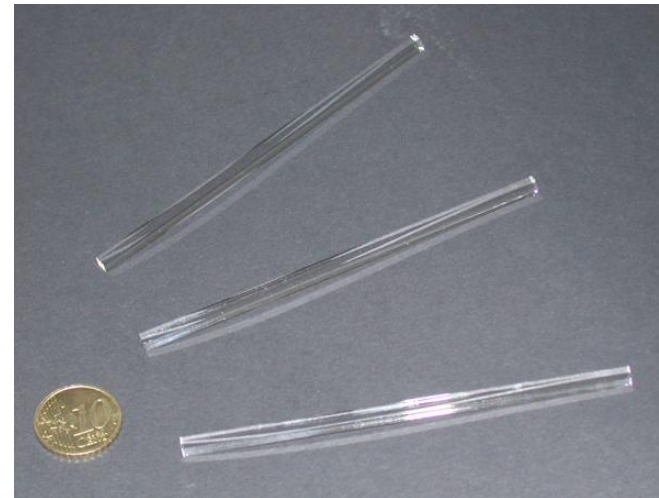
Crystals are staggered by 2 mm. Crystals and WLS strips are read out on alternate sides to allow maximum packing density.



The **scintillator crystals** are Ce doped LYSO ( $\text{Lu}_{1.8}\text{Y}_{0.2}\text{SiO}_5:\text{Ce}$ ) single crystals, fabricated by Saint Gobain and commercialized under the trade name PreLude 420.

The main characteristics are:

Density [g/cm <sup>3</sup> ]	7.1
Attenuation length for 511 keV [cm]	1.2
Wavelength of maximum emission [nm]	420
Refractive index at W.L. of max. emission	1.81
Light yield [photons/keV]	32
Average temperature coefficient [%/K]	-0.28
Decay time [ns]	41
Intrinsic energy resolution [%, FWHM]	~8
Natural radioactivity [Bq/cm <sup>3</sup> ]	~300
Effective optical absorption length [mm]	~420

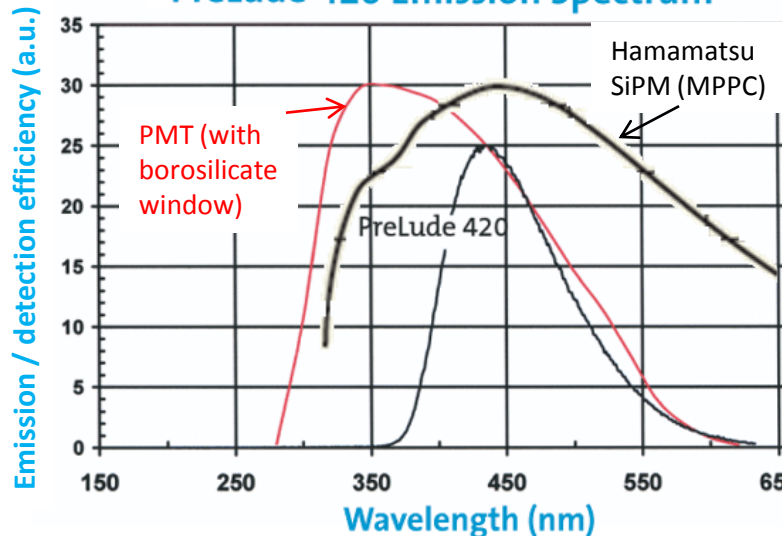


One end is read out, the other end is mirror-coated (evaporated Al-film).

Dimensions: 3 x 3 x 100 mm<sup>3</sup>

This determines the transverse resolution (1 module).  
 Expect:  $\sigma_x = \sigma_y = 3/\text{sqrt}(12) \sim 0.86 \text{ mm}$   
 (2 mm FWHM)

PreLude 420 Emission Spectrum

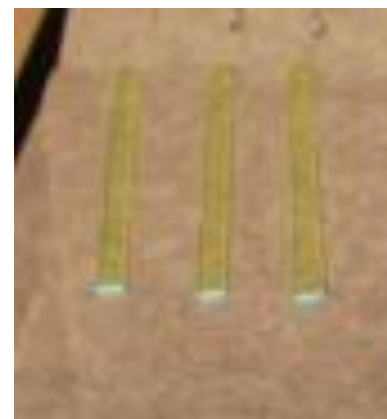
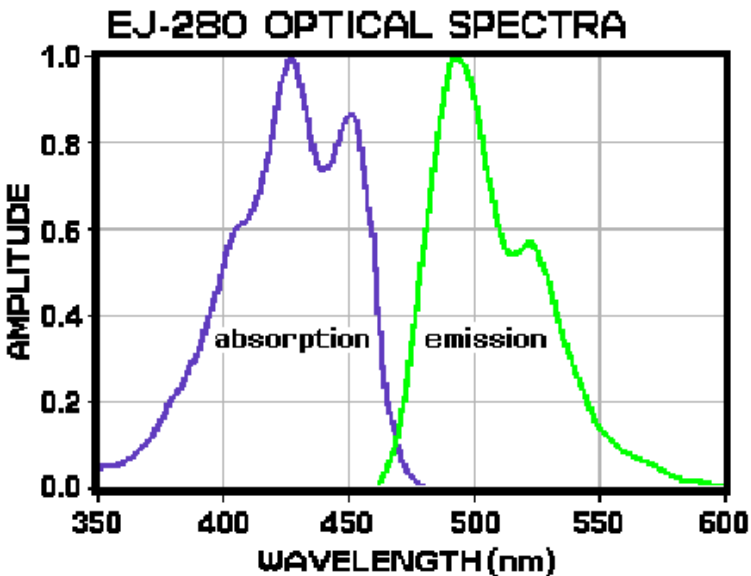
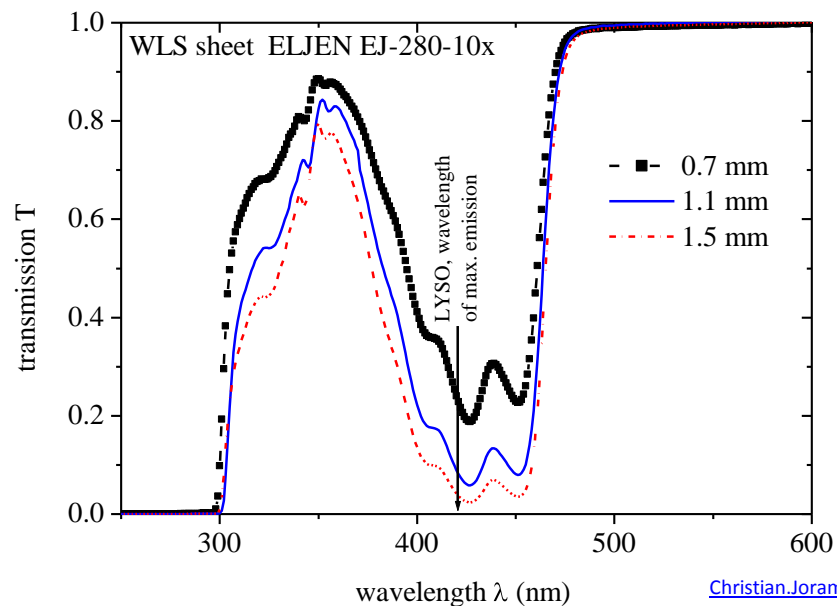


The **WLS strips** are of type EJ-280-10x from Eljen Technologies

- Shift light from blue to green
- Density: 1.023 g/cm<sup>3</sup>
- Absorption length for blue light: 0.4mm (10 x standard concentration)
- Index of reflection: 1.58
- Decay time: 8.5ns
- Size: 0.9x3x40mm<sup>3</sup>

$\sigma_z = 3/\text{sqrt}(12) \sim 0.86 \text{ mm}$   
(2 mm FWHM).

Use COG algorithm on top.



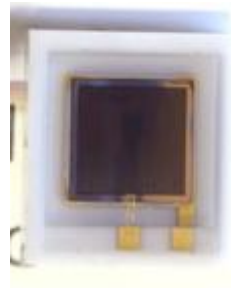
One end is read out, the other end is mirror-coated (evaporated Al-film).

The **photodetectors** are SiPMs of type MPPC from Hamamatsu.

Two different types are used:

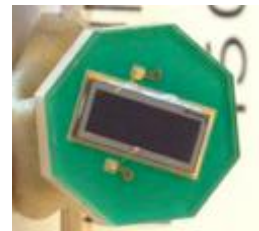
**MPPC S10362-33-050C → Crystal readout**

- sensitive area:  $3 \times 3 \text{ mm}^2$ .
- pixel size:  $50 \times 50 \mu\text{m}^2$  ( $60 \times 60 = 3600$  pixels)
- typical operational voltage: 70 V.
- Typical gain:  $7 \cdot 10^5$ .
- Photon detection efficiency:  $\sim 40 \%$  (400 nm)



**MPPC 3.22x1.19OCTAGON-SMD → WLS readout**

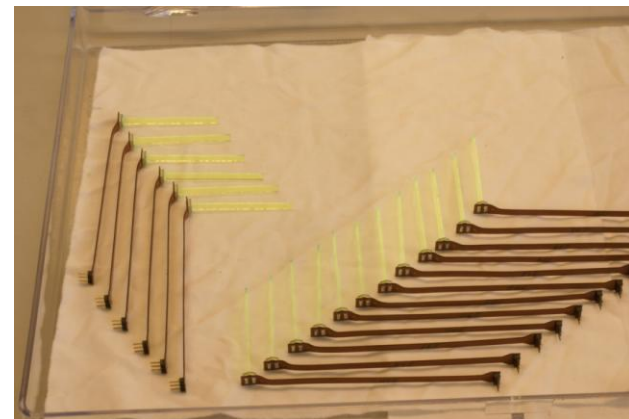
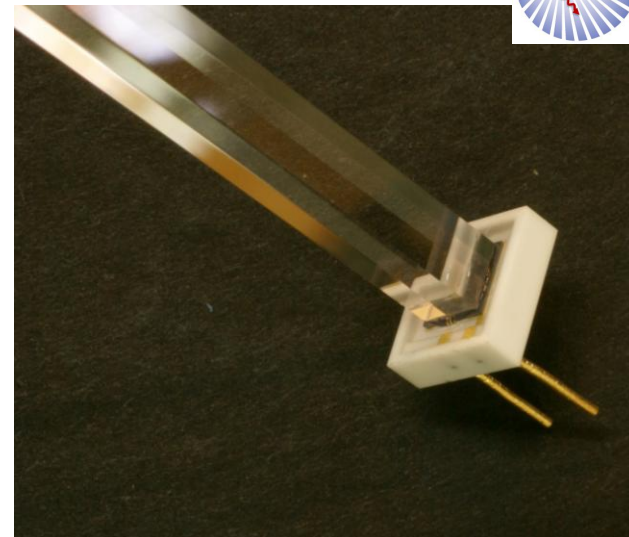
- custom specific device
- sensitive area.  $3.22 \times 1.19 \text{ mm}^2$
- The pixel size is  $70 \times 70 \mu\text{m}^2$ , ( $46 \times 17 = 782$  pixels).



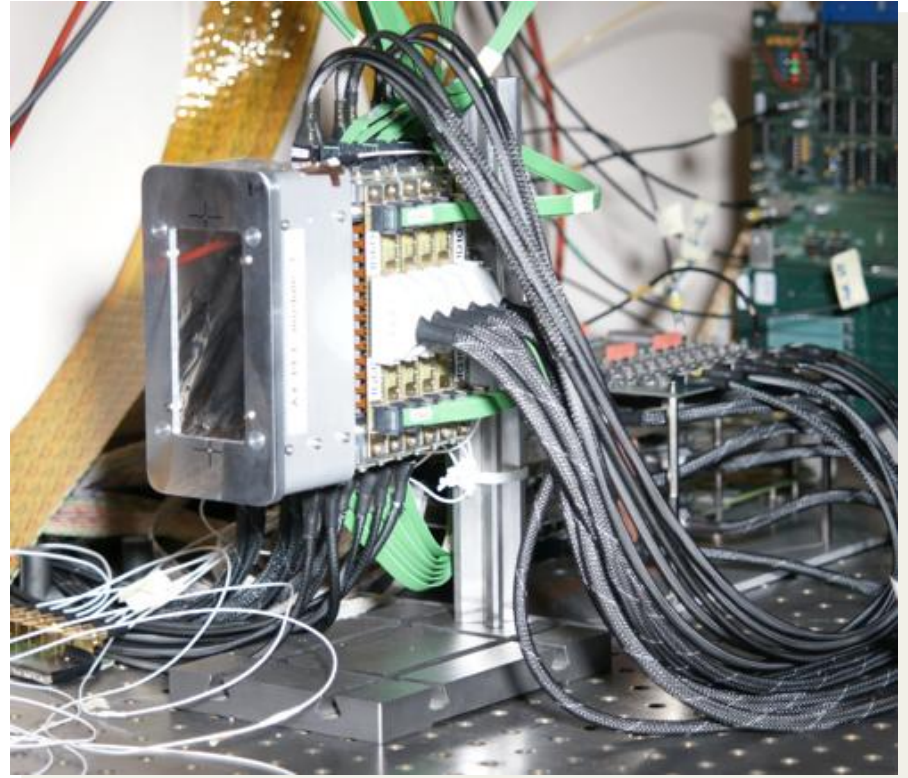
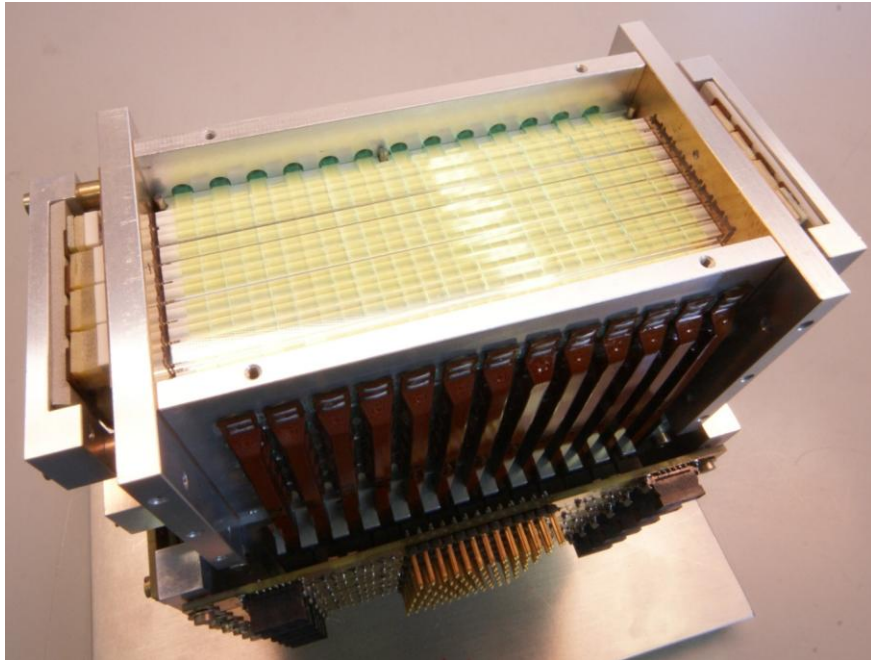
**Some MPPC 'features'**

- Gain is temperature dependent ( $\sim 5\%/^\circ\text{K}$ ) → T monitoring
- Limited dynamic range → saturation effects → correction
- Thermal noise, O(100 kHz) at 1 photon level. → set threshold

The electrical connections to the MPPCs are made via special Kapton cables soldered to the MPPCs.



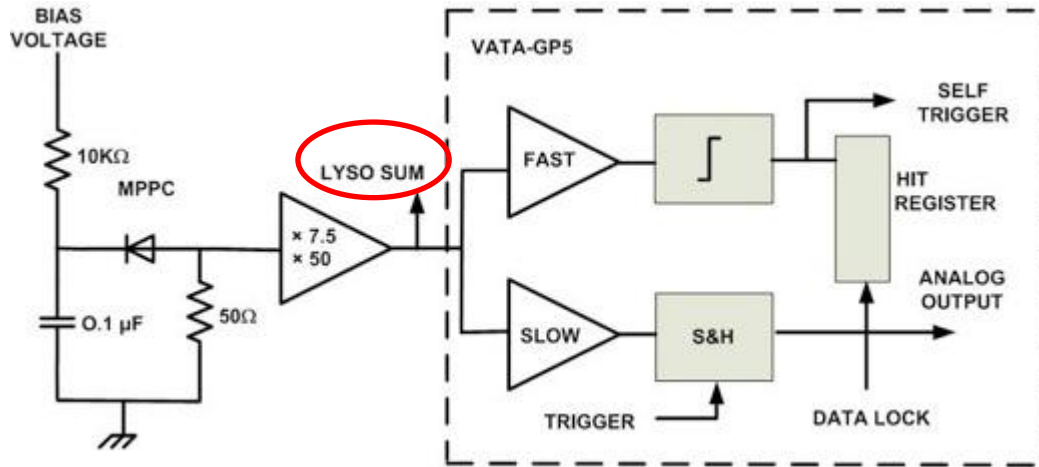
Fully assembled module (48 crystals, 156 WLS stips)  
+ lots of cables: 204 x (bias + signal out)



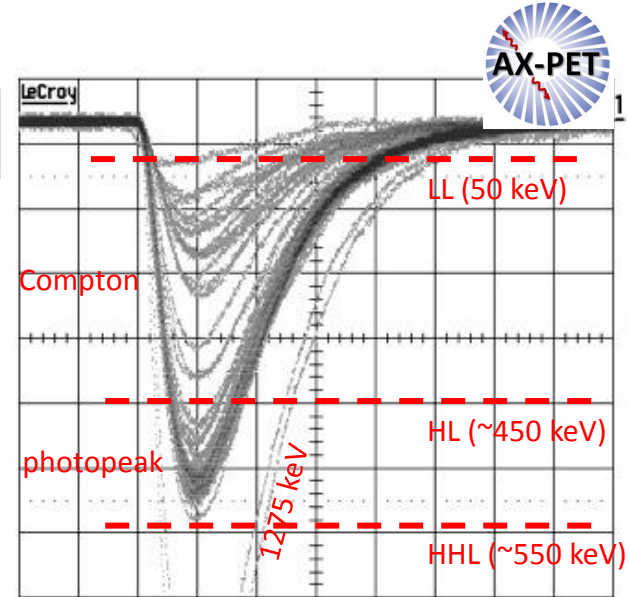


Fully analog, but relatively slow ...

1 channel.

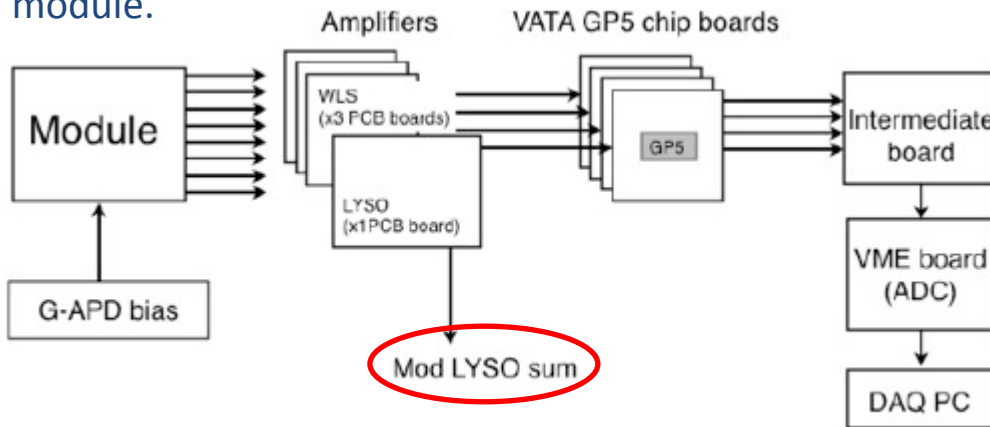


26-Nov-09  
18:34:16  
50 ns  
50 mV  
-59 steps

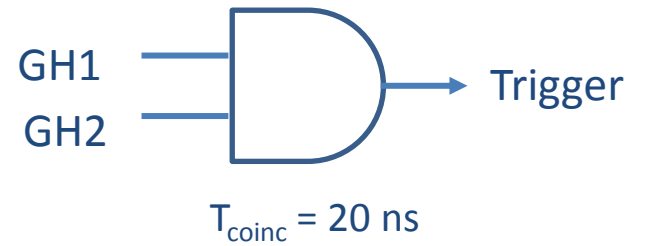


Mod 1: Energy sum of all LYSO crystal of 1 module. <sup>22</sup>Na source

1 module.

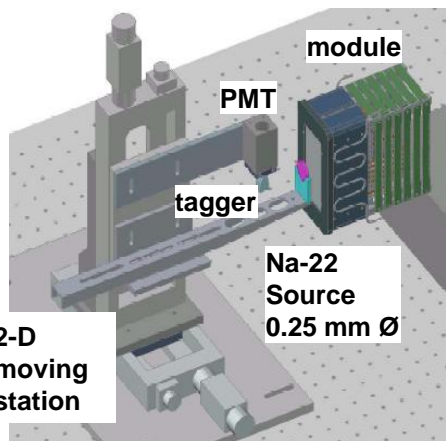


$$\text{Good hit in 1 module} = \text{LL} \times \text{HL} \times \text{HHL}$$

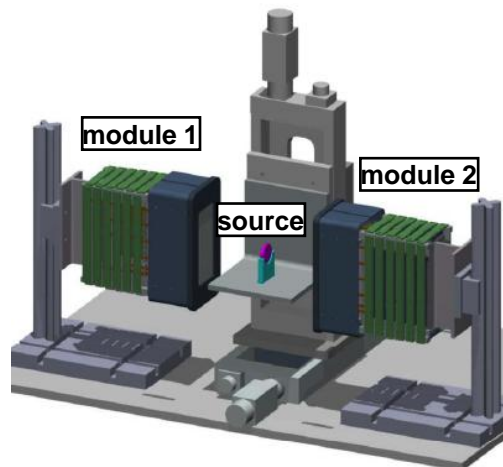


Max Readout rate ~ 20 kHz

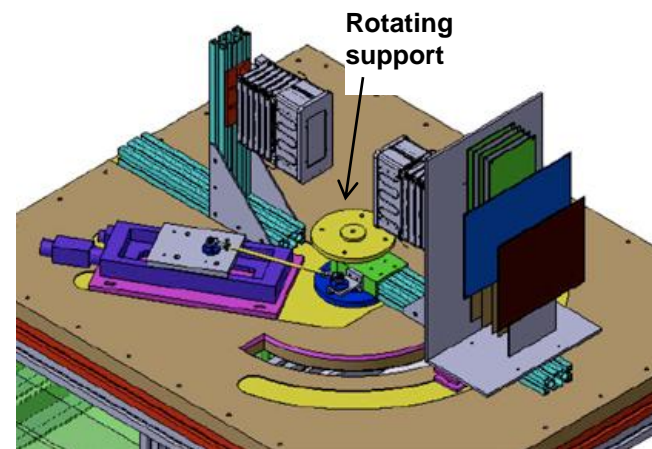
## I. Single module characterization



## II. Coincidence of 2 modules

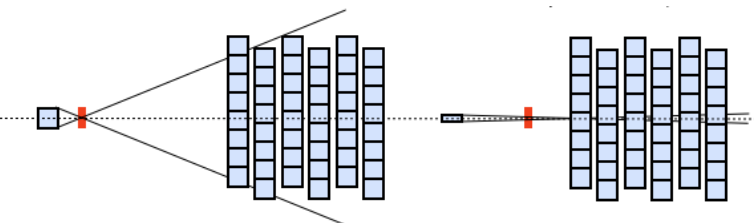


## III. Gantry for tomographic measurements



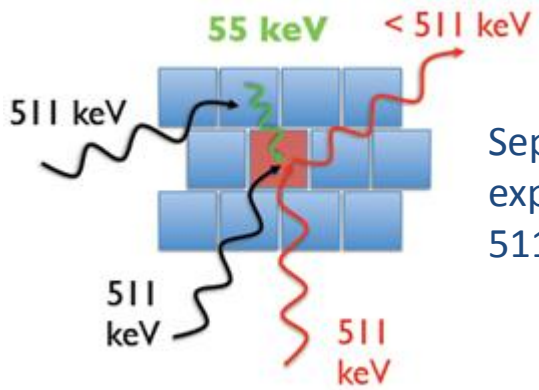
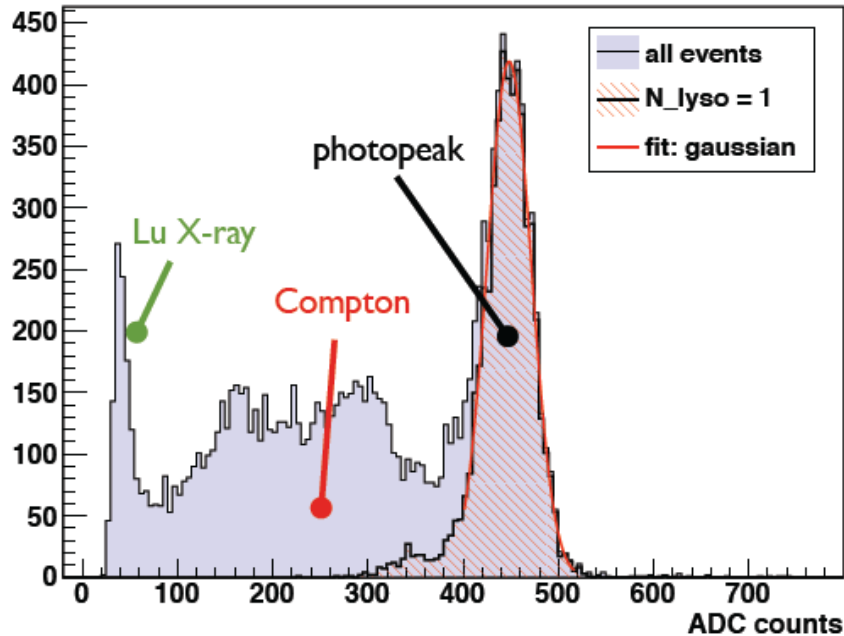
- Module in coincidence with a tagging scintillator
- Use of different tagging crystals

- Distance between modules = 15 cm



## Typical charge spectrum from 1 LYSO crystal

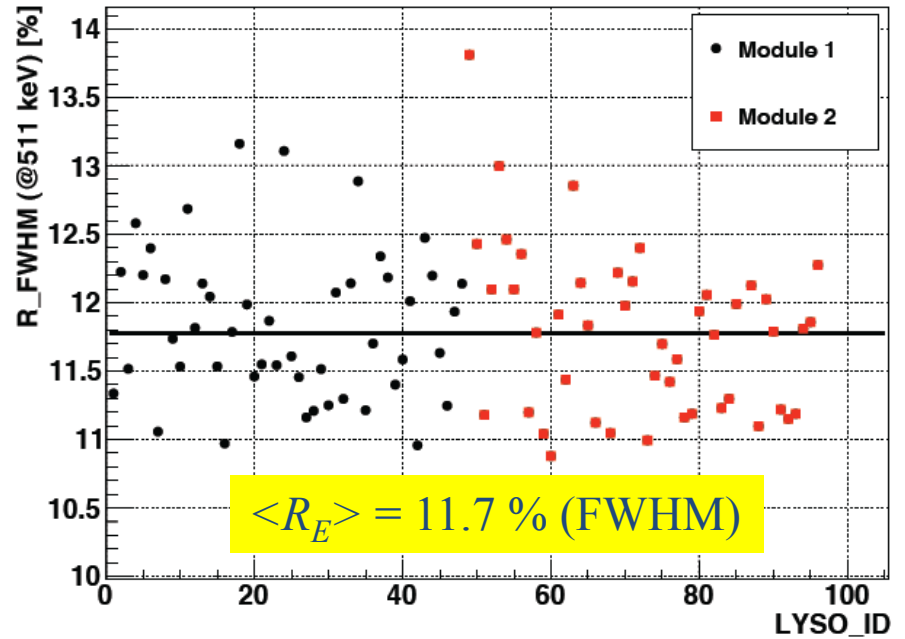
LYSO No. 21 - <sup>22</sup>Na coinc. trigger



Separate calibration experiment:  
511 keV ~ 1100 pe in SiPM

## Energy resolution of all 96 LYSO crystals

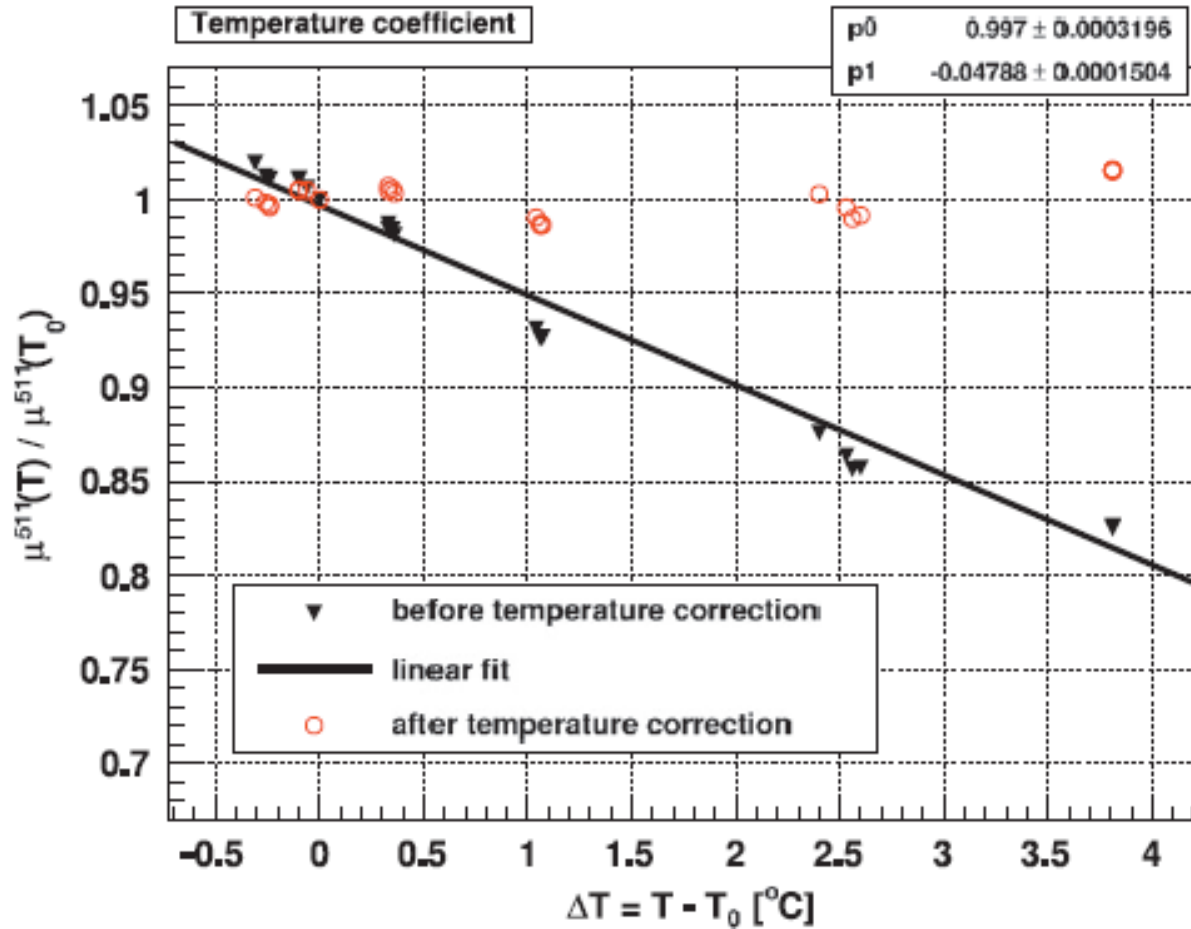
Energy resolution



In the ideal case:  $R_E = R_E^{intr.} \oplus \frac{1}{2.35 \cdot \sqrt{N_{pe}}}$

→ Expect  $R_E \sim 10.7\%$

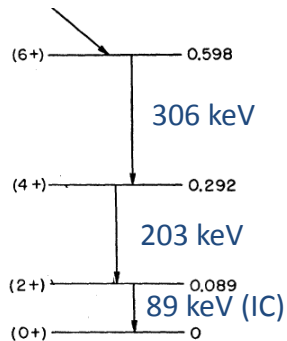
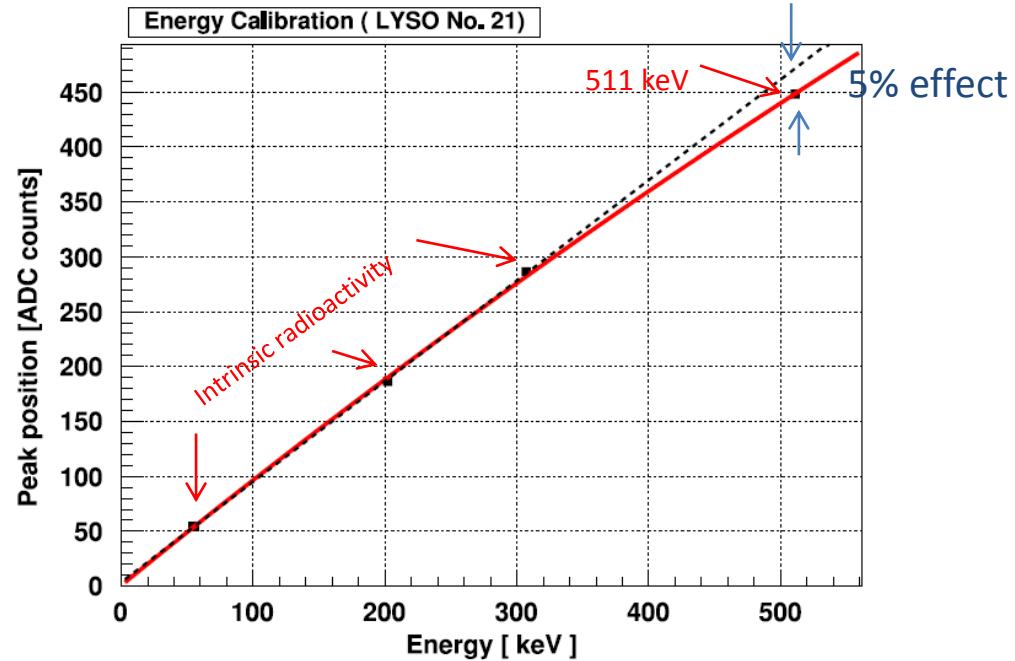
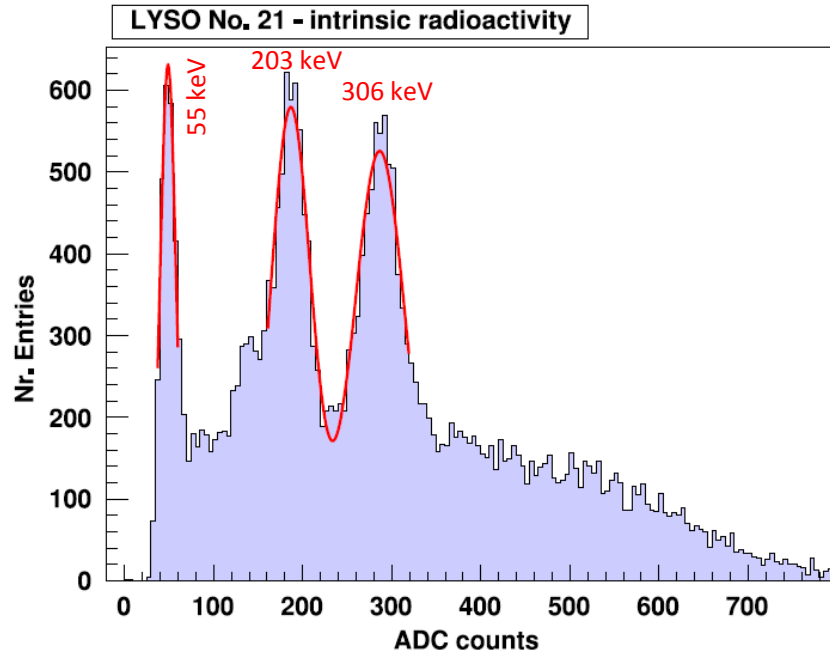
First correct for possible temperature changes  
 SiPM gain drops by ~5% per degree K.





Lutetium in LYSO is radioactive.  
 ~ 250 Bq per crystal.

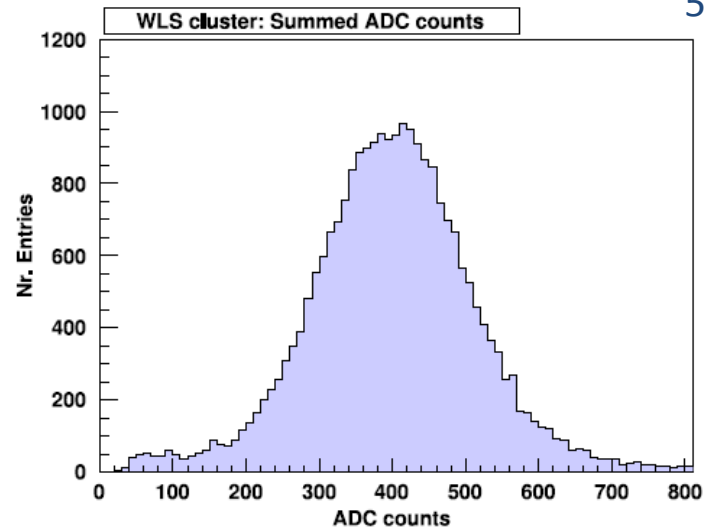
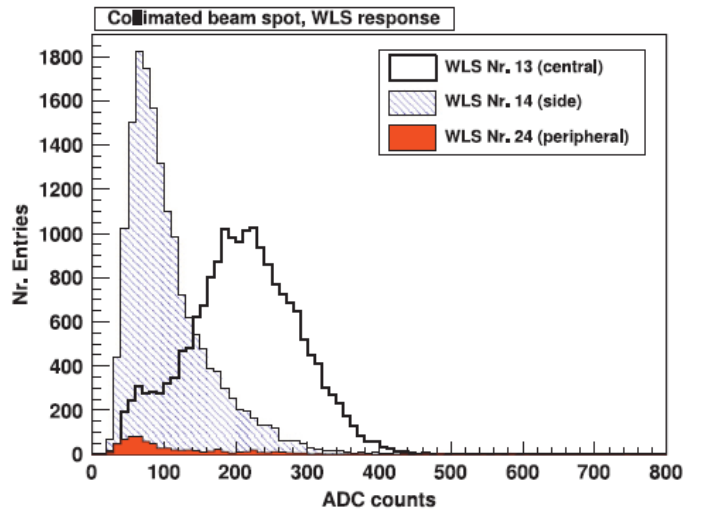
Small non-linearity due to limited pixel number of SiPM (3600)



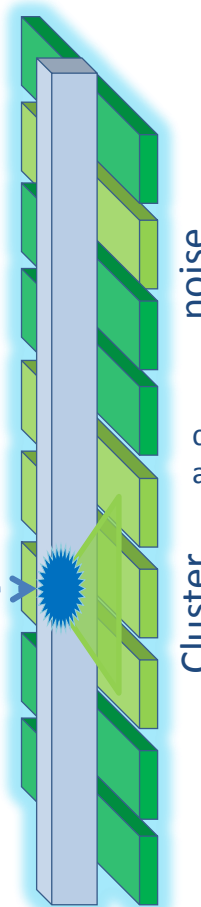
The formula would predict a 15% effect

$$N_{fired} = N_{available} \left( 1 - \exp\left(-\frac{N_{\gamma, true}}{N_{available}}\right) \right)$$

LYSO photons arrive over ~100 ns. Some hit pixels will have recovered when the 2<sup>nd</sup> hit arrives.

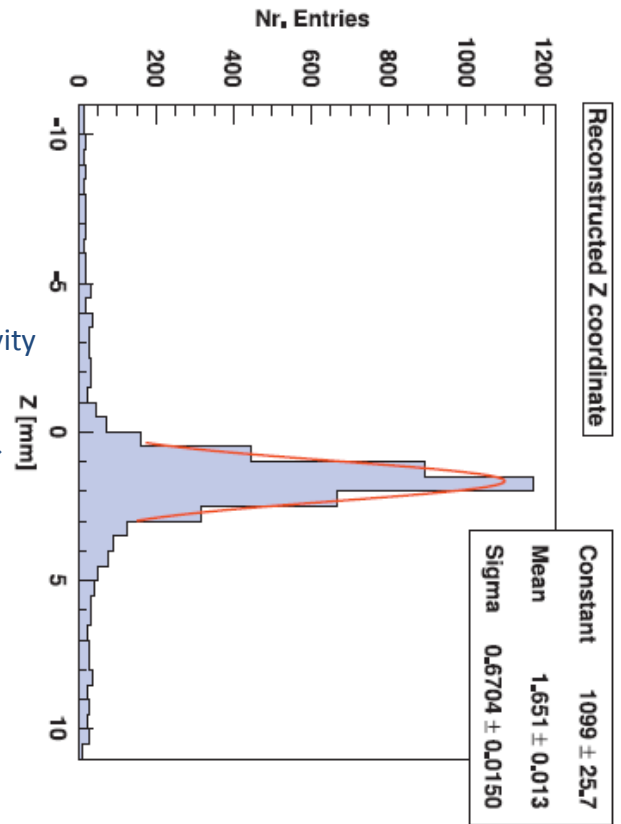


511 keV



noise

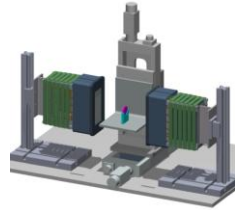
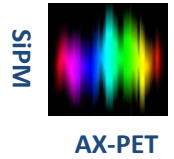
centre-of-gravity algorithm



$\sigma_z \sim 0.75$  mm  
(average over whole module, after correction for  $e^+$  annihilation physics).

Calibration (separate set-up):  
511 keV → 100 pe in WLS cluster

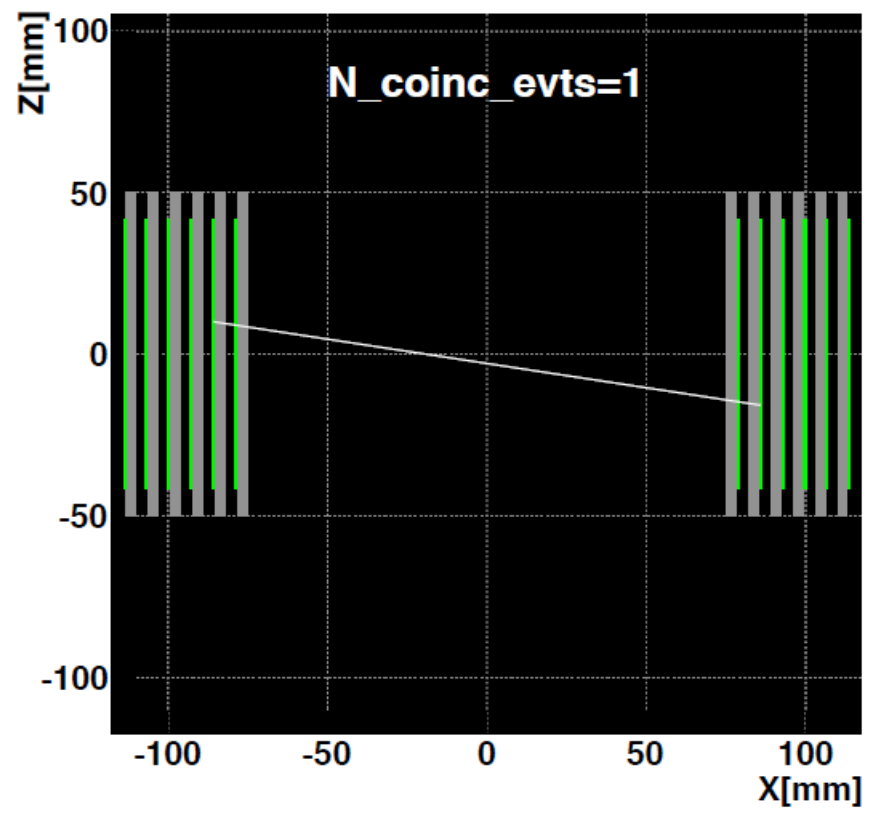
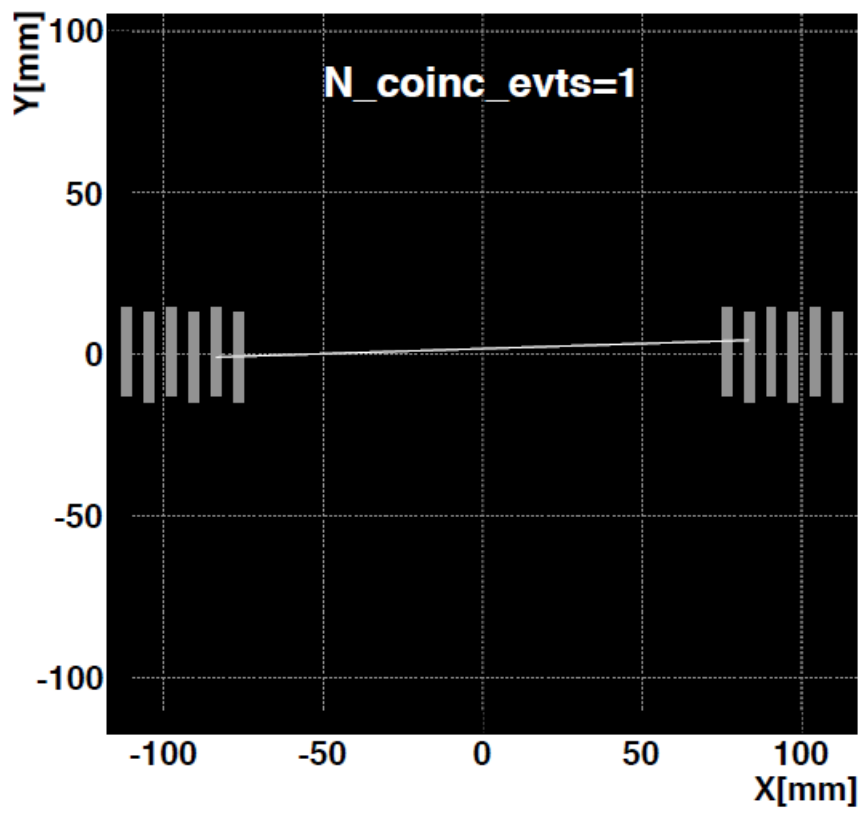
# First coincidence measurements



- Point-like  $^{22}\text{Na}$  source
- Photoelectric events only (1 hit crystal per module)
- Draw “LOR” (pure geometrical, no tomographic reconstruction)

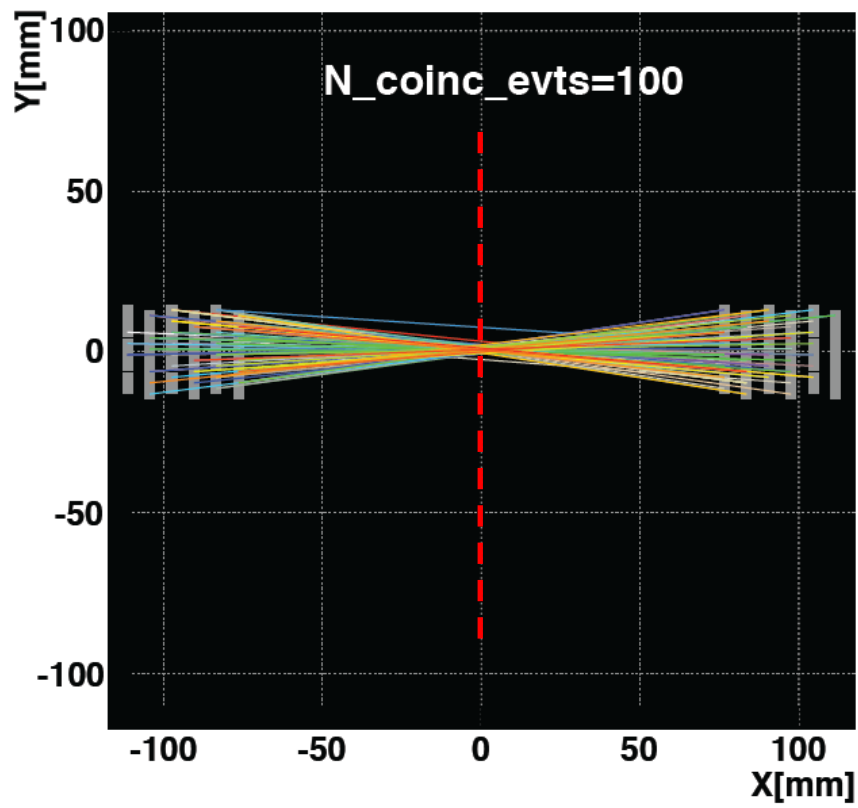
TOP View -  $d(\text{Mod1}, \text{Mod2}) = 150 \text{ mm}$

SIDE View -  $d(\text{Mod1}, \text{Mod2}) = 150 \text{ mm}$

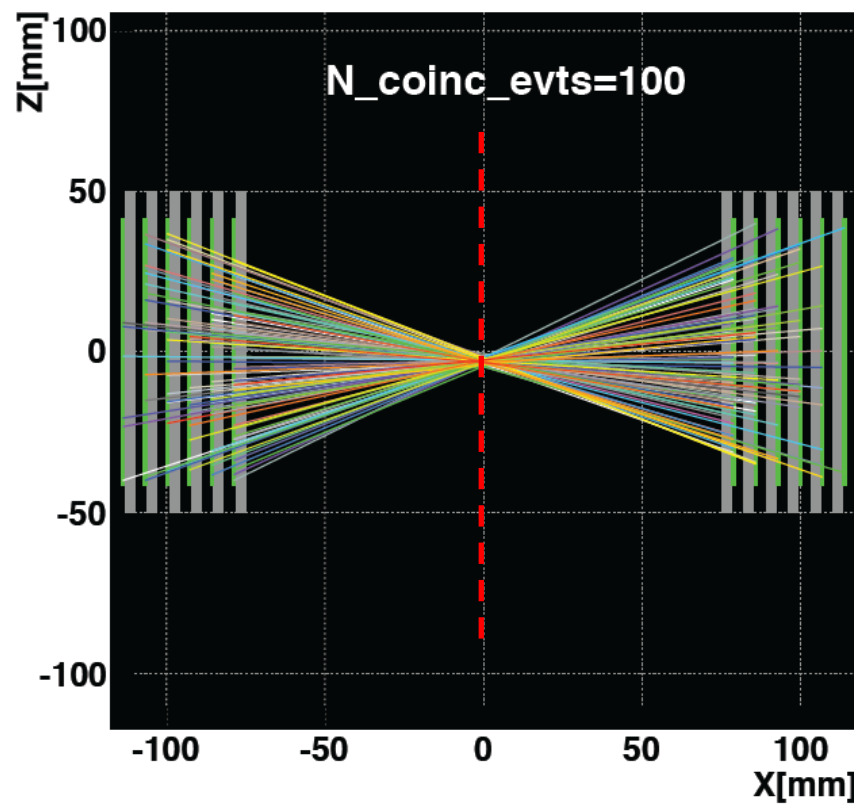




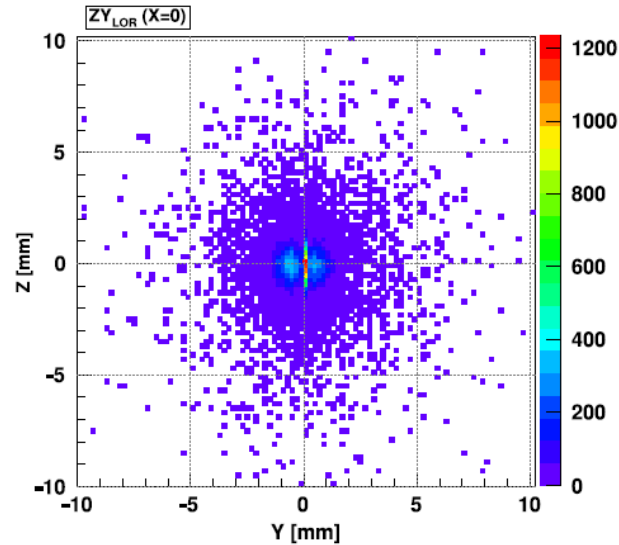
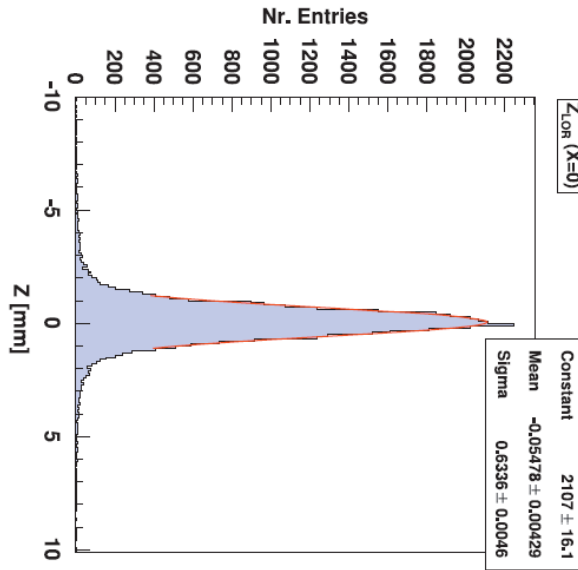
TOP View -  $d(\text{Mod1}, \text{Mod2}) = 150 \text{ mm}$



SIDE View -  $d(\text{Mod1}, \text{Mod2}) = 150 \text{ mm}$



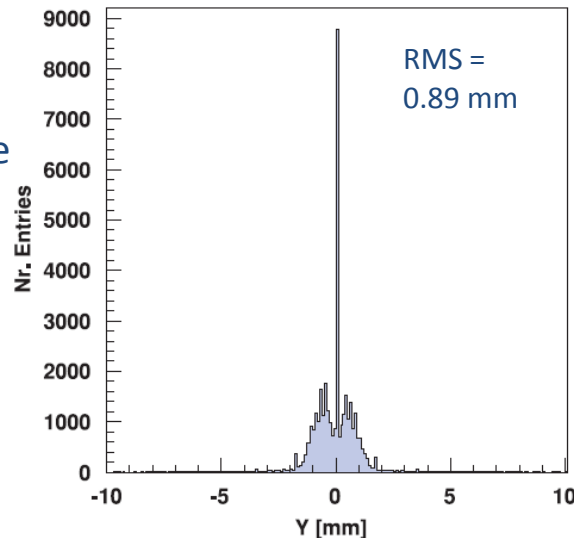
Look at the YZ distribution at x=0 (“confocal reconstruction”)



$\sigma_z = 0.63$  mm (coincidence) is compatible with the single detector resolution.

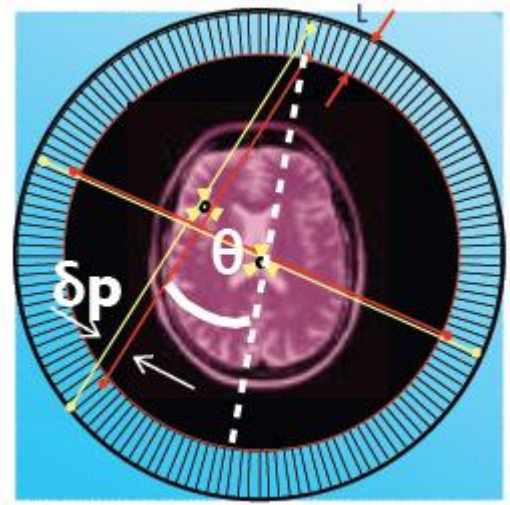
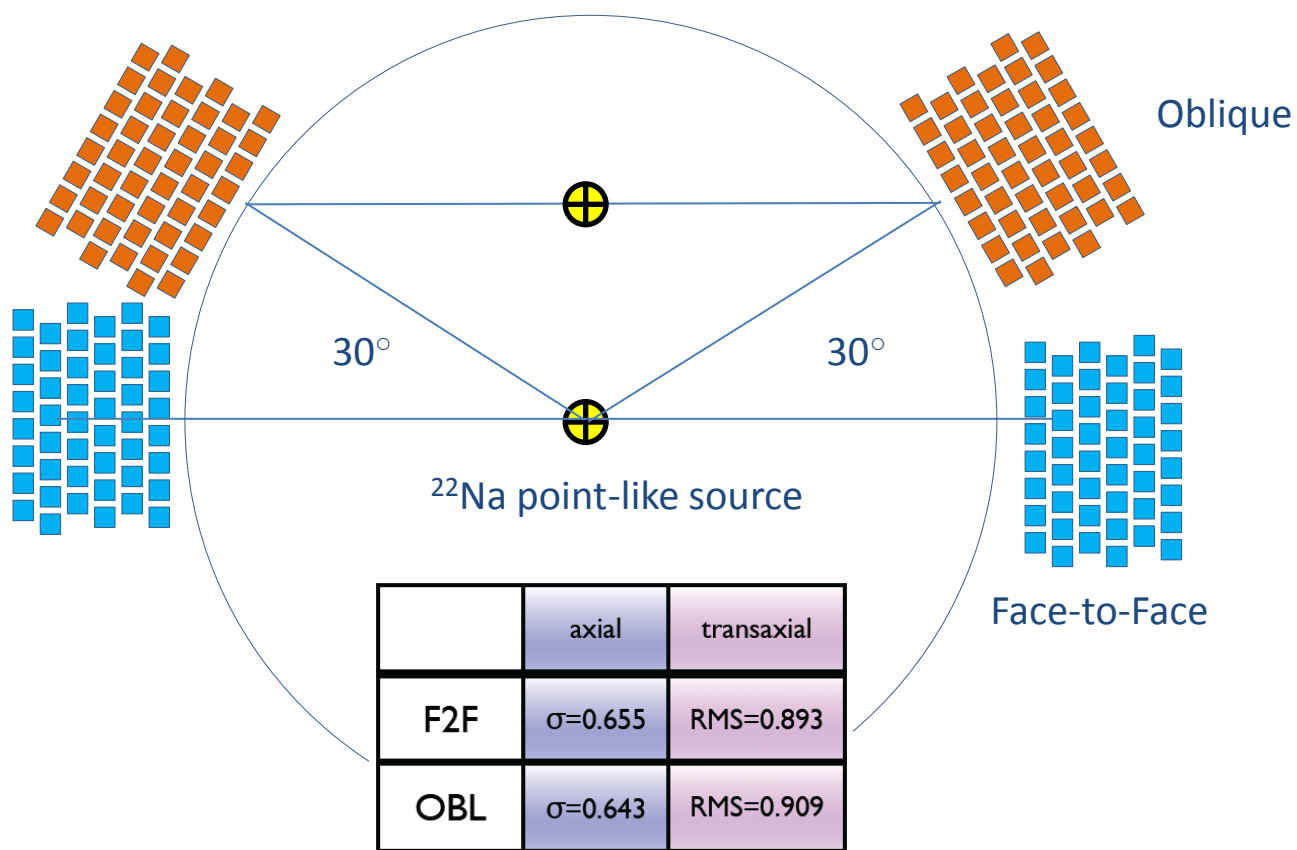
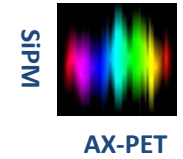
After correction of the  $e^+$  annihilation physics:

$$\sigma_z(\text{coinc.}) \sim \sigma_z(\text{detector}) / \sqrt{2}$$



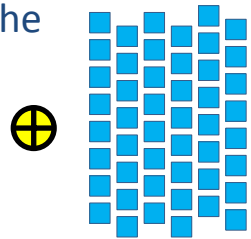
y coordinate is quasi-discrete (crystal positions).

# Experimental check: Are there parallax errors ?



As expected from the design, there is no noticeable parallax error, neither in the axial nor transaxial plane.

There is however an unavoidable degradation of the resolution, when the source is very close to one detector. The coincidence resolution loses the  $1/\sqrt{2}$  'bonus'





**Basics of tomographic imaging** (in AX-PET this is the speciality of the team from Valencia (M. Rafecas et al.))

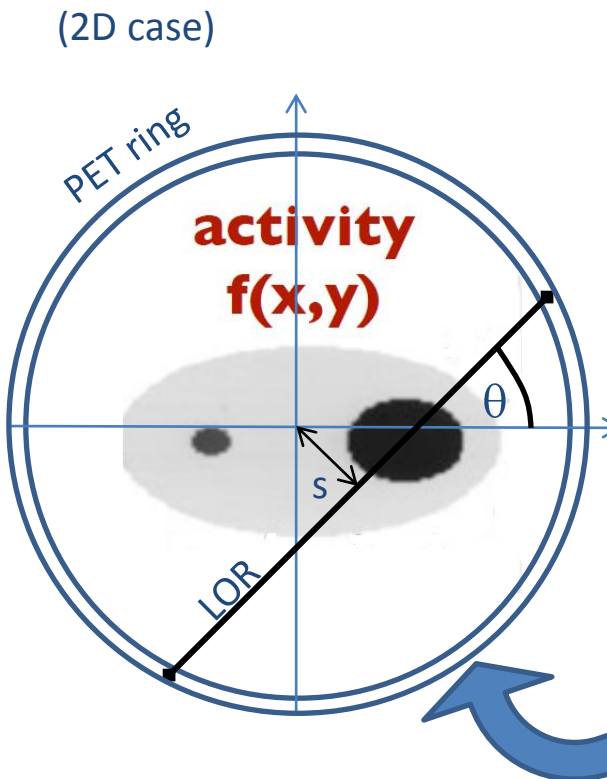
A PET scanner measures projections of the activity distribution. Reconstruction means to calculate from these projections the actual 3D distribution of the activity. There are two groups of methods:

1. Analytical algorithms

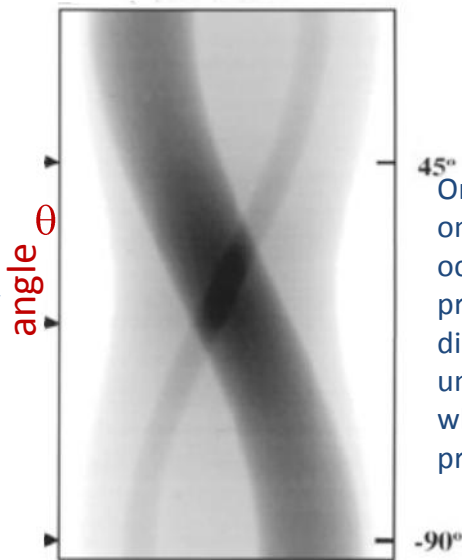
(usually based on sinograms)

2. Iterative algorithms

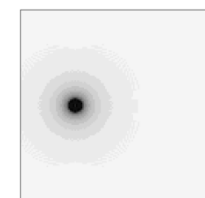
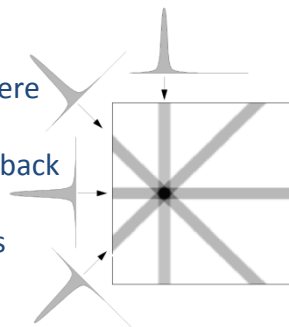
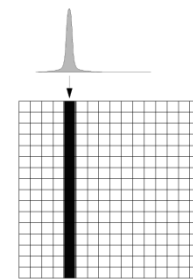
(mainly used in AX-PET, see back-up slides)



“sinogram”  
a 2D histogram  
of all projections  $g(s,\theta)$



One doesn't know where on the LOR the count occurred. Therefore, “back projection” means re-distributing the counts uniformly to all pixels which fall within the projection path.



The more angles, the better!

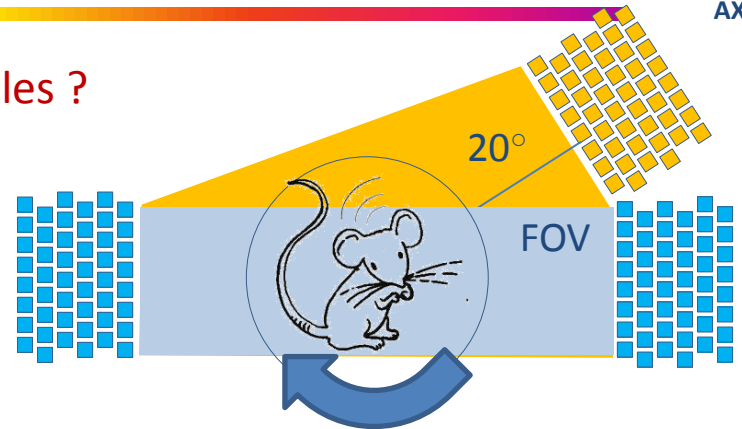
(Filtered) Back Projection

## How do we get all these angles with just 2 modules ?



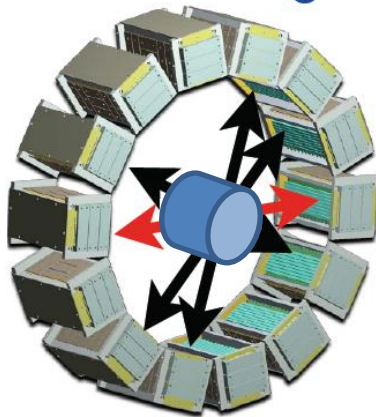
“Step and shoot”

Rotate object in 9 steps of 20 deg.



“Step and shoot”

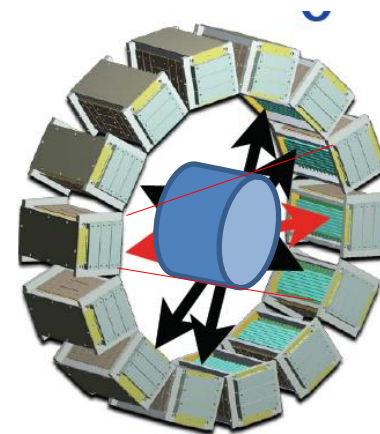
- 1.) Rotate object in 9 steps of 20 deg.
- 2.) Rotate 1 module by 20 deg.
- 3.) Rotate object in 18 steps of 20 deg.



Price to pay:

- Longer acquisition times (several h).
- Decaying activity
- Changing conditions (pile-up, dead time)

We mimic a 18-module scanner, however with a very limited FOV (width and length of 1 module). We allow only coincidences between opposite modules.



Now we allow coincidences between opposite  $\pm 1$  modules.  $\rightarrow$  Larger FOV.

The AX-PET set-up has exactly the size of a EURO palette. Very useful for measurement campaigns at other places



Measurements with phantoms or animals can't be made at CERN!

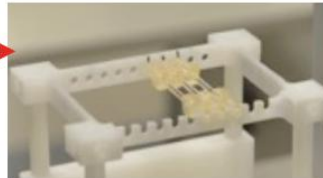
- ETH Zurich, PET lab, 2010
  - AAA (Saint GENis), F) 2010
  - AAA (Saint GENis), F) 2011
  - ETH Zurich, PET lab 2012
- } phantoms
- } animals



Phantoms are just containers which can be filled with a radiotracer. We usually work with F18 in aqueous solution. Some ink is added to see air bubbles.

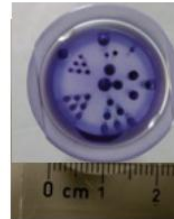
**(1) capillaries**

L = 3cm ;  
Diam = 1.4 mm ;  
Pitch = 5 mm



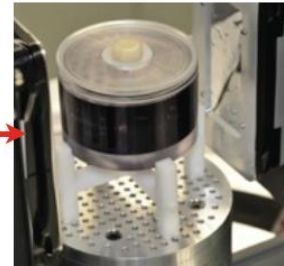
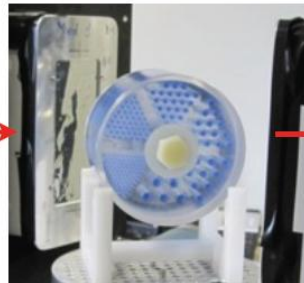
**(2) micro Derenzo**

H = 1.5 cm ;  
Diam = 2 cm ;  
Rods\_Diam = 0.8±2 mm



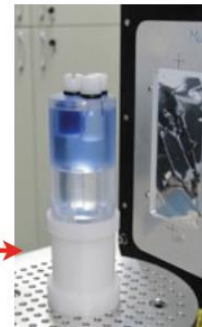
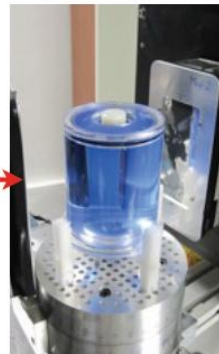
**(3) mini DeLuxe**

H = 5 cm ;  
Diam = 7.5 cm ;  
Rods\_Diam = 1.2±4 mm



**(4) homogeneous cylinder**

H = 9 cm ;  
Diam = 6 cm ;

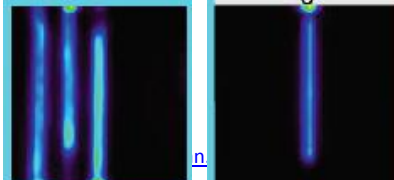
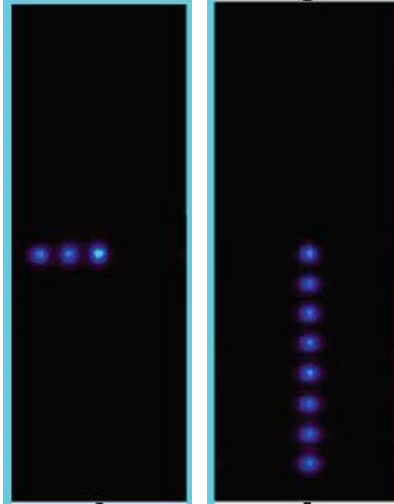
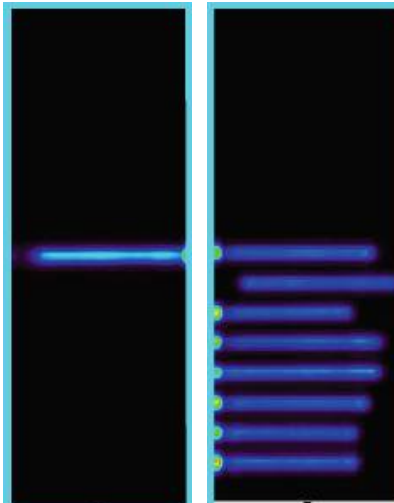
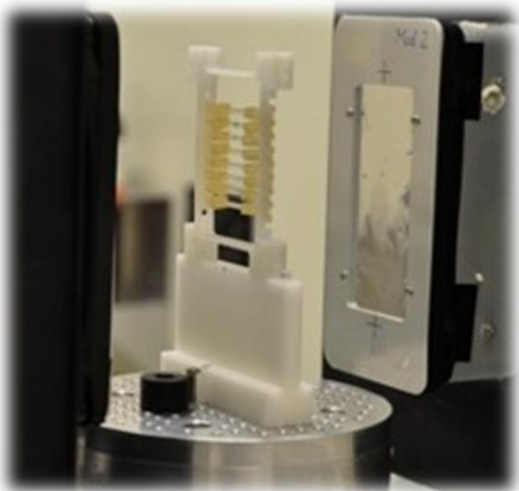
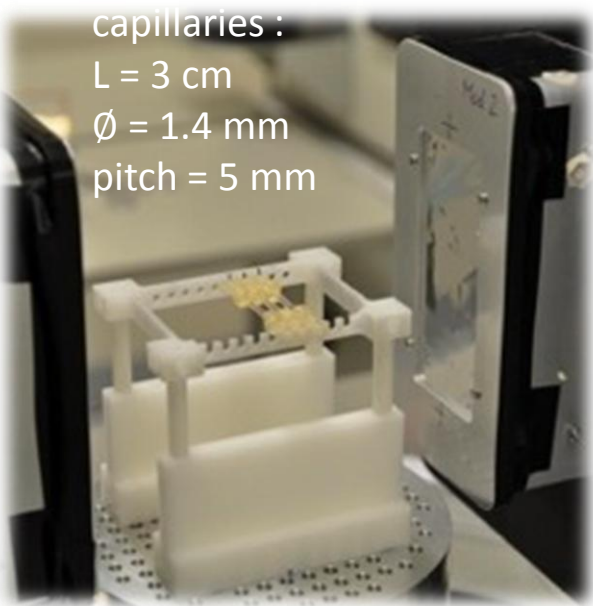


**(5) NEMA phantom**

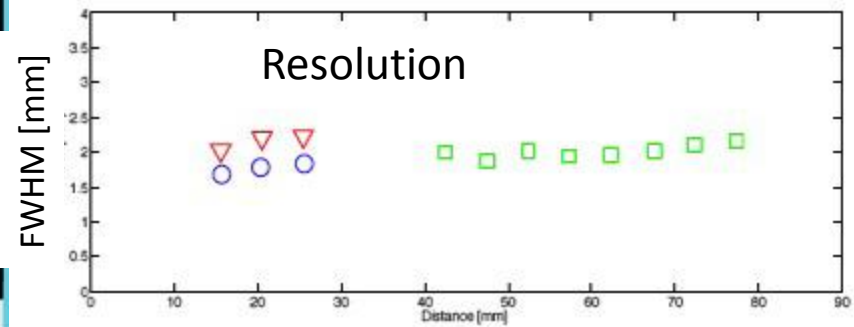
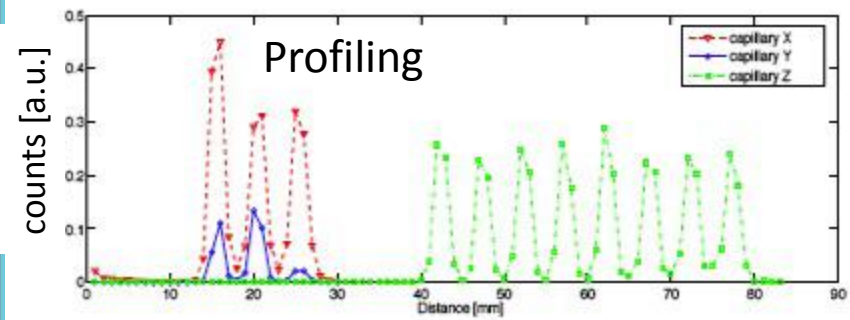
H = 6.3 cm ;  
Diam = 3.3 cm ;



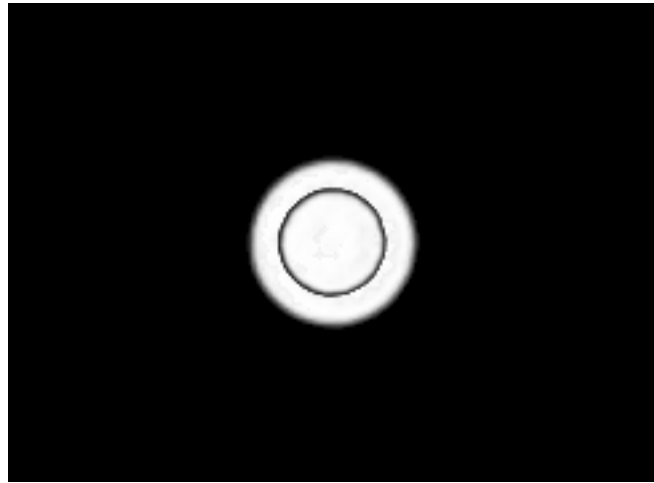
capillaries :  
 $L = 3 \text{ cm}$   
 $\varnothing = 1.4 \text{ mm}$   
 pitch = 5 mm



ETH 2010



Three regions in the same phantom to address three different aspects



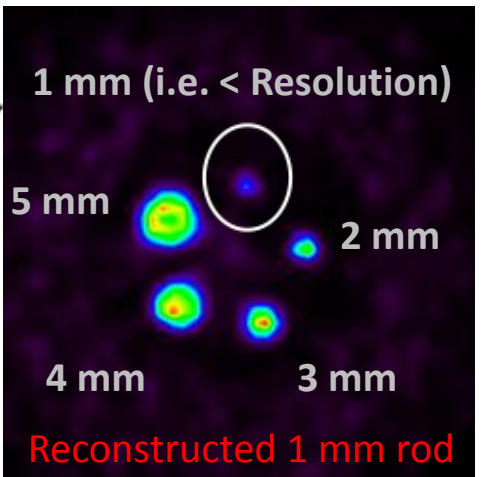
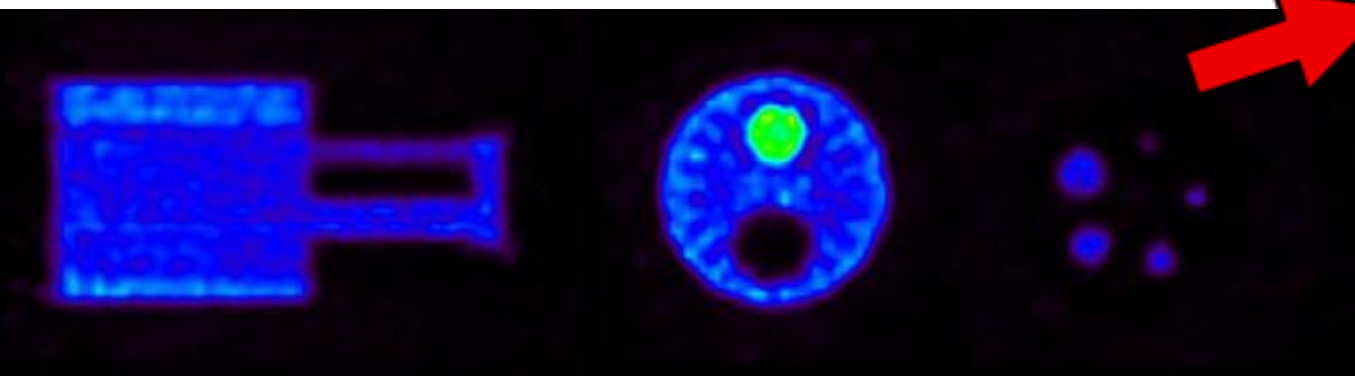
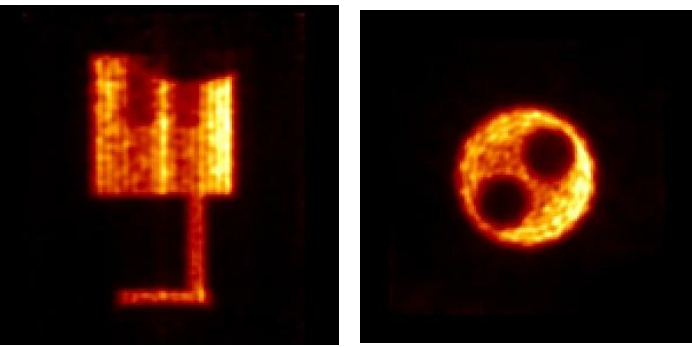
Hot & Cold rods for contrast

Homogeneous cylinder for assessing the ability to reconstruct homogeneous distributions

Series of small rods for resolution



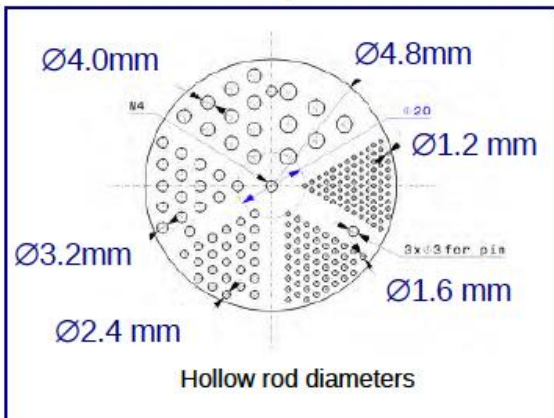
NEMA mouse phantom



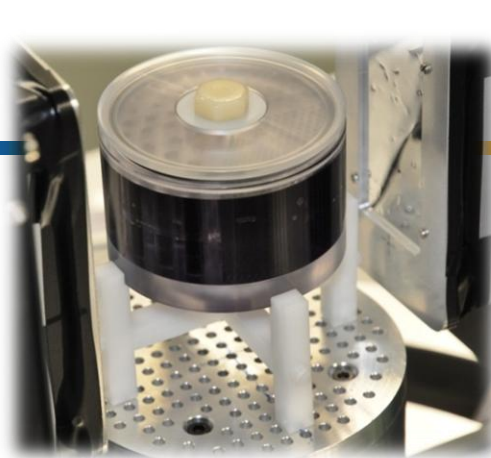
Reconstructed 1 mm rod  
=> FWHM ~ 1.6 mm



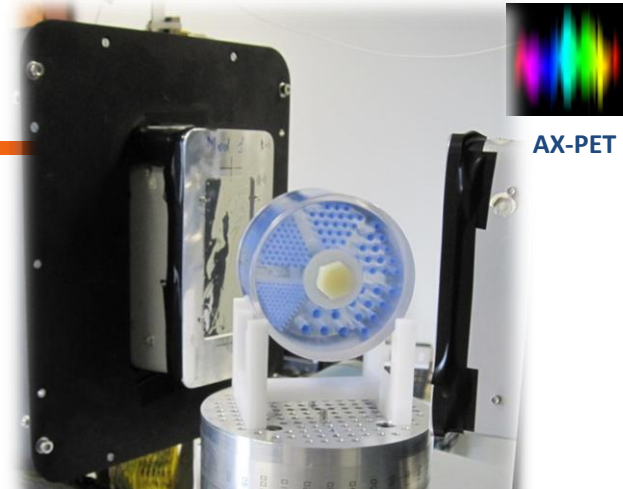
## Mini Deluxe phantom



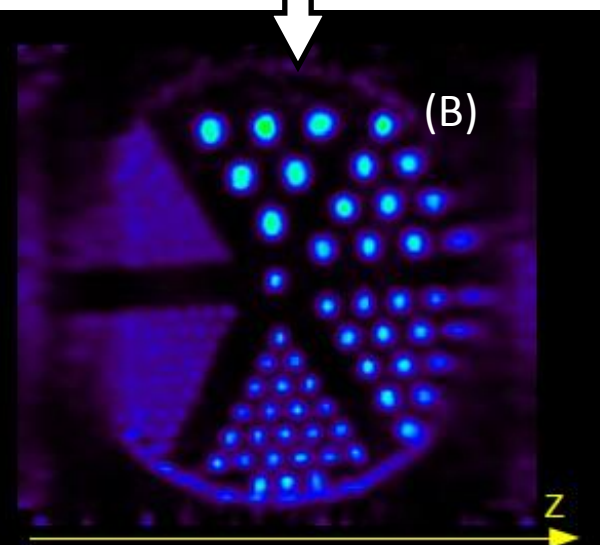
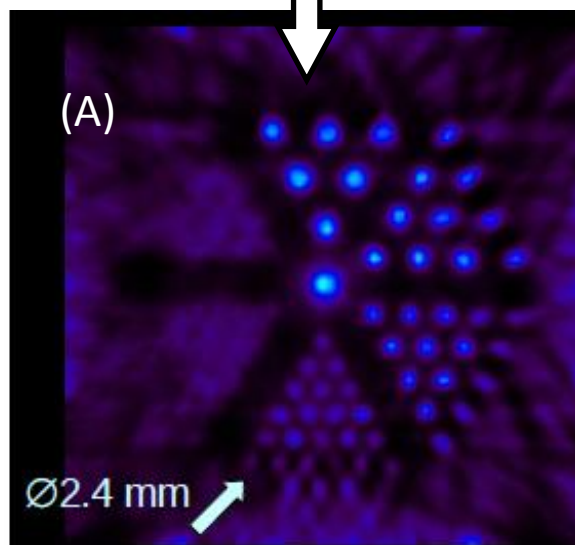
- High density resolution phantom
- Diameter (75 mm) is larger than the extended FOV



Rods oriented parallel to Z axis



Rods oriented perpendicular to Z axis

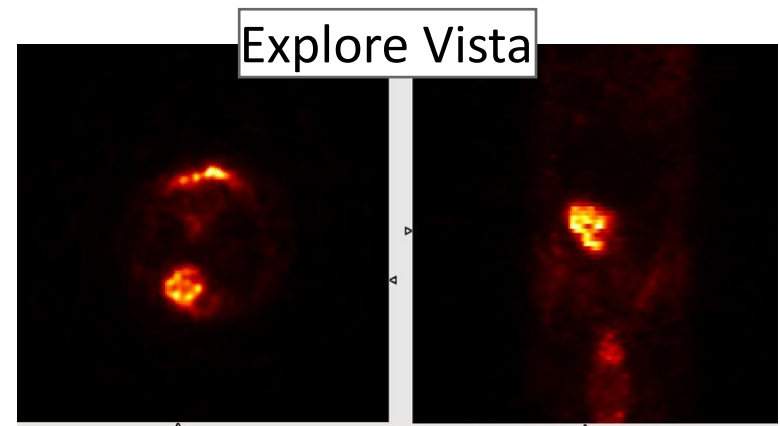
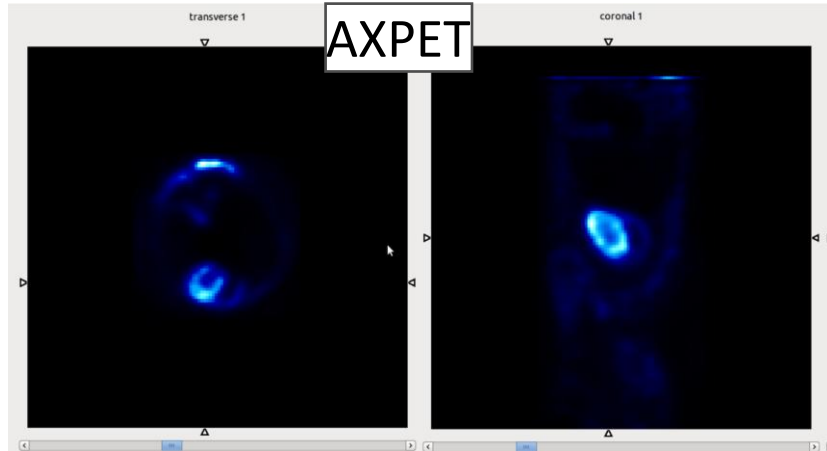


- Fixed time acquisition: 120 s /step
- 60 iterations + post-reconstruction smoothing
- No corrections
- Artefacts due to data truncation (FOV too small...)

- June 2012, small animals tests campaign at ETH Zurich, Radiopharmaceutical Inst.
- Possibility to use their GE Explore Vista PET/CT scanner as reference. This is a dedicated small animal scanner with 1.45 x 1.45 mm crystals. Block readout. DOI via Phoswich approach.
- one mouse, FDG } => organs structure
- one (young) rat, FDG }
- one (young) rat, 18-F } => bones, skeleton structure

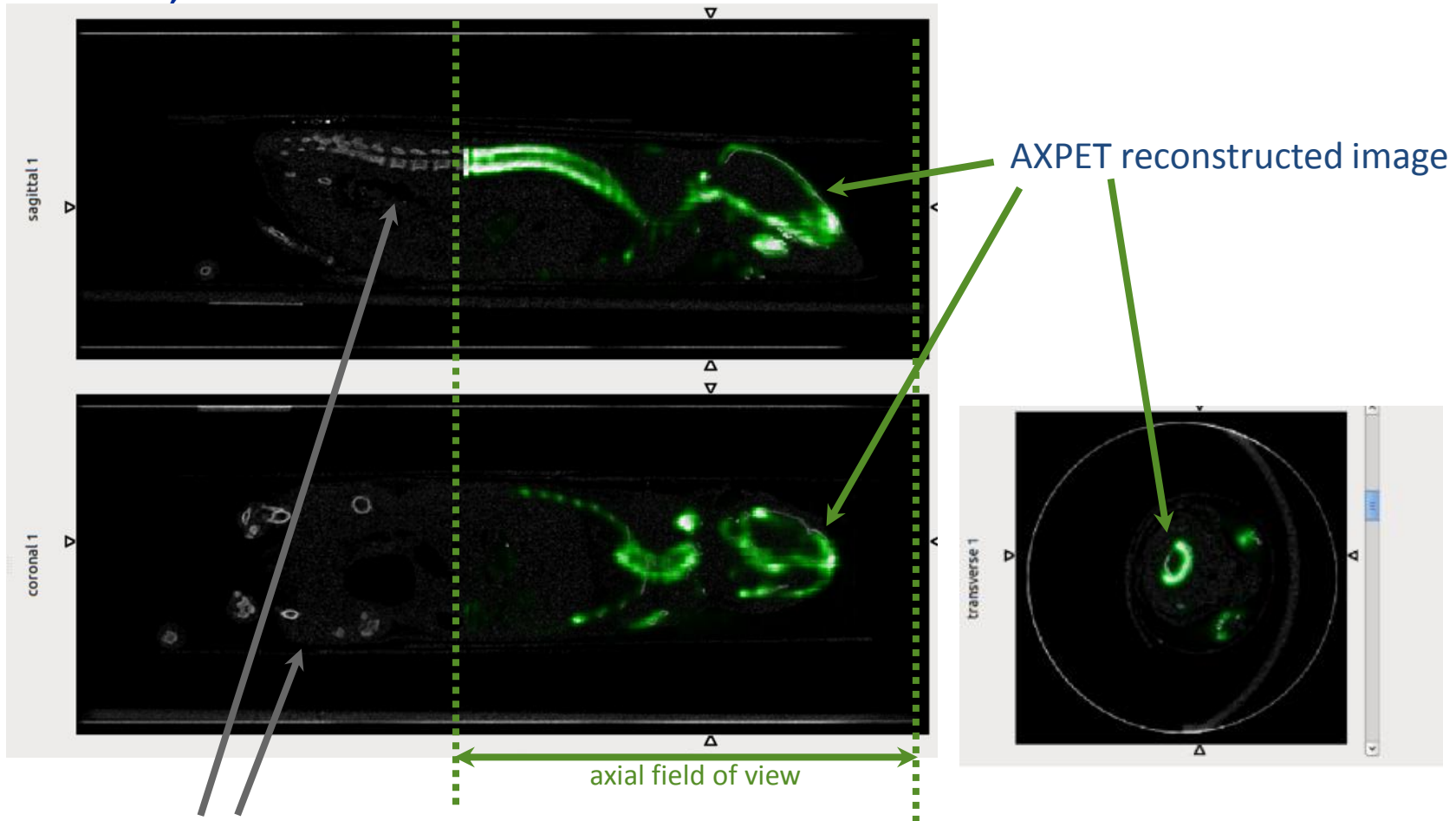


## Rat, FDG - Details of the heart





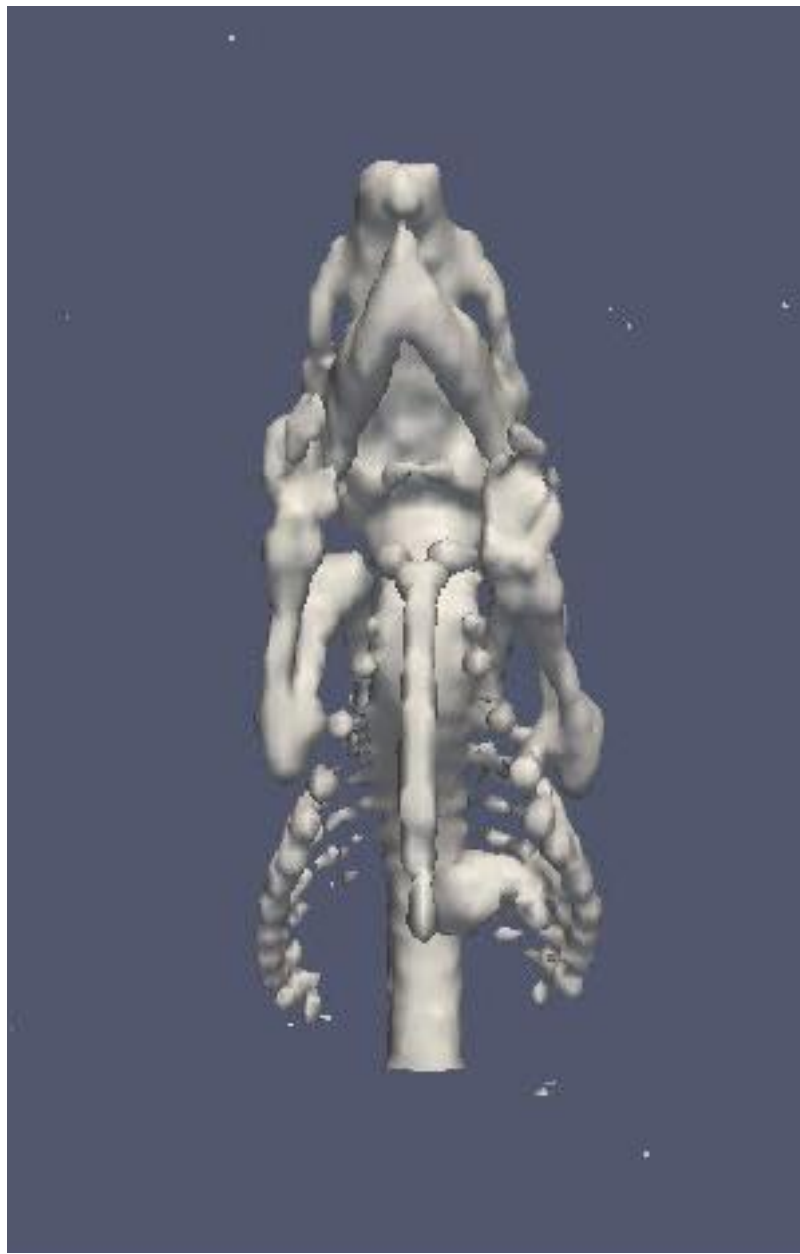
### Rat, F-18 - Details of the skeleton



CT image from Explore Vista  
(not enough activity left for the PET acquisition with Explore Vista)

# Rendered F-18 image of rat

(click to animate)

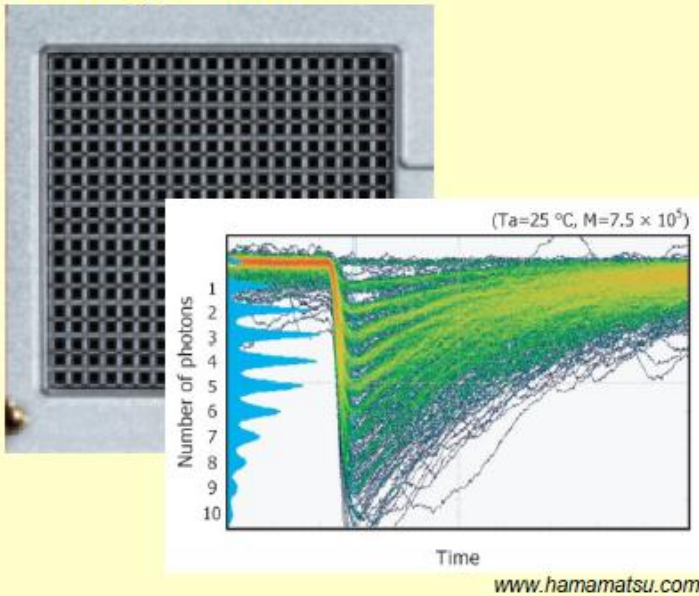




With the GM-APD being a binary device... one could also conceive a fully digital SiPM, where the output is just the digital count of the number of fired cells.

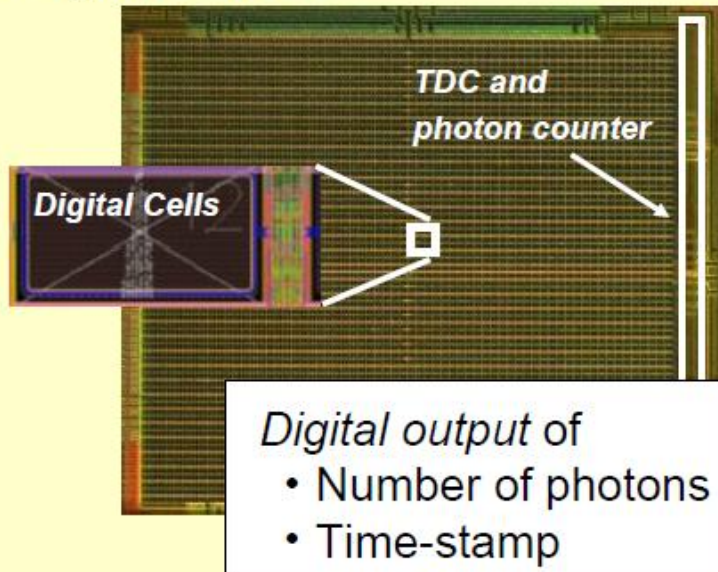
Philips

## Analog SiPM



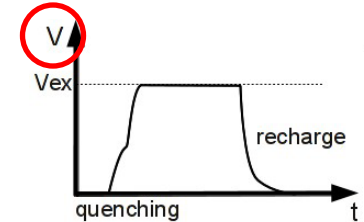
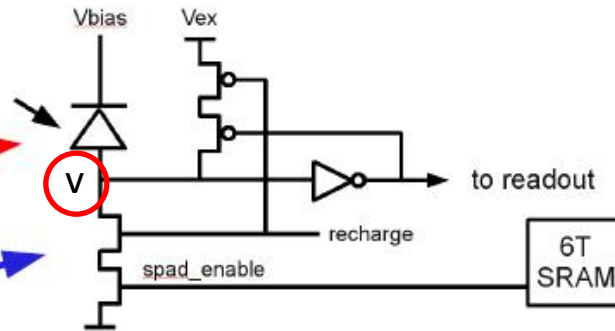
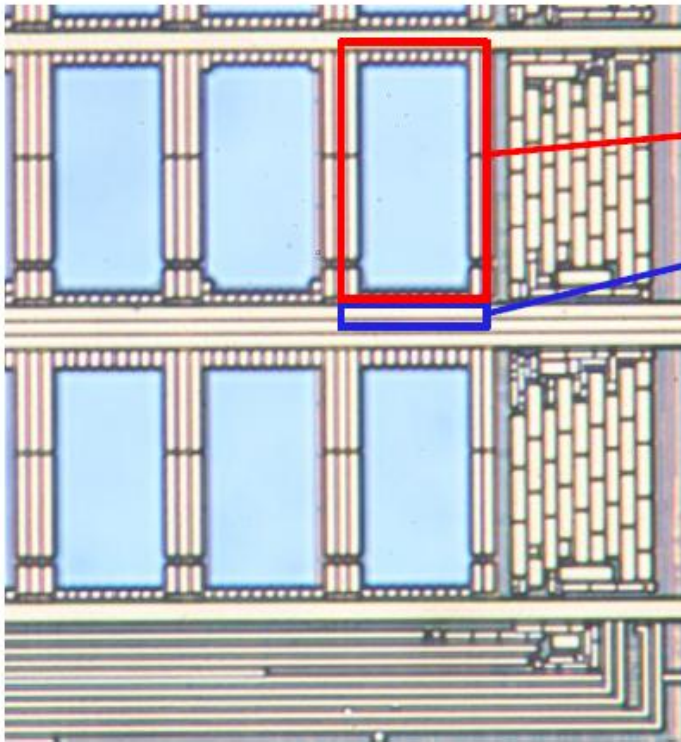
- Cells connected to common readout
- Analog sum of charge pulses
- Analog output signal

## Digital SiPM



- Each diode is a digital switch
- Digital sum of detected photons
- Digital data output

1 digital cell (area depends on type, e.g. 30 x 50  $\mu\text{m}$ )



- Cell electronics area: 120 $\mu\text{m}^2$
- 25 transistors including 6T SRAM
- ~6% of total cell area
- Modified 0.18 $\mu\text{m}$  5M CMOS
- Foundry: NXP Nijmegen

Philips

Different from analog SiPMs: Upon the detection of a photon, the avalanche is actively quenched using a dedicated transistor, and a different transistor is used to quickly recharge the diode back to its sensitive state.



Compared to the analog technology, the digital one (so far only offered by Philips) has a number of

## advantages

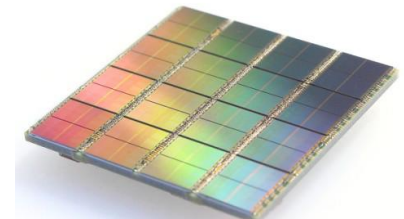
- + Integration of bias supply, amp, TDC, counter...
- + Fast active quenching → no afterpulses
- + Possibility to de-activate noisy cells → potentially lower dark noise
- + Reduced sensitivity to voltage and temperature variations
- + Compactness
- + Possibility to add local intelligence

## ... problems shared with analog

- High dark noise (a discharging cell doesn't know whether it is digital or analog)
- Signal saturation (limited number of cells)

## ... and also has some drawbacks

- The local electronics is a source of heat → cooling advisable
- The readout functionality is designed into the sensor. In case of mismatch with the needs, relatively expensive modifications of the sensor/FPGA may be required.

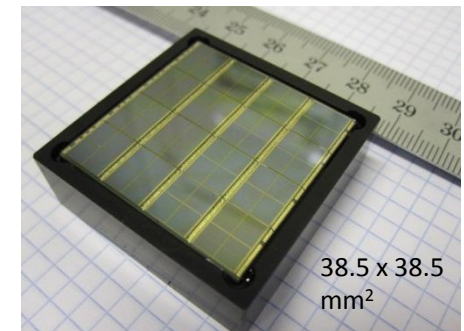


Front and back sides of a 64 channel digital tile (DPC6400-22-44) or (DPC3200-22-44)



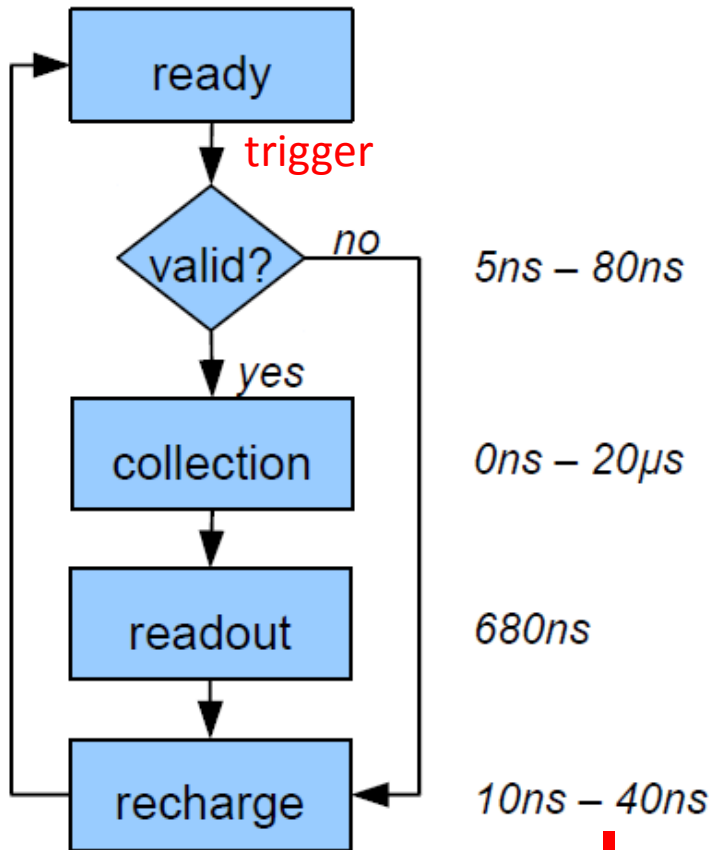
Philips

Packaged module, as delivered to clients (DPC3400-22-44). Includes a 100 μm thick protective glass layer.



38.5 x 38.5 mm<sup>2</sup>

## Digital SiPM – State Machine

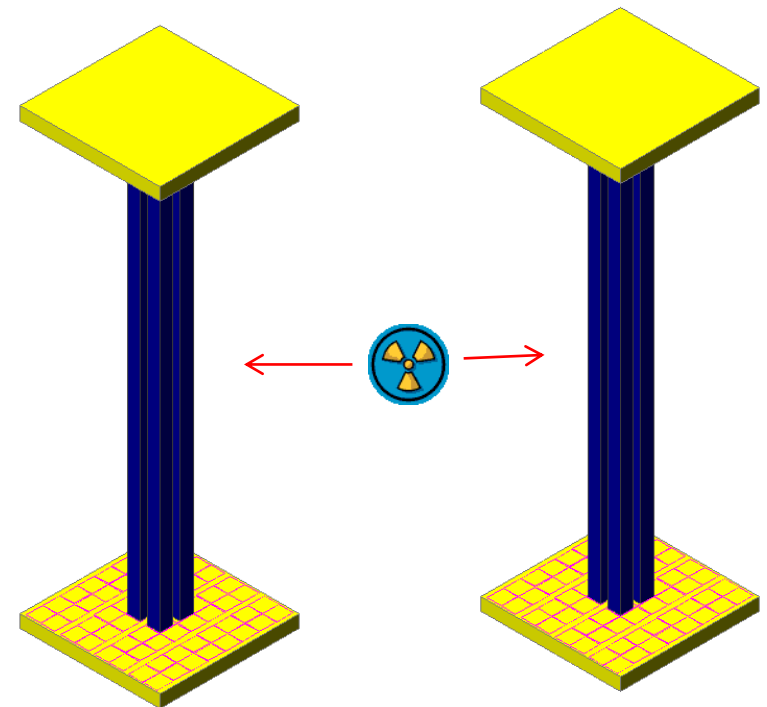
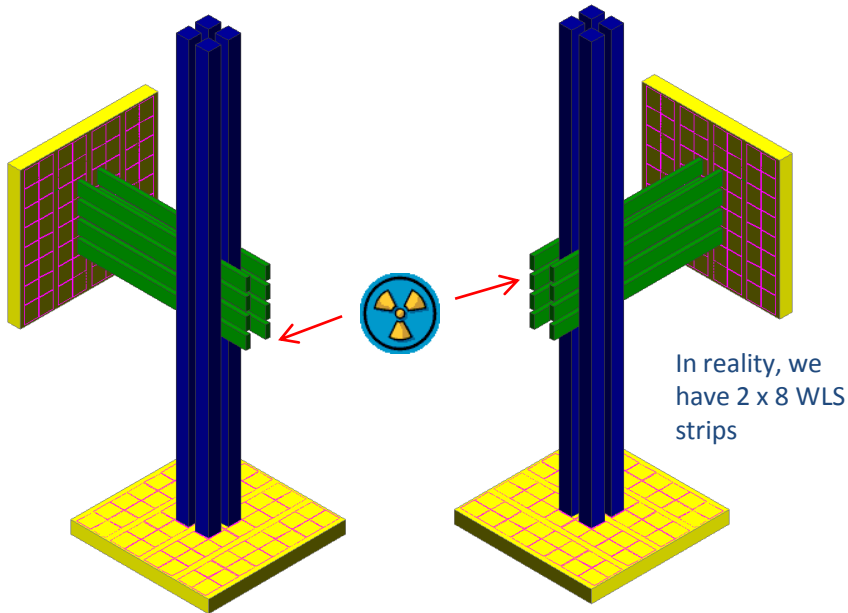


- 200MHz (5ns) system clock
- Variable light collection time up to 20µs
- 20ns min. dark count recovery
- dark counts => sensor dead-time
- data output parallel to the acquisition of the next event (no dead time)
- Trigger at 1, ≥2, ≥3 and ≥4 photons
- Validate at ≥4 ... ≥64 photons (possible to bypass event validation completely)

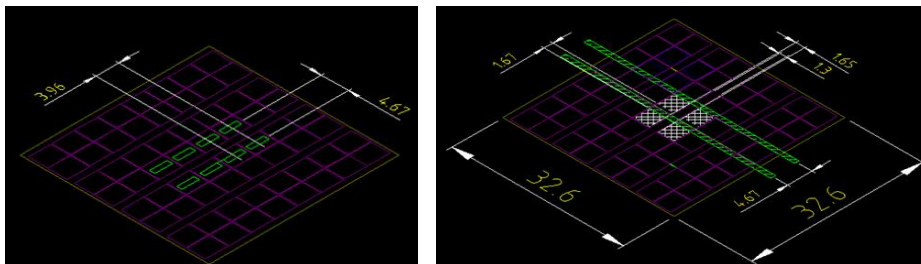
Every non-validated trigger leads in principle to the recharging of all cells. Without cooling, the device can loose efficiency/availability.

$\Sigma < 1 \mu s$  Expect readout rate up to O(1 MHz)

We got fascinated by the idea of a digital AX-PET module, mainly in view of a possible TOF-PET extension.

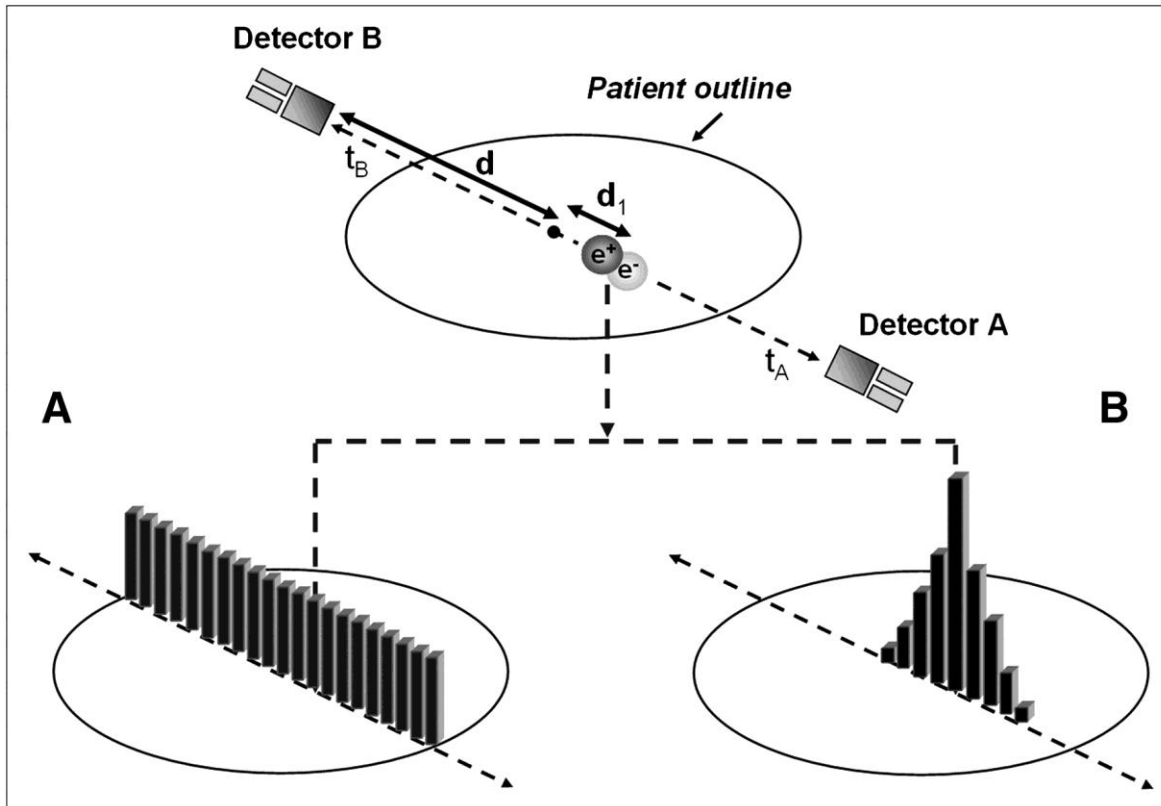


Luckily, crystals and WLS would just fit (without big compromises) on the existing Philips 64 channel DSiPM modules DLS-3200 (6400)



Aim for dual sided readout of long crystals to get rid of propagation delays

**Idea:** use time information to localize annihilation along the line of response. LOR does no longer contribute uniformly to all pixels but according to the measured time and its resolution. Images contain **less noise and show better contrast** (particularly noticeable for large scanners and big patients)



$$\Delta t = 2 \cdot \Delta x / c$$

→ Need  $\delta t = 66$  ps  
for  $\delta x = 1$  cm

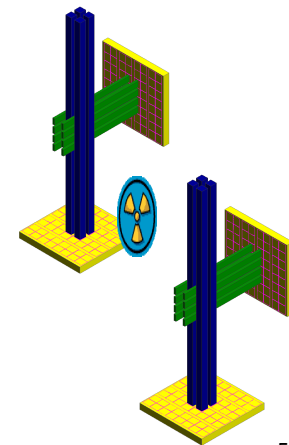
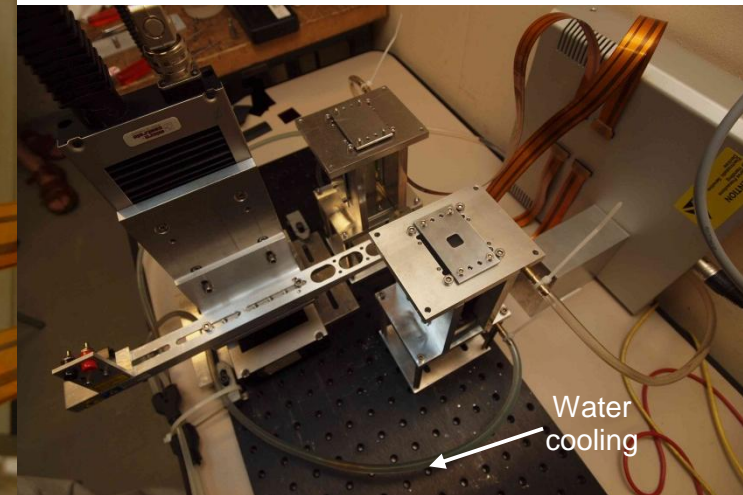
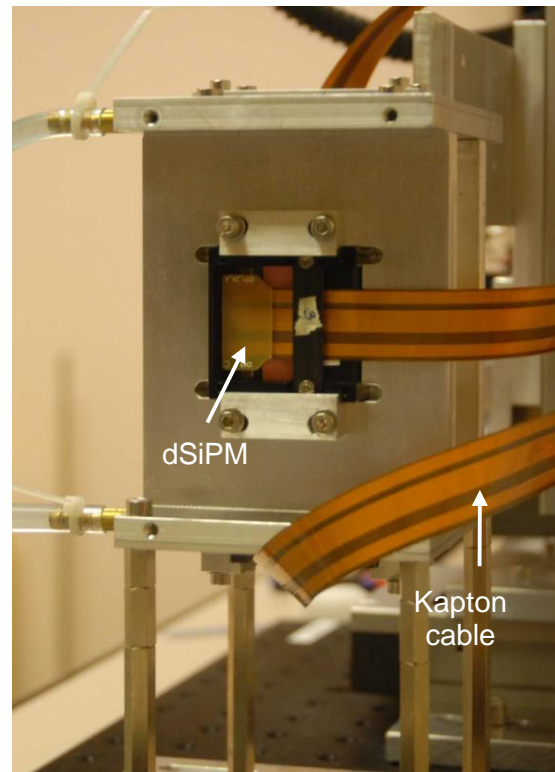
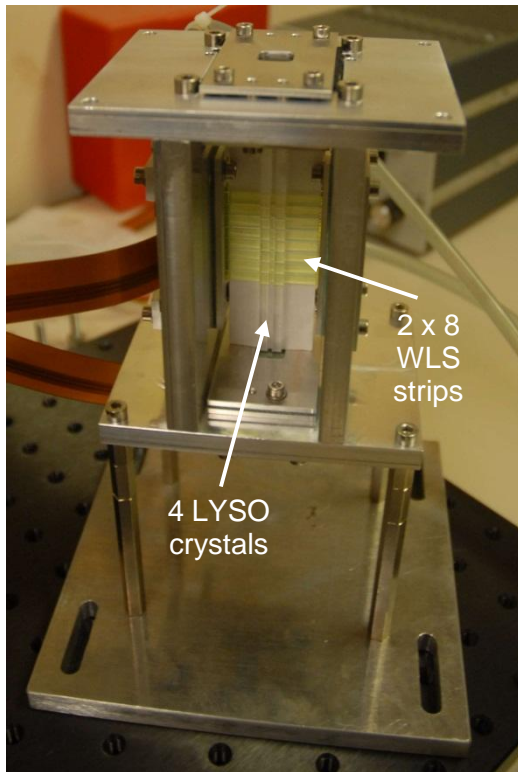
Gain of a TOF system over a non-TOF system is

$$G = 2D / c \cdot \delta t$$

$D$  = dimension of object being imaged.

# Verification of normal AX-PET characteristics

Two modules setup. Single sided readout plus WLS strips.





## Energy calibration and resolution

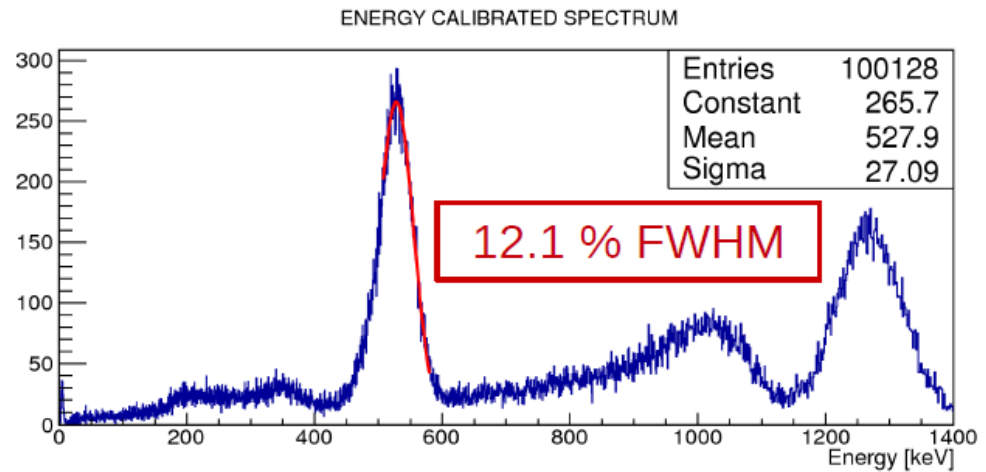
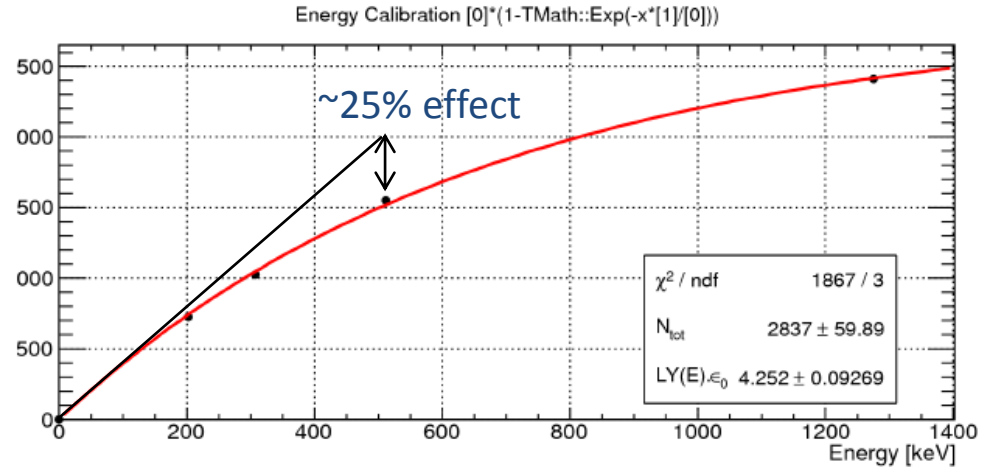
(single sided readout)

Saturation effect is much larger:

- More detected p.e.
- Fewer pixels (3200 vs 3600)
- Recharging only after readout!

In the end we get a comparable  
Energy resolution.

(analog AX-PET was 11.7 %).

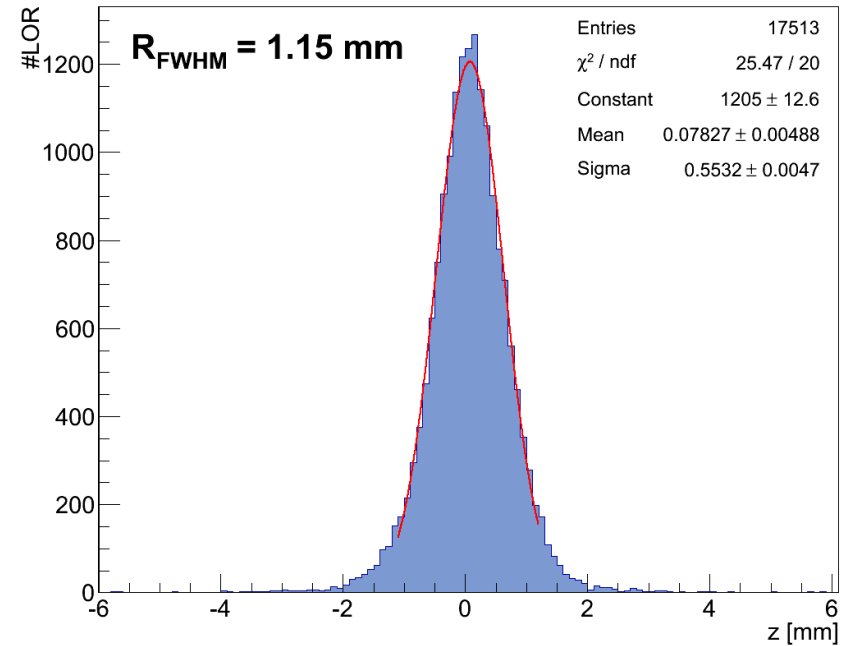
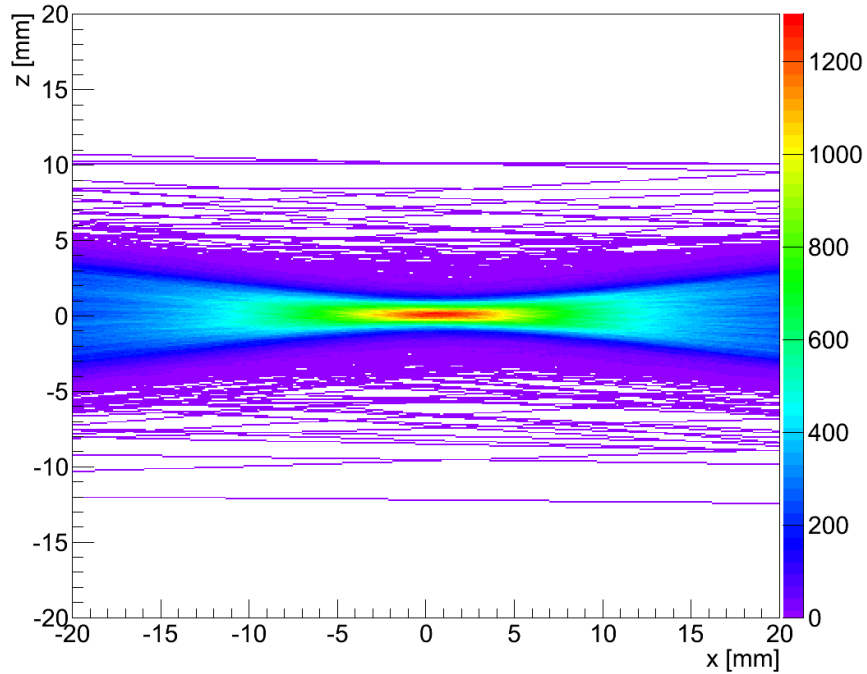




## Confocal reconstruction in axial direction (WLS array)

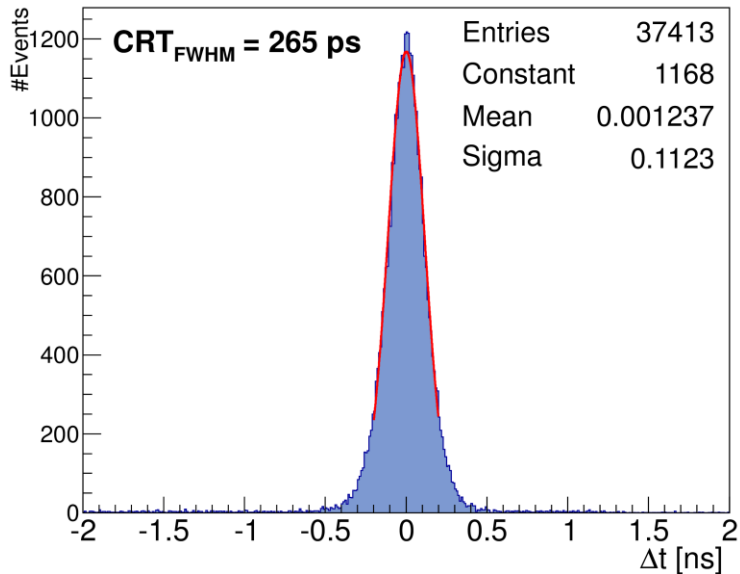
$^{22}\text{Na}$  source of 250 microns diameter, 150 mm between the two modules

Entries 7005200

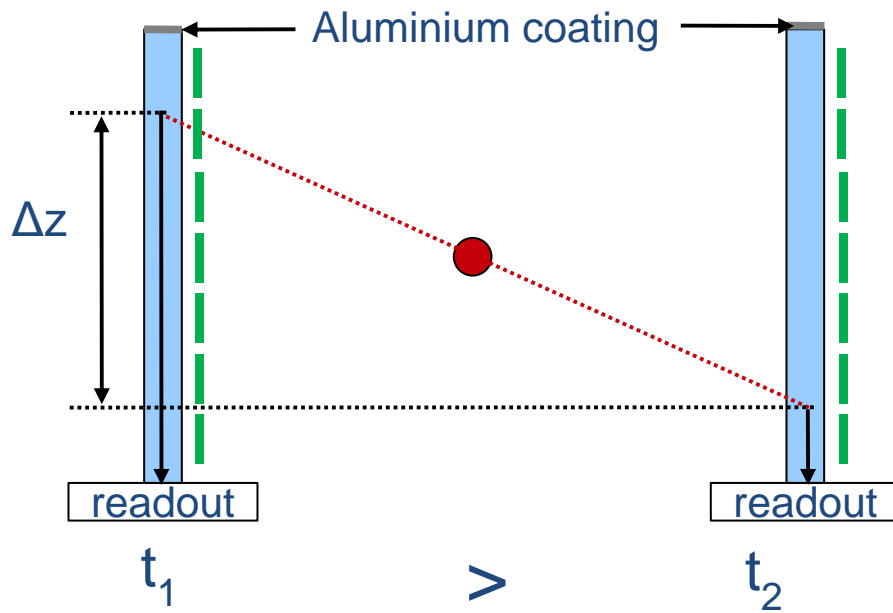


Slightly better than with the analog AX-PET set-up (1.48 mm)

## Coincidence time resolution (single sided readout)

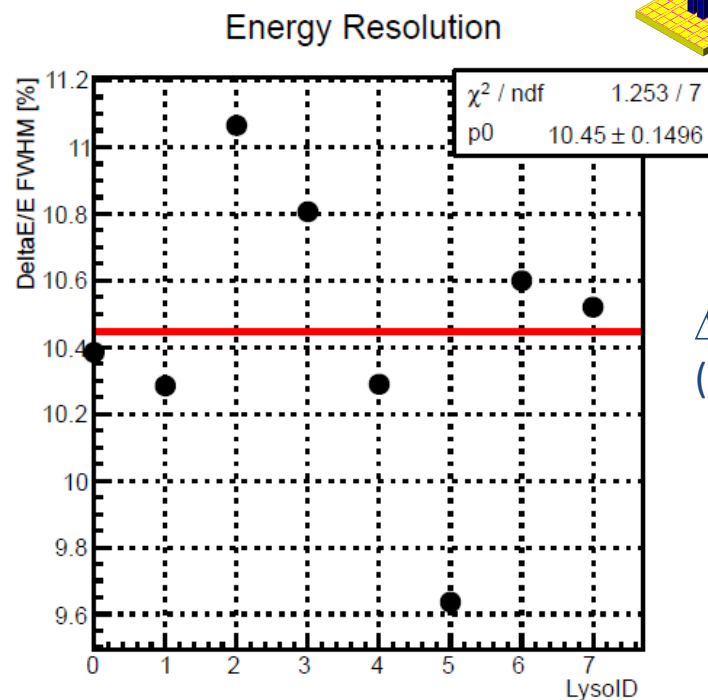
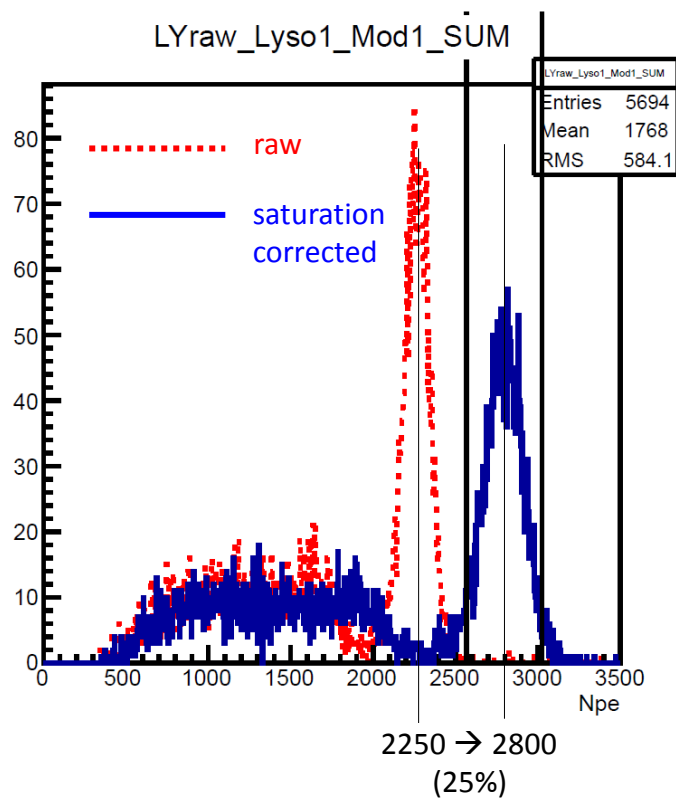
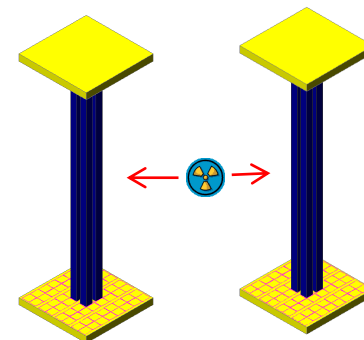


This is only possible after correcting for light paths using WLS information



# Energy calibration and resolution

(Double sided readout)



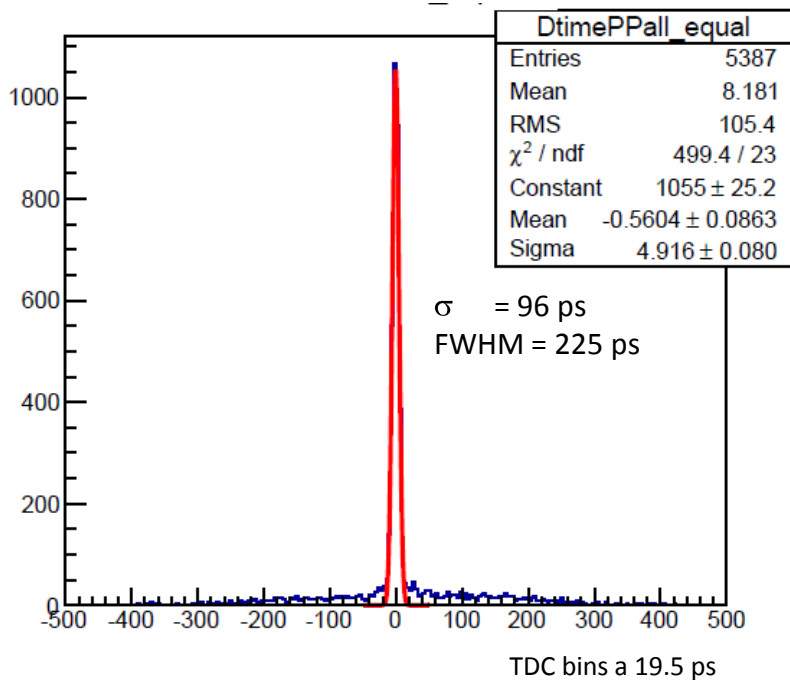
$\Delta E = 10.45\%$   
(FWHM)

# Coincidence time resolution by mean timing

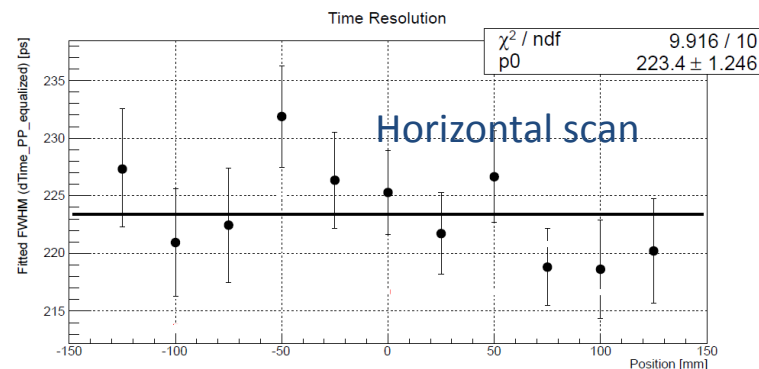
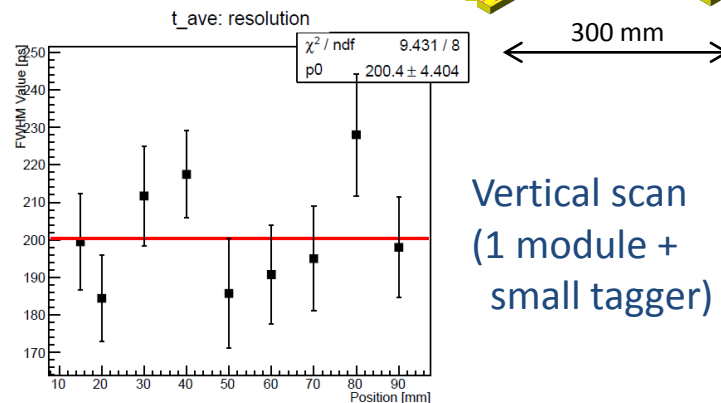
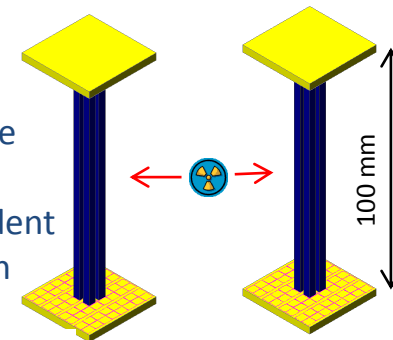
(Double sided readout)

$$\Delta t = \langle t_{mod1} \rangle - \langle t_{mod2} \rangle = \frac{t_{1,up} - t_{1,down}}{2} - \frac{t_{2,up} - t_{2,down}}{2}$$

Small differences in timing of pixels (offsets) can be eliminated.



Mean Timing corrects automatically for light propagation times in the crystals. The resolution becomes fully independent of the source position in the FOV.



The SiPM technology wasn't mature enough when the choices were made for LHC (>10 years ago). But we start to see SiPMs in R&D for the LHC upgrade.

**The obvious applications are readout of scintillators and scintillating fibres.  
Also demonstrated: Detection of Cherenkov light (even with digital SiPM).**

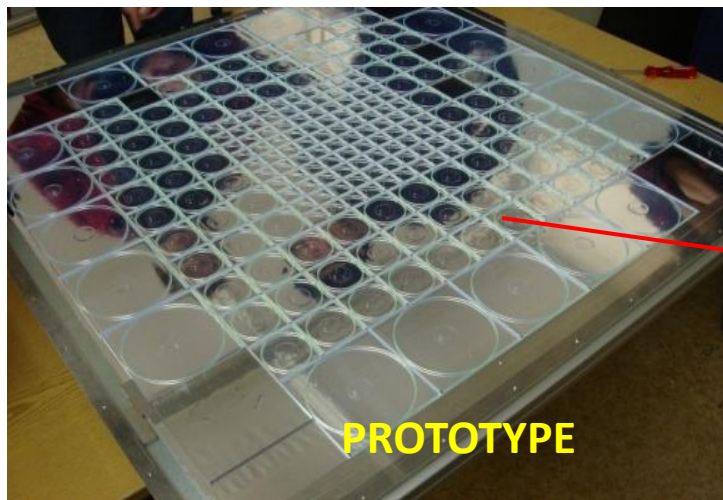
- First major project was T2K (scintillator tracker + ECAL). ~65k SiPMs.
- The CALICE collaboration builds HCAL and ECAL prototypes based on small scint. plastic tiles (ILC). ~8k SiPMs.
- CMS is working on an upgrade of HCAL barrel (SiPMs replacing HPDs).
- LHCb is working on a study of SciFi tracker to replace Si strips and gas straw tubes. ~ 300k SiPMs
- CLIC detector study for a W/scint ECAL. Many 100k SiPMs.

High granularity hadronic calorimeter optimised for the Particle Flow measurement of multi-jets final state at the ILC

photo-detector requirements:

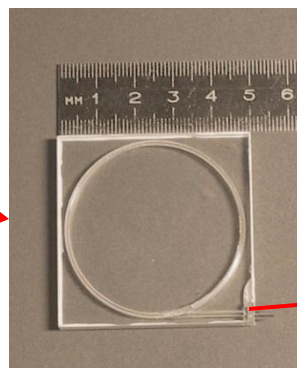
- insensitive to magnetic field ( $\sim 5T$ )
- coupling with a scintillator (blue emission)
- stability (T-control or T-monitoring)
- rel. large dynamic range
- low cost

CALICE tests with MePHI/PULSAR, HAMAMATSU, KETEK SiPMs

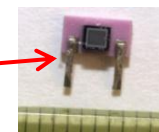


**PROTOTYPE**

216 tiles/layer (38 layers in total)  $\sim 8000$  channels



3 x 3 cm<sup>2</sup> plastic scintillator tile with embedded WLS fiber + SiPM



SiPM  
1 mm<sup>2</sup>

Readout of SiPMs by the SPIROC ASIC (LAL)

e<sup>+</sup> e<sup>-</sup> collider (1 TeV)

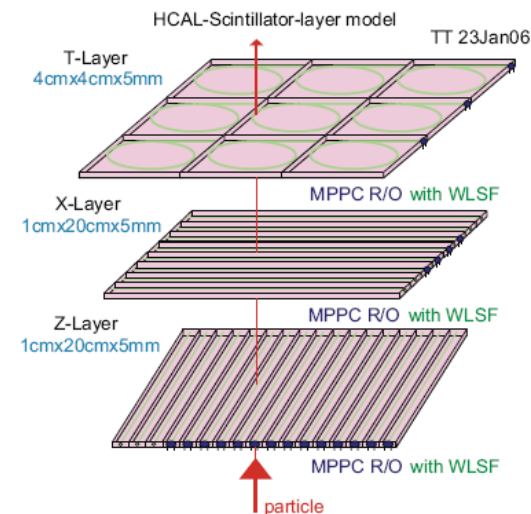
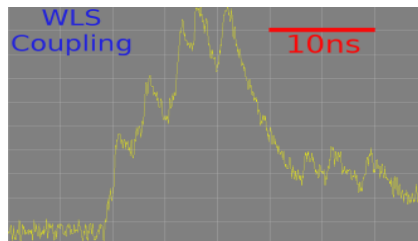
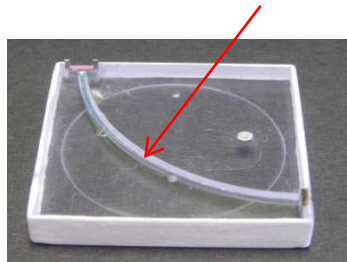


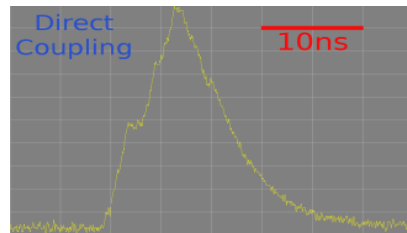
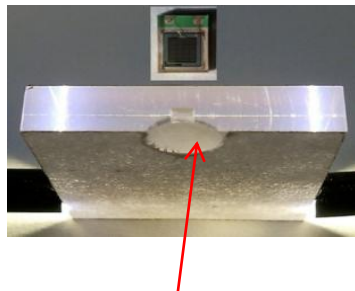
Fig. 6. A possible scintillator strip/tile sequence of the analog HCAL.



Different SiPM couplings to scintillator tile with WLS fiber (for MEPHI SiPM)



direct coupling (for MPPC)

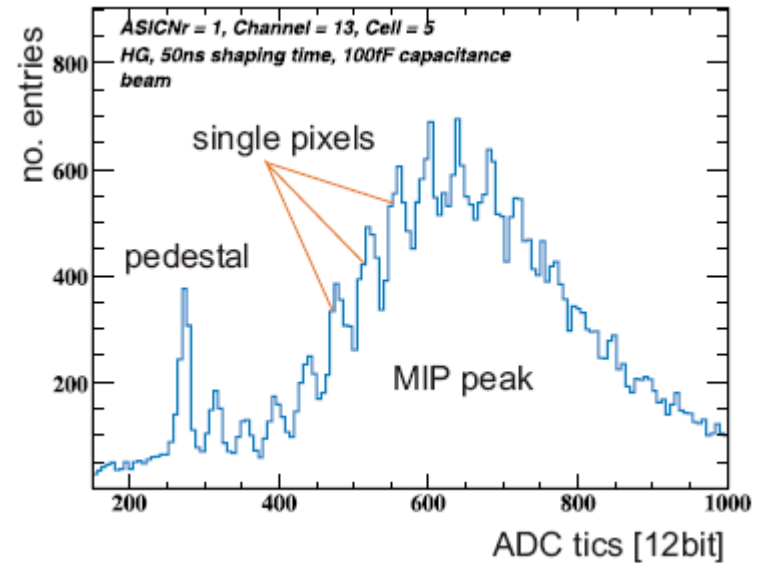


hole (“dimple”) for more uniform light yield close to photodetector

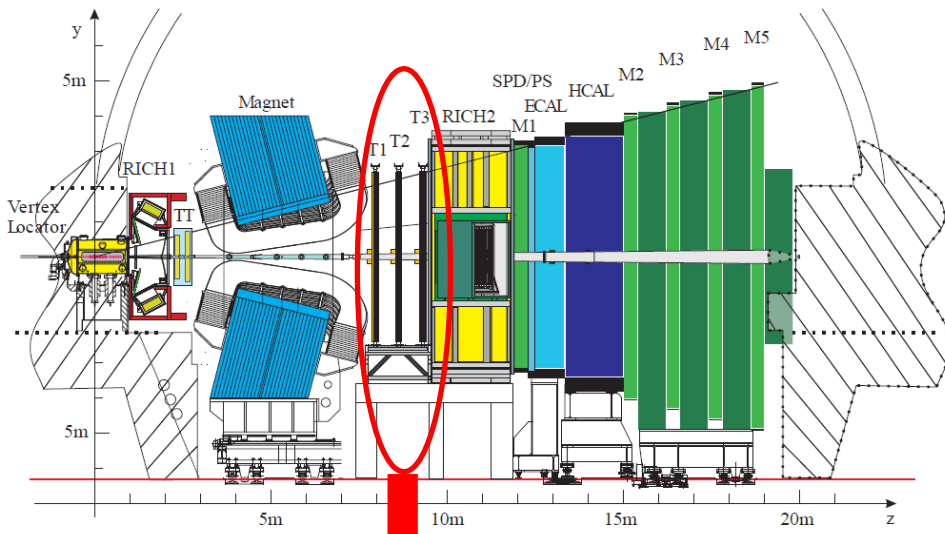
Calibration & monitoring

- test beam (absolute)
- LED monitoring system (stability)

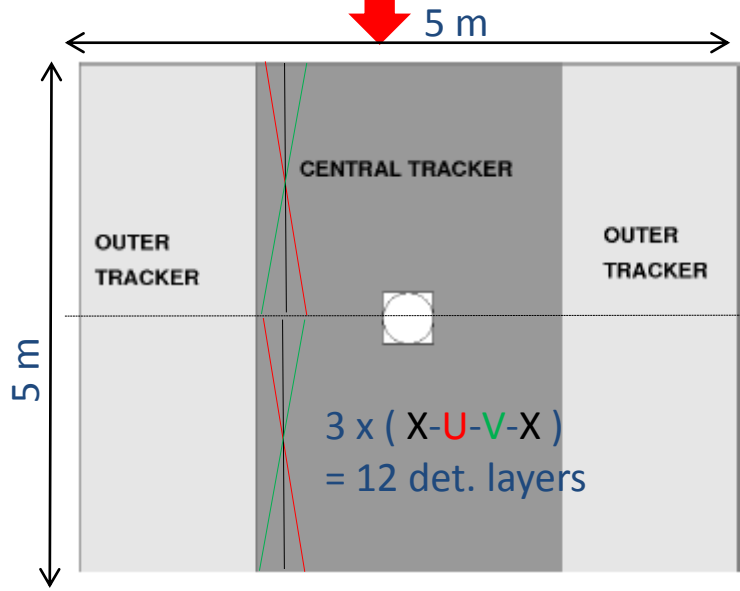
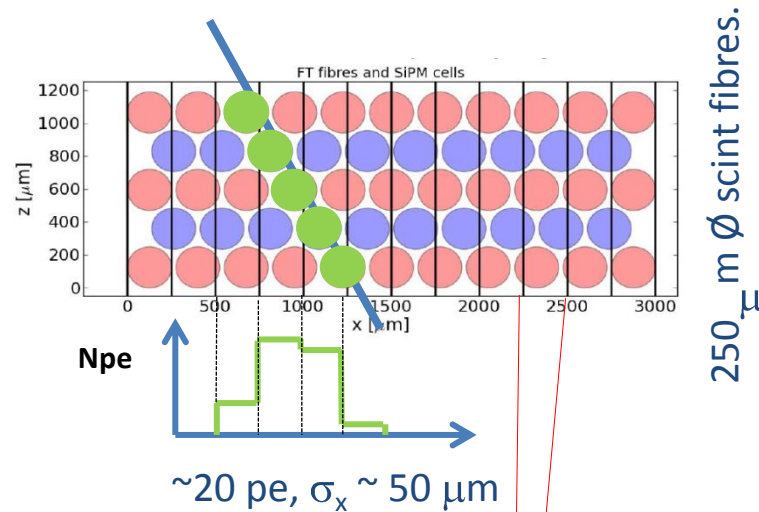
DESY 3 GeV electron testbeam



- Channel energy calibration by ~3 GeV electrons (MIPs).
- Multi-photon peaks allow simple absolute calibration.



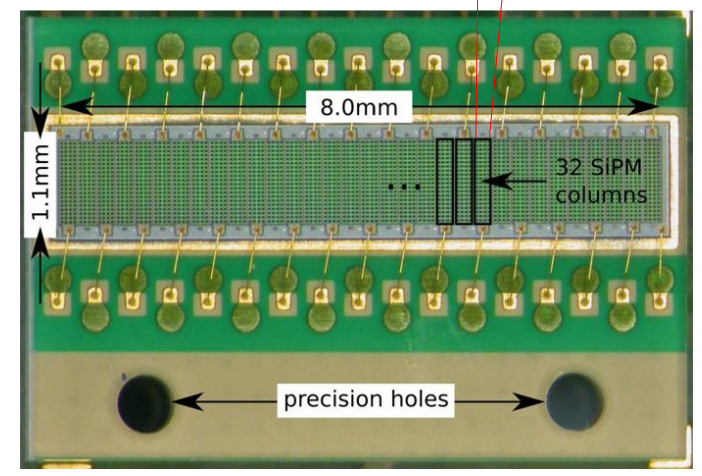
1 det. layer = 5 fibre layers



Detector concept follows largely the work of the Aachen group

(S. Schael et al.)  
NIM A 622 (2010)  
542-554

~ 300 k SiPM channels



## Main challenges:

- **Rad hardness of SiPM** (10 years  $\sim 6 \cdot 10^{11}$  n/cm<sup>2</sup>)
- (Rad hardness of scint. Fibres (10 years  $\sim 30$  kGy))

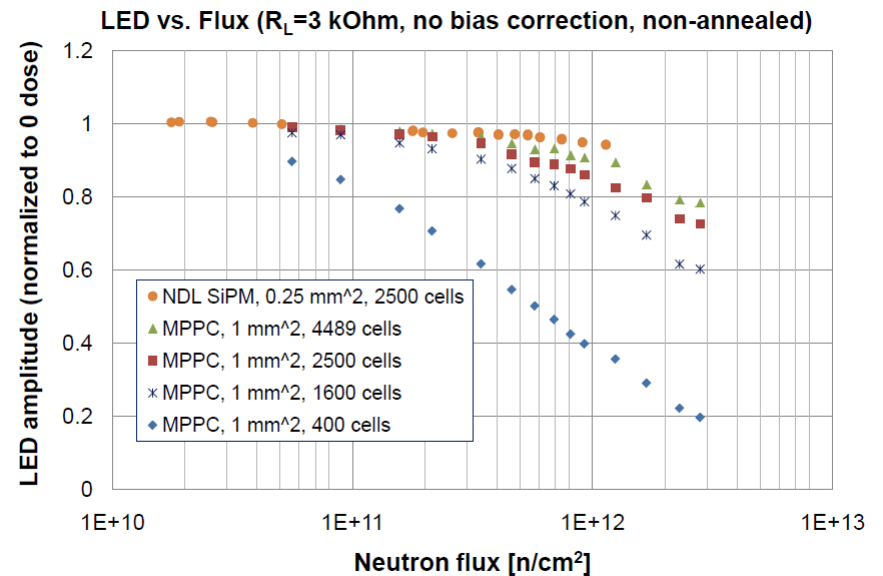
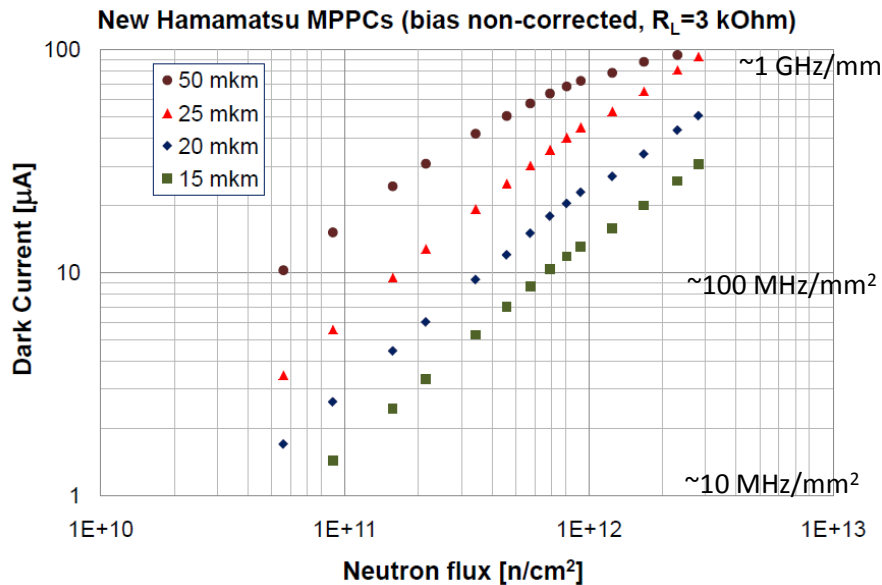
Main observation: dark current / dark rate increase linearly with the NIEL

In analogy to a standard pn detector...

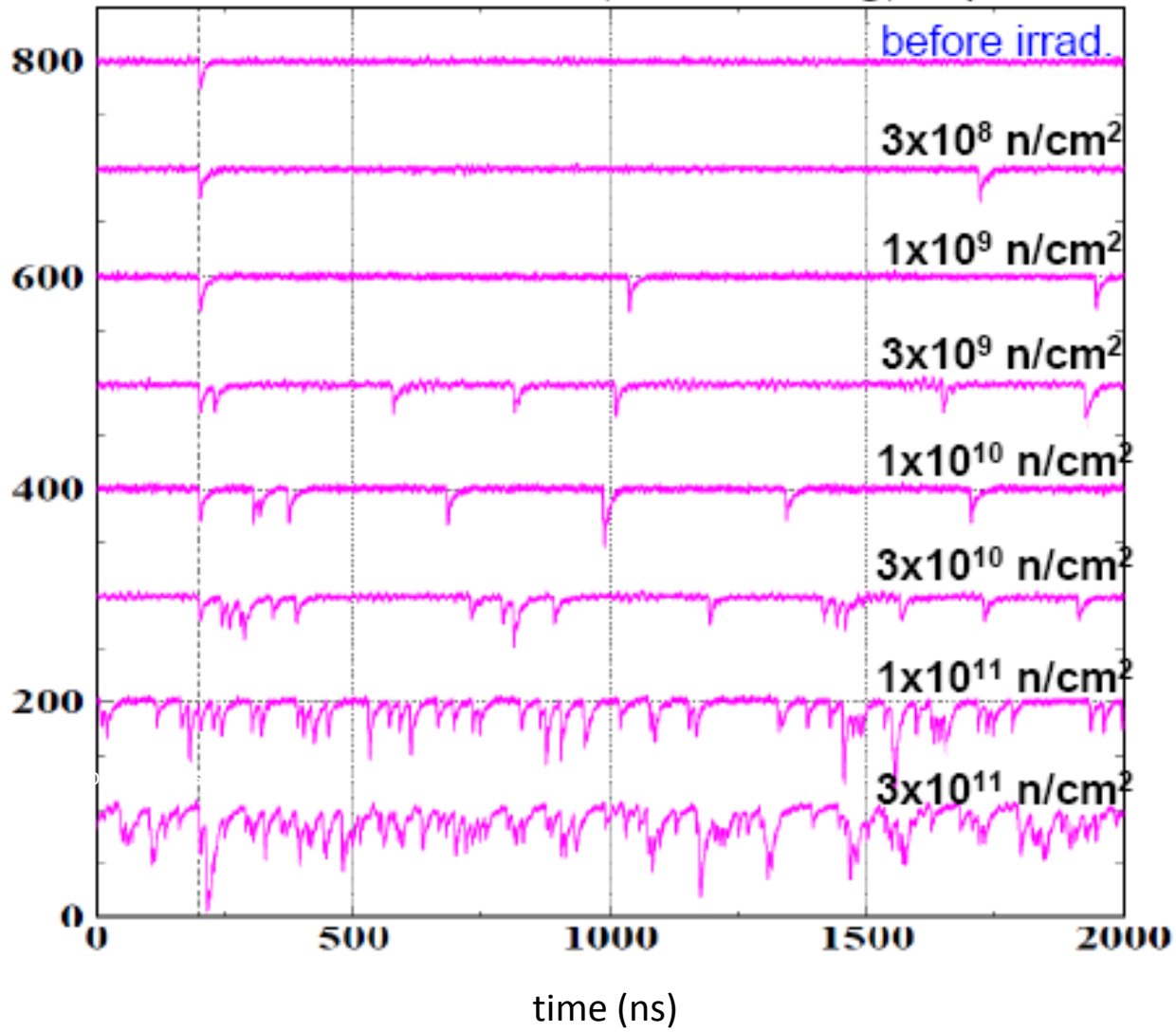
$$I_d \sim \alpha \cdot \Phi_{(1 \text{ MeV n eq.})} \cdot V_{\text{eff}} \cdot G \quad (\alpha = 3 \cdot 10^{17} \text{ A} \cdot \text{cm})$$

But also gain starts to drop

Devices with smaller cell size and fast cell recovery survive longer

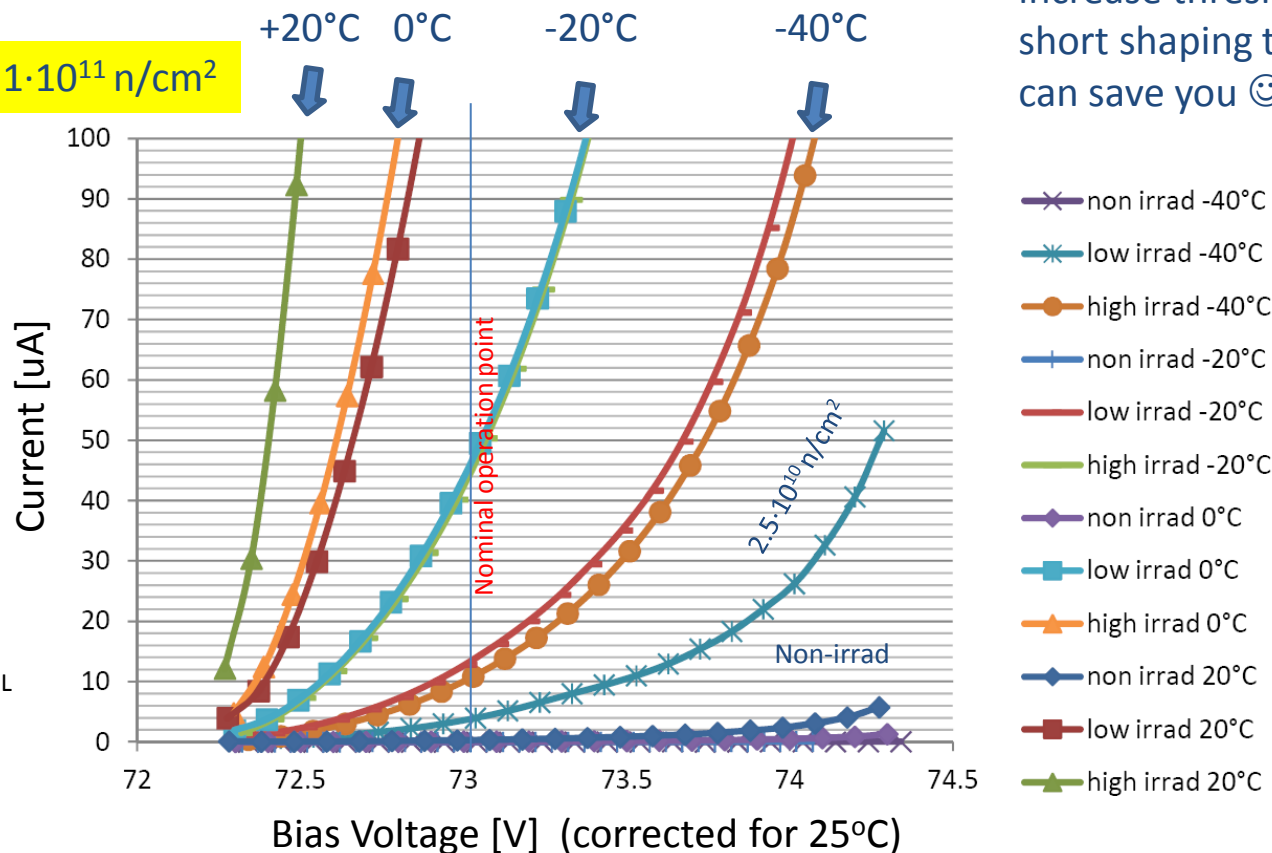


I.Nakamura, JPS meeting, Sep. 2008



Cooling helps a lot. Every 8K reduce the dark noise by a factor 2

After  $1 \cdot 10^{11} \text{ n/cm}^2$



But also reducing overvoltage, increase threshold, clustering, short shaping time, ... can save you 😊

G. Häfeli, EPFL (LHCb SciFi)

Dark current (Hamamatsu SiPM module of 128 ch à  $0.25 \times 1.1 \text{ mm}^2 \sim 35 \text{ mm}^2$ )

SiPMs are photodetectors with **great properties** (sensitivity, gain, compactness, simplicity) and a few limitations (dark noise, rad. tolerance, dynamic range, rel. high cost).

In the past decade they have stimulated huge interest (by research teams, industry) and **their properties improved a lot**. They enabled new applications and will continue to do so.

**Digital SiPM technology is a consequent next step**. Their acceptance by the market depends on many other aspects.

**AX-PET** is an example of a detector concept which would be very difficult to implement without SiPMs. It **overcomes the sensitivity-resolution dilemma** of standard PET detectors. Its acceptance by the market ...

Many thanks to my AX-PET colleagues Chiara Casella (ETH Zurich) and Matthieu Heller (CERN) for many plots and schematics used in this talk. Thanks also to Felix Sefkow for CALICE material.



*Many thanks for  
your interest !*

